Thomas Heubrandtner

Theoretical Models for Signal Generation in Resistive Plate Chambers[1]

Dissertation

zur Erlangung des akademischen Grades
Doktor der Technischen Wissenschaften
eingereicht an der

Technischen Universität Graz

Begutachter

Univ.-Prof.Dr.phil. B. Schnizer
Institut für Theoretische Physik, Technische Universität Graz

Univ.-Prof.Dr.techn. K.D. Rendulic
Institut für Festkörperphysik, Technische Universität Graz

Mai 1999

[1]unterstützt vom Fonds zur Förderung der wissenschaftl. Forschung, Wien; Projekt Nr.: P10648-NAW.

Abstract

Simple theoretical models for the signal generation in Resistive Plate Chambers (RPC's) are developed, which permit one to give simple formulae to calculate the current induced in the anode strips by the electron cloud, under simplifying assumptions: The electron cloud is approximated by a point charge moving at constant velocity on a trajectory normal to the resistive plates. The calculations are done by the theory of Green's functions. The corresponding equations and conditions involving the piece-wise constant parameters of several layers are rendered self-adjoint by introducing a suitable definition of the scalar product of the eigenfunctions consisting of several pieces. Comparison of the solution of the full time-dependent Maxwell equations and a new method of a quasi-static approximation for weakly conducting media shows that the latter gives very satisfactory results in most cases, at least for conductivities we are interested in, say $0 \leq \sigma \leq 10^{-3}\ S/m$. The signal strength as a function of instantaneous position of the point charge, of the geometrical and the electrical parameters of the resistive plates and of the anode strip width is assessed. The effect of the gap between two neighbouring anode strips is investigated using two-dimensional models and conformal maps.

It turns out that the influence of the weak conductivity of the dielectric layer is small, so the quasi-static approximation for an isolating dielectric layer is applicable. The wanted current is given by three equivalent representations. Two are either based on an eigenfunction expansion or on an integral representation. The third one is given as an triple-sum with a very simple summand and is calculated by the method of images. Additionally, for the special case of a half-filled condensor a closed form for the current can be given; an approximate expression in closed form is found for the case of a dielectric layer very thin as compared to the distance of the electrodes.

Zusammenfassung

Einfache theoretische Modelle für die Signalerzeugung in einer "Widerstandsplattenkammer" (RPC) werden entwickelt, die die Berechnung einfacher Formeln für den Strom, der in den Anodenstreifen durch die Elektronenwolke induziert wird, erlauben. Dabei werden vereinfachende Annahmen getroffen: Die Elektronenwolke wird näherungsweise durch eine Punktladung ersetzt, die sich mit konstanter Geschwindigkeit senkrecht auf die Widerstandsplatte zubewegt. Die Berechnung erfolgt mit Hilfe Green'scher Funktionen. Die zugehörigen Gleichungen und Bedingungen, die die stückweise konstanten Parameter des Mehrschichtproblems enthalten, werden selbstadjungiert gemacht, indem eine passende Definition des Skalarproduktes stückweise stetiger Eigenfunktionen

eingefürt wird. Der Vergleich der Lösungen, die man aus den vollen zeitabhängigen Maxwell'schen Gleichungen und aus einer neuen Methode einer quasistatischen Näherung für schwach leitende Medien erhält zeigt, daß die letztere sehr genaue Ergebnisse liefert, zumindest für Leitfähigkeiten, die für uns von Interesse sind ($0 \leq \sigma \leq 10^{-3}\ S/m$). Die Stärke des Signals in den Anodenstreifen wird als Funktion der momentanen Lage der Punktladung, der geometrischen und elektrischen Parameter der Widerstandsplatten und der Breite der Anodenstreifen berechnet. Die Wirkung des Spaltes zwischen zwei benachbarten Anodenstreifen wird anhand zwei-dimensionaler Modelle und konformer Abbildung untersucht.

Es zeigt sich, daß der Einfluß der schwachen Leitfähigkeit gering ist, sodaß die quasistatische Näherung für eine isolierende dielektrische Schicht anwendbar ist. Der gesuchte Strom wird in drei äquivalenten Darstellungen angegeben: Zwei basieren auf einer Eigenfunktions-Entwicklung und einer Integraldarstellung. Die dritte ist gegeben durch eine Dreifach-Summe mit sehr einfachen Summanden, berechnet mit Hilfe der Spiegelladungstechnik. Zusätzlich wird ein geschlossener Ausdruck für den Strom im speziellen Fall eines halb-gefüllten Kondensators angegeben; eine Näherungsformel in geschlossener Form kann im Falle einer sehr dünnen dielektrischen Schicht im Vergleich zum Abstand der beiden Elektroden gefunden werden.

Contents

Chapter 1

Introduction

A Resistive plate chamber (RPC) is a new type of particle detectors now under development at CERN, Geneva. Such a device consists of two weakly conducting dielectric panels bounding a gap filled by a gas (see Fig.1.1). The panels are made either both of melamine-phenolic laminate [1] or one of melamine-phenolic laminate and the other one of glass [2]. They are in turn covered by the electrodes. The cathode is a continuous sheet of metal. The anode consists of strips; this division gives the opportunity to get information on the position of the event. Such a design permits the application of mass production techniques developed in the semiconductor industry. A high energy particle passing through the detector produces ion clusters by ionizing atoms of the gas in the gap. A static voltage (about 1 kV) applied to the electrodes sets the ions and the electrons into motion. The latter grow into an avalanche and hit the melamine-phenolic laminate panel in front of the anode strips. These moving charges induce a current on the opposite anode strip or strips. The contribution to the signal due to ion motion is negligible. An extensive report on the development of RPC's is in [3].

1.1 Simple Models for Resistive Plate Chambers

In this work simple theoretical models for the signal generation in RPC's are developed. The aim is to give approximate simple formulae and theory, which permit one to calculate the current induced in the anode strips by the electron cloud, under simplifying assumptions. In particular, this electron cloud is approximated by a point charge moving at constant velocity on a trajectory normal to a dielectric layer, Fig.1.2.

One is interested to give the strength of the signal in dependence of the instantaneous position of the charge. Also the influence of the geometrical and electrical parameters of the configuration is to be assessed. The value of the relative dielectric constant is low

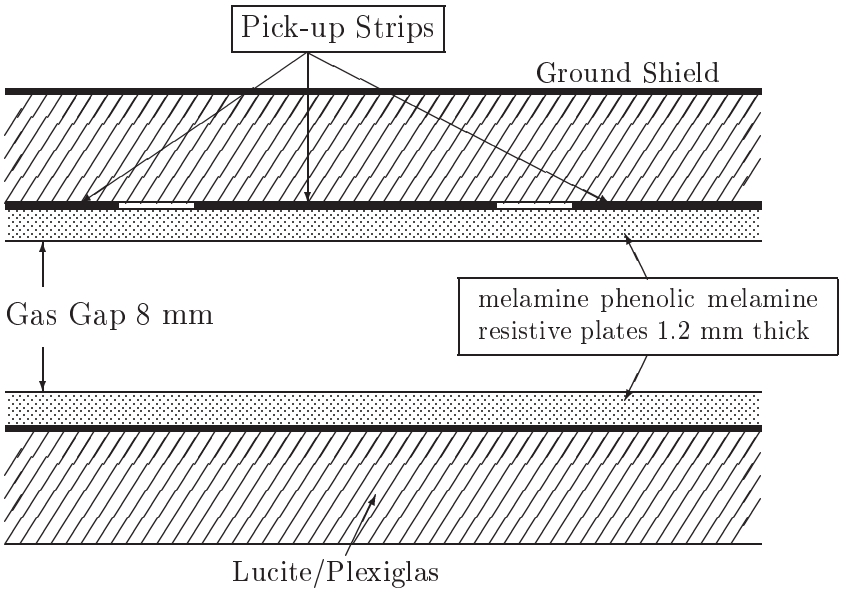

Figure 1.1: *Drawing of a Resistive Plate Chamber [1].*

(2 to 4). The conductivity of these panels is small but not zero (about 10^{-9} S/m). This serves to carry off charges induced on the dielectric; on an ideally isolating dielectric they would accumulate and disturb the normal functioning of the chamber.

The philosphy of presentation in this work is to start from very simple models and to proceed to more complicated ones, which are nearer to reality. As a consequence, some of the simplifying assumptions used in the first chapters are justified and validated in later chapters. The general dynamical model, in which the fields generated by a point charge moving in a plane condensor filled with two dielectric layers are calculated with the help of time-dependent electrodynamic theory, is defered to Chapter 7. The wanted current is given by two equivalent representations, which are based either on an eigenfunction expansion or on an integral represenation of the solution. The numerical evaluation of these, performed in Chapter 8, and previous investigations [6] show that the quasi-static approximation gives good results; the reason is the slow motion of the charge. This quasi-static approximation elaborated in the earlier chapters has far-reaching consequences; it yields expressions for the currents in the electrodes, which are much simpler and need considerably less effort in their numerical evaluations. The results of Chapter 8 show also - what was also found in [5], [6] - that the influence of the weak conductivity of the dielectric layer(s) on the signal is negligible. This result is used at the end of Chapter 4. There the general quasi-static solution for the case of a weakly conducting panel is specialized to the simple case of an isolating dielectric layer in a plane condensor. A completely different approach for solving the purely electrostatic problem with two

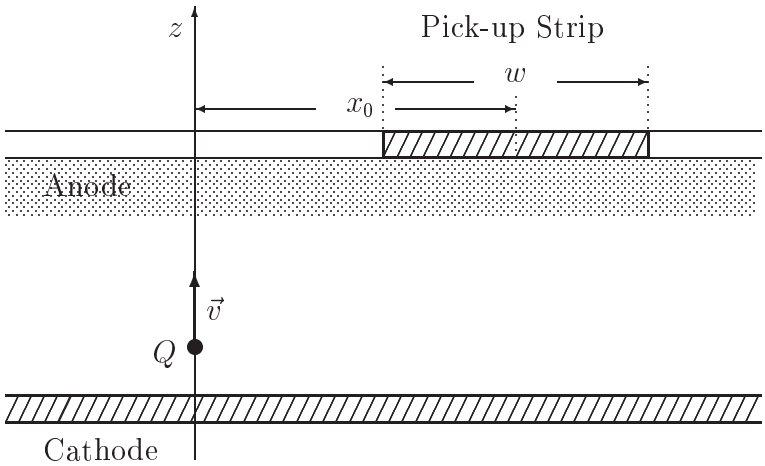

Figure 1.2: *A simple model for a Resistive Place Chamber.*

isolating dielectric layers is the method of images. This is presented in Chapter 5. It produces a result equivalent to that of Chapter 4 represented as a triple sum. Since the summand has quite a simple analytic expression the latter method can compete with that of Chapter 4 in the numeric evaluation. These sums also have the advantage that there are no critical values of the parameters, where convergence becomes difficult and must be checked very carefully. In addition, a simple approximate formula for the signal current can be given for a very thin dielectric layer.

In all models described in the preceding paragraph the structure of the anode strips has been treated in a very approximate way: At first the problem is solved and the surface charge density is calculated as if the anode were a continuous metallic sheet. The charge on a strip is obtained by integrating the charge density over this strip. Thus the gaps separating the anode strips have been disregarded. In order to get some insight what the influence of a real gap is, in Chapter 6 some models are investigated with electrodes having a gap. These are two-dimensional so that the method of conformal maps can be applied. Here also the result found in other chapters is used that the influence of the dielectric on the signal is small. So the 4 models treated in this chapter do not contain dielectric layers. For the sake of comparison models with continuous and with split electrodes are considered. So a charge is moving slowly in the following structures: 1) above a continuous conducting plate; 2) two parallel conducting plates (= a plane condensor); 3) a plate with a gap; 4) two parallel plates, one of which is cut by a gap. Comparison of the results obtained for these different models permits one to estimate the influence of the gap and of the other electrode on the signal. It turns out that the procedure described at the beginning of this paragraph, in which the surface charge density is integrated over a strip of the continuous plate is justified except for

the particular situation, where the charge is moving very near to the gap.

The new method for weakly conducting dielectrics used extensively in this work was proposed by Dedek and Barchorec [9], but only for numeric field calculations. But we recognized immediately that this approach has far-reaching consequences. In the electrodynamic literature and in the research community the opinion prevails that the solution methods of electrostatics are no longer applicable when the dielectric has conductivity, even if this is extremely small. The only method to solve such transient problems is the solution of the full time-dependent Maxwell equations. This opinion is revised in the present work. A quasi-static method for slowly changing fields and not too high a conductivity ($< 10^{-3} S/m$) using only a scalar potential is shown to work by comparison with the result of the rigorous theory.

We hope that the methods to accelerate or induce converge of slowly converging or even diverging series, which are rarely used up to now, will be better known through this work.

Chapter 2

The Quasi-Static Approximation for Isolating and Weakly Conducting Media

The ionization of the gas in a counter produces positive ions and electrons. So neutral atoms are transformed into two clouds of charges. This generates a shock wave, which process is only of theoretical interest as its signal is hardly observed. The main signal results from the motion of the charges. At first this is accelerated. But the gas brackes the motion of these clouds; so it is an acceptable approximation to regard the velocity of this motion as constant. It depends on the type and the regime of the counter whether it is the motion of the ions or that of the electrons, which accounts for the predominant contribution to the signal. This distinction is not very relevant for the treatment in this work. We just assume that a point charge is moving at constant speed on a trajectory perpendicular to the plane electrodes.

We assume the dielectric constant of the medium traversed by the charge to be that of the vacuum. But we pay considerable attention to the dielectric which is between the gas gap (or more generally the space where the motion of the charge takes place) and the electrodes. In the first section it is assumed that the conductivity of this dielectric is zero or negligible. In the second section a new method proposed in [9] is elaborated which is very useful to treat fields propagating in weakly conducting media. This permits one to solve the slow transient problems with a quasi-static method by a scalar time-dependent potential and to avoid the involved machinery of Green's tensors and vector solutions needed in the genuine treatment of transient fields, which is based on the solution of the full Maxwell equations. The quasi-static approximation is applicable since the velocity of the charges emanating the fields is slow as compared to the velocity of electromagnetic wave propagation in the media considered. This point has been discussed in more detail in [7].

2.1 Isolating Media. Scalar Potential as an Approximation to the Liénard-Wiechert Potentials

The quasi-static approximation for the field of a point charge Q moving with velocity $\vec{v}$ may start from the Liénard-Wichert potentials [11]:

$$\Phi(\vec{r},t) = \frac{Q}{4\pi\varepsilon_0\varepsilon}\,\frac{1}{|\vec{R}(t_R)-\vec{R}(t_R)\cdot\vec{v}(t_R)/v_{ph}|}\;; \tag{2.1}$$

$$\vec{A}(\vec{r},t) = \frac{Q}{4\pi\varepsilon_0\varepsilon}\,\frac{\vec{v}}{|\vec{R}(t_R)-\vec{R}(t_R)\cdot\vec{v}(t_R)/v_{ph}|}\;. \tag{2.2}$$

t is time of observation; $t_R = t - R/v_{ph}$ is retarded time; v_{ph} is the phase velocity in the medium. $\vec{r}$ is the point of observation; $\vec{r}_0(t_R)$ is the position of the charge at the instant t_R it emits the field; $\vec{R} = \vec{r} - \vec{r}_0$. The electric field is given by:

$$\vec{E}(\vec{r},t) = -\nabla\Phi(\vec{r},t) - \frac{\partial\vec{A}}{\partial t}\;. \tag{2.3}$$

In the quasistatic approximation it is assumed that the charge moves with a constant velocity small as compared to the phase velocity v_{ph}

$$|\vec{v}| \ll v_{ph} \;\Rightarrow\; v/v_{ph} \approx 0\;,$$

that the distance between the observation and the source point is small (which fact implies $t \approx t_R$) and that the transient fields due to the generation (say by ionization of an atom) and acceleration of the charge have gone away. In that approximation we get for the potentials and the electric field:

$$\Phi(\vec{r},t) \approx \frac{Q}{4\pi\varepsilon_0\varepsilon}\,\frac{1}{R}\;, \tag{2.4}$$

$$\vec{E}(\vec{r},t) \approx -\nabla\Phi(\vec{r},t)\;, \tag{2.5}$$

$$\vec{A}(\vec{r},t) \approx 0\;. \tag{2.6}$$

The formulae above apply to an infinite homogeneous medium characterized by a relative dielectric constant ε. If there are ideally conducting surfaces S, then the tangential electric field $\vec{E}_{tang}$ along these electrodes must be zero; the potential and the Greens function must fulfil the following boundary condition:

$$\vec{r}_S \in S \;:\quad \Phi(\vec{r_S},t) = 0\;,\quad G(\vec{r}_S,\vec{r}_0) = 0\;. \tag{2.7}$$

The electric field induces a surface charge density on these electrodes:

$$\eta(\vec{r}_S, t) = \varepsilon_0 \varepsilon \ \vec{n} \cdot \nabla_S \ \Phi(\vec{r_S}, t) \ . \tag{2.8}$$

$\vec{n}$ is the unit normal pointing from the dielectric into the metal. The charge contained in an subarea A of an electrode is obtained by integrating eq.(2.8) over this area. This charge depends on the position of the source; it is time-dependent when the source moves. We assume that this motion has constant velocity v and is in the direction of $\vec{n}$ so that we may write

$$\vec{r}_0(t) = \vec{n} \ vt \ . \tag{2.9}$$

The time derivative gives the current flowing from (or to) this area:

$$\boxed{I_A = \frac{dq_A}{dt} = Qv(\vec{n} \cdot \nabla_0)(\vec{n} \cdot \nabla_S) \iint_A d\vec{r}_S \ G(\vec{r}_S, \vec{r}_0) \ .} \tag{2.10}$$

$\vec{n} \cdot \nabla_S = \partial / \partial n_S$ denotes the derivation w.r.t. the variable normal to the boundary. The above formula is the main result of the quasi-static theory as we shall use it for isolating dielectrics.

2.2 Weakly Conducting Media. Scalar Potential for a Time-Dependent Field

The derivation of the formulae for the quasi-static approximation in the more general case of weakly conducting linear media starts with the Maxwell equations:

$$\nabla \times \vec{E} = \frac{\partial \vec{B}}{\partial t} , \tag{2.11}$$

$$\nabla \times \vec{H} = \vec{j} + \frac{\partial \vec{D}}{\partial t} = \sigma \vec{E} + \varepsilon_0 \varepsilon \frac{\partial \vec{E}}{\partial t} + \vec{j}_e \ ; \tag{2.12}$$

$$\nabla \cdot \vec{B} = 0 \ , \tag{2.13}$$

$$\nabla \cdot \vec{D} = \nabla \cdot (\varepsilon_0 \varepsilon \vec{E}) = \rho \ . \tag{2.14}$$

σ is the conductivity, ε the dielectric constant of the medium (or media). $\vec{j}_e$ is the impressed current. Now we start to use the assumptions that the conductivity σ of the media is small and that the motion of the charges producing the impressed curren $\vec{j}_e$ is slow, which entails that the fields changes also slowly. We now apply the method proposed by Dedek and Bachorec [9]. From the foregoing assumptions if follows that variation of the magnetic induction with time is vanishingly small, which entails that the electric field is free of vortices and may be derived from a time-dependent scalar potential:

$$\nabla \times \vec{E} = \frac{\partial \vec{B}}{\partial t} \approx 0 \ \Rightarrow \ \vec{E} = -\nabla \Phi \ . \tag{2.15}$$

We take the divergence of eq.(2.12):

$$\nabla \cdot \left(\sigma \vec{E} + \varepsilon_0 \varepsilon \frac{\partial \vec{E}}{\partial t} \right) = -\nabla \cdot \vec{j}_e = \frac{\partial \rho_e}{\partial t} \ . \tag{2.16}$$

In making the last change in the above equation we used the fact that the impressed current fulfils the following continuity relation:

$$\nabla \cdot \vec{j}_e = -\frac{\partial \rho_e}{\partial t} \ .$$

The impressed charge density ρ_e results from the moving point charges we consider. Inserting eq.(2.15) into (2.16) gives the wanted equation for the quasi- static potential in a weakly conducting medium:

$$\boxed{\sigma \nabla^2 \Phi + \varepsilon_0 \varepsilon \frac{\partial}{\partial t} \nabla^2 \Phi = -\frac{\partial \rho_e}{\partial t} \ .} \tag{2.17}$$

This is a third order partial differential equation which resembles somewhat a diffusion equation. It is solved by a Fourier transform in time t. Inserting

$$\Phi(\vec{r},t) = \frac{1}{2\pi}\int_{-\infty}^{\infty}\Phi(\omega,\vec{r})\ e^{-i\omega t}\ d\omega\ , \tag{2.18}$$

$$\rho_e(\vec{r},t) = \frac{1}{2\pi}\int_{-\infty}^{\infty}\rho_e(\omega,\vec{r})\ e^{-i\omega t}\ d\omega\ , \tag{2.19}$$

gives the follwing second order equation for the Fourier transform of the potential:

$$\sigma\nabla^2\Phi(\omega,\vec{r}) - i\omega\varepsilon_0\varepsilon\nabla^2\Phi(\omega,\vec{r}) = i\omega\rho_e(\omega,\vec{r})\ . \tag{2.20}$$

With the help of the complex dielectric constant

$$\epsilon := \left(\varepsilon + \frac{i\sigma}{\omega\varepsilon_0}\right)\ ,$$

the above differential equation assumes again the shape of the Poisson equation

$$\nabla^2\Phi(\omega,\vec{r}) = -\frac{\rho_e(\omega,\vec{r})}{\varepsilon_0\epsilon}\ . \tag{2.21}$$

Now eq.(2.17) is treated by a Laplace transform:

$$\bar{\Phi}(\vec{r},s) \ = \ \mathcal{L}[\Phi(r,t)] \ := \ \int_0^{\infty}\ e^{-st}\ \Phi(\vec{r},t)\ dt. \tag{2.22}$$

From this it follows:

$$\mathcal{L}[\frac{\partial}{\partial t}\Phi(r,t)] \ := s\ \bar{\Phi}(\vec{r},s) - \Phi(\vec{r},t=0); \qquad \mathcal{L}[\frac{\partial}{\partial t}\rho(r,t)] \ := s\ \bar{\rho}(\vec{r},s) - \rho(\vec{r},t=0). \tag{2.23}$$

$\Phi(\vec{r},t=0)$ and $\rho(\vec{r},t=0)$ are the initial data of the potential and of the charge. If both are zero we get in place of eq.(2.17) the follwing one:

$$\nabla^2\bar{\Phi}(\vec{r},s) \ = \ -\frac{\bar{\rho}(\vec{r},s)}{\varepsilon_0\epsilon} \quad \text{with} \quad \epsilon := \varepsilon + \sigma/(s\varepsilon_0). \tag{2.24}$$

In the quasi-static approximation we get an equation which resembles a Poisson equation in place of a Helmholtz equation. This is very advantangeous as the toolbox for solving the former equation is much richer than that for solving the latter.

Chapter 3

An Empty Condensor as a Model of a Chamber

A plane condensor, whose interior is vacuum, represents the simplest model of a chamber. A point charge moving in it with constant speed on a normal to the plates induces a charge distribution varying in time on these electrodes. This current is the signal we want to investigate. The full time-dependent problem with a weakly conducting layer has been solved by Schöpf [4], [6], [5]. In this works it has been shown by solving Maxwell's equations for a charge moving in such a configuration, that the influence of a small conductivity of a layer screening an electrode on the signal is negligible and that the main contribution to the signal results from the uniform motion of the charge. There also the static approximation has been developed, more as a check. Here it is used to derive formulae for the current on the electrodes.

3.1 Basis Equations for the Potential

The configuration is shown in Fig.3.1. A charge Q is located at the point $(0, z_0)$ between two ideally conducting grounded electrodes passing through the points $z = 0$, $z = D$, respectively. The potential is expressed by a Green's function

$$\Phi(r, z, z_0) = \frac{Q}{\varepsilon_0}\, G(r, z; r' = 0, z_0)\ . \tag{3.1}$$

The configuration is symmetric around the z-axis. So neither the potential nor the Green's function depend on the azimuthal angle. The Green's function is a solution of the following differential equation

$$\Delta G(r, z; z') = \left[\frac{\partial^2}{\partial r^2} + \frac{1}{r}\frac{\partial}{\partial r} + \frac{\partial^2}{\partial z^2}\right] G(r, z; z') = -\frac{\delta(r)}{2\pi r}\ \delta(z - z')\ , \tag{3.2}$$

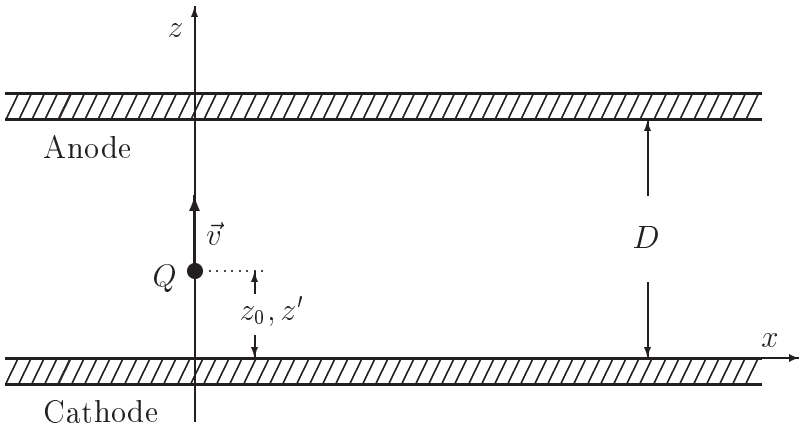

Figure 3.1: *A charge Q beween to parallel conducting planes. At first it is regarded as being at rest. When calculating the signal it is assumed to have velocity v.*

fulfilling the boundary conditions

$$G(r, z; z')\Big|_{z=0,D} = 0 \ . \tag{3.3}$$

In view of the axial symmetry the azimuthal coordinate has been omitted everywhere.

3.2 Eigenfunction Expansion of the Green's Function

Solutions of the homogeneous equation belonging to eq.(3.2) are products of Bessel functions of order 0 (due to the axial symmetry) and trigonometric functions. One may start from the completeness relation

$$\int_0^\infty d\rho \ \rho J_0(\rho r) = \frac{\delta(r)}{r} \ , \tag{3.4}$$

and make an ansatz for the Green's function:

$$G(r, z; z') = \frac{1}{2\pi} \int_0^\infty d\rho \ \rho J_0(\rho r) \ g(\rho; z, z')$$

Inserting both into eq.(3.2) and equating integrands leaves us with the following equation for the amplitude g:

$$\Big[\frac{d^2}{dz^2} + \rho^2\Big] g(\rho; z, z') = -\delta(z - z') \ . \tag{3.5}$$

Only trigonometric functions $\sin(m\pi z/D)$, with $m = 0, 1, 2, \ldots$, fulfil the boundary conditions (3.3). Their completeness relation is:

$$\delta(z - z') = \frac{2}{D} \sum_{m=0}^{\infty} \sin\Big(\frac{m\pi z}{D}\Big) \sin\Big(\frac{m\pi z'}{D}\Big) \ .$$

Making a similar ansatz for the function $g(\rho; z, z')$ and inserting this together with the completeness relation into (3.5) yields

$$g(\rho; z, z') = \frac{2}{D} \sum_{m=0}^{\infty} \frac{\sin(m\pi z/D)\ \sin(m\pi z'/D)}{\rho^2 + (m\pi/D)^2} \ ,$$

and with this the eigenfunction expansion:

$$G(r, z; z') = \frac{2}{D} \sum_{m=0}^{\infty} \sin\Big(\frac{m\pi z}{D}\Big) \sin\Big(\frac{m\pi z'}{D}\Big) \int_0^{\infty} d\rho \ \frac{\rho\ J_0(\rho r)}{\rho^2 + (m\pi/D)^2} \ .$$

The integration over ρ can be done

$$\int_0^{\infty} d\rho \ \frac{\rho\ J_0(\rho r)}{\rho^2 + (m\pi/D)^2} = K_0\Big(\frac{m\pi r}{D}\Big) \ ,$$

to give the final form of the axially symmetric Green's function:

$$G(r, z; z') = \frac{2}{D} \sum_{m=0}^{\infty} \sin\Big(\frac{m\pi z}{D}\Big) \sin\Big(\frac{m\pi z'}{D}\Big) K_0\Big(\frac{m\pi r}{D}\Big) \ . \tag{3.6}$$

3.3 Integral Representations of the Green's Function

Another representation of the Green's function is derived from that for free space [13] :

$$G_F(r, z; z') = \frac{1}{4\pi} \ \frac{1}{\sqrt{r^2 + (z - z')^2}} = \frac{1}{4\pi} \int_0^{\infty} d\lambda \ J_0(\lambda r)\ e^{-\lambda|z - z'|} \ .$$

This function is augmented by a solution of the homogeneous equation corresponding to (3.2):

$$H(r, z; z') = \frac{1}{4\pi} \int_0^{\infty} d\lambda \ J_0(\lambda r) \Big[A(\lambda)\ e^{\lambda z} + B(\lambda)\ e^{-\lambda z} \Big]$$

The sum $G(r, z; r' = 0, z') = G_F(r, z; z') + H(r, z; z')$ is required to fulfil the boundary conditions (3.3); this gives two equations for the two unknown functions $A(\lambda)$ and $B(\lambda)$.

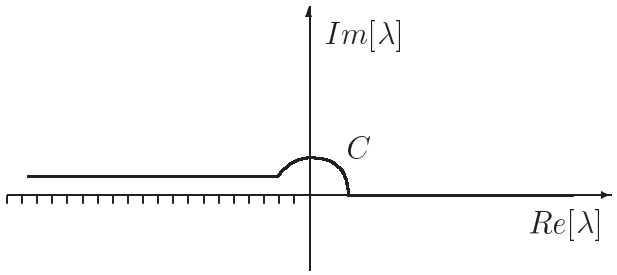

Figure 3.2: *The complex λ-plane. Branch cut and path of integration C for integral (3.9).*

Solving for these and inserting the results in the above integral gives after some algebra the following integral representation for the axially symmetric Green's function:

$$G(r,z;z') = \frac{1}{2\pi}\int_0^\infty d\lambda\ J_0(\lambda r)\left[\frac{\sinh[\lambda(D-z_>)]\sinh[\lambda z_<]}{\sinh \lambda D}\right], \tag{3.7}$$

with

$$z_> = \max[z,z'] \quad \text{and} \quad z_< = \min[z,z']\ . \tag{3.8}$$

This representation may also be rewritten as:

$$G(r,z;z') = \frac{1}{4\pi}\int_{-\infty}^\infty d\lambda\ H_0^{(1)}(\lambda r)\left[\frac{\sinh[\lambda(D-z_>)]\sinh[\lambda z_<]}{\sinh \lambda D}\right] \tag{3.9}$$

Since the Hankel function $H_0^{(1)}(\lambda r)$ has a branch point at $\lambda = 0$ a branch cut must be applied along the negative real axis of the complex λ-plane; and the path of integration C must lie above it (see Fig.3.2). The equivalence of these two representations is proved by splitting the path of integration into three parts $(-\infty, -\epsilon)$, a semicircle of radius ϵ and (ϵ, ∞). The integral around the semicircle tends to zero as $\epsilon \to 0$; in the first integral λ is replaced with $\lambda e^{i\pi}$ and the half circuit relation $H_0^{(1)}(r\lambda e^{i\pi}) = -H_0^{(2)}(r\lambda)$ is inserted; this and the third integral are combined and $H_0^{(1)}(r\lambda) + H_0^{(2)}(r\lambda) = 2J_0(r\lambda)$ is used to transform (3.9) into (3.7).

The integral in (3.9) may be evaluated by Cauchy's residue theorem. The path of integration C is closed by an semi-circle of infinite radius. The contour so obtained encloses an infinite number of first order poles at $\lambda = im\pi/D$. This yields the series (3.6) after the hyperbolic functions of imaginary argument have been replaced by the corresponding trigonometric functions and the Hankel function of imaginary argument by the modified Bessel function.

3.4 Surface Charge and Current on a Whole Electrode

The charge density is obtained from eqs.(3.1) and (3.7) according to:

$$\eta(r,z') = \varepsilon_0 Q \frac{\partial \Phi}{\partial z}\Big|_{z=D} = Q \frac{\partial G}{\partial z}\Big|_{z=D} = -\frac{Q}{2\pi}\int_0^\infty d\lambda\ J_0(\lambda r)\frac{\lambda \sinh \lambda z'}{\sinh \lambda D}\ . \tag{3.10}$$

The charge on the whole electrode is:

$$q_T(z') = -2\pi Q \int_0^\infty d\lambda \frac{\lambda \sinh \lambda z'}{\sinh \lambda D} \underbrace{\int_0^\infty dr\ r J_0(\lambda r)}_{=\ \delta(\lambda)/\lambda} = -\frac{Q}{D}\ z'\ .$$

The integral over r is evaluated by the completeness relation (3.4). The remaining integral over λ involves a δ-distribution; in its evaluation one may argue that in the resulting limit $\lambda \to 0$ the fraction of hyperbolic functions becomes z'/D.

The above slightly ambiguous step is avoided if the series expansion (3.6) of the Greens function is used:

$$\eta(r,z') = \varepsilon_0 Q \frac{\partial \Phi}{\partial z}\Big|_{z=D} = \frac{Q}{D^2}\sum_{m=1}^\infty \Big[m(-1)^m \sin\Big(\frac{m\pi z'}{D}\Big) K_0\Big(\frac{m\pi r}{D}\Big)\Big]\ . \tag{3.11}$$

The total charge on the electrode is:

$$\begin{aligned} q_T(z') &= 2\pi \int_0^\infty dr\ r\eta(r,z') = \frac{2\pi Q}{D^2}\sum_{m=1}^\infty \Big[m(-1)^m \sin\Big(\frac{m\pi z'}{D}\Big) \underbrace{\int_0^\infty dr\ r K_0\Big(\frac{m\pi r}{D}\Big)}_{=\ (D/m\pi)^2}\Big] = \\ &= \frac{2Q}{\pi}\sum_{m=1}^\infty \Big[\frac{(-1)^m}{m}\sin\Big(\frac{m\pi z'}{D}\Big)\Big] = -\frac{Q}{D}\ z'\ . \end{aligned}$$

In the intervall under consideration the above Fourier series over m sums up to the final linear function.

By the method of the quasistatic approximation described in sect.2.1, one gets for the current:

$$I_T(z') = \frac{dq_T(z')}{dt} = v\frac{dq_T(z')}{dz'}\Big|_{z'=z_0} = -\frac{Qv}{D}\ . \tag{3.12}$$

So the current on each electrode is completely independent of the position of the charge Q. Fig.3.1 just shows the configuration. Through the sign of the velocity v the current depends on the direction of the motion.

3.5 Charge on and Current through a Strip

The charge density (3.10) is integrated over a strip of width w centered at $x = x_0$ and extending to infinity at both ends of the y-axis (see Fig.3.3).

$$\begin{aligned} q_S(z') &= \int_{x_0-w/2}^{x_0+w/2} dx \int_{-\infty}^{\infty} dy\ \eta(r,z') = \\ &= -\frac{Q}{2\pi}\int_0^{\infty} d\lambda\ \frac{\lambda \sinh \lambda z'}{\sinh \lambda D} \int_{x_0-w/2}^{x_0+w/2} dx \int_{-\infty}^{\infty} dy\ J_0(\lambda\sqrt{x^2+y^2})\ . \end{aligned} \tag{3.13}$$

The integral over y is done according to [16]:

$$\int_{-\infty}^{\infty} J_0(\lambda\sqrt{x^2+y^2})\ dy = 2\ \frac{2^{-1/2}\ \Gamma(1/2)}{\lambda^{1/2}\ x^{-1/2}}\ J_{-1/2}(\lambda x) = \frac{2\cos\lambda x}{\lambda}\ .$$

Now the integration over x is easy:

$$\Big[\int dx \int_{-\infty}^{\infty} J_0(\lambda\sqrt{x^2+y^2})\ dy\Big]_{x=x_0-w/2}^{x=x_0+w/2} = \frac{2}{\lambda^2}\sin\lambda x\Big|_{x=x_0-w/2}^{x=x_0+w/2}\ .$$

The charge on the strip is:

$$q_S(z') = -\frac{Q}{\pi}\Big[\int_0^{\infty} d\lambda \frac{\sinh\lambda z' \sin\lambda x}{\lambda \sinh\lambda D}\Big]_{x=x_0-w/2}^{x=x_0+w/2}\ . \tag{3.14}$$

The current through the strip is:

$$\begin{aligned} I_S(z') &= \frac{dq_S(z')}{dt} = v\frac{dq_S(z')}{dz'}\Big|_{z'=z_0} = -\frac{Qv}{\pi}\Big[\int_0^{\infty} d\lambda \frac{\cosh\lambda z_0 \sin\lambda x}{\sinh\lambda D}\Big]_{x=x_0-w/2}^{x=x_0+w/2} = \\ &= \frac{Qv}{2D}\left[\frac{\sinh[\frac{\pi(x_0+w/2)}{D}]}{\cos[\frac{\pi z_0}{D}]+\cosh[\frac{\pi(x_0+w/2)}{D}]} - \frac{\sinh[\frac{\pi(x_0-w/2)}{D}]}{\cos[\frac{\pi z_0}{D}]+\cosh[\frac{\pi(x_0-w/2)}{D}]}\right]\ . \end{aligned} \tag{3.15}$$

This formula differs from corresponding ones given in earlier work [7], [8] by the value 2 (in place of 4) in the denominator on the right hand side. An error occured in these earlier calculations.

The above formula is an approximation to the current flowing through the anode strip in a RPC. Recall that the dielectric supporting the anode strips and the gaps separating them are neglected. The influence of the dielectric on the signal is indeed small as will be shown in Chapters 4, 5 and 7. The influence of a gap separating the strips is more complex. This is investigated in Chapter 6.

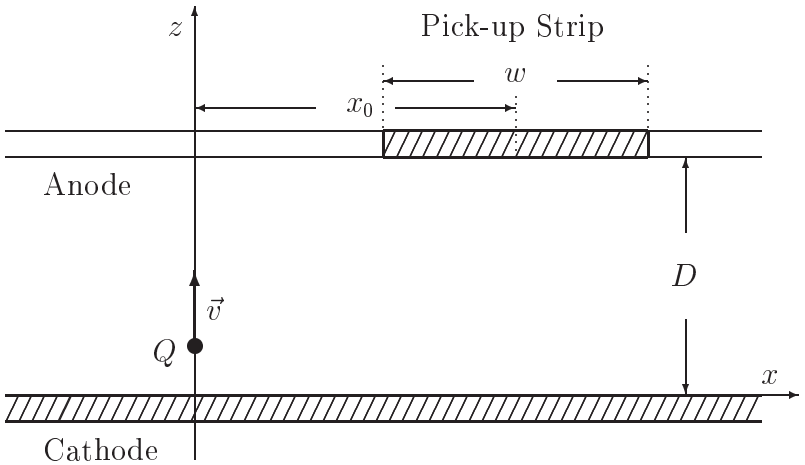

Figure 3.3: *Point charge moving in a very simplified model of a RPC. w indicates the width of the anode strip.*

Chapter 4

Condensor with 2 Layers in the Quasi-Static Approximation

4.1 Quasi-Static Approximation for a Weakly Conducting Layer

There are two layers ($i = 1, 2$) of thickness p, $|q|$, each having its own complex relative dielectric constant ϵ_i :

$$\epsilon_i = \varepsilon_i + \frac{i\sigma_i}{\omega\varepsilon_0} \ .$$

The whole configuration extends till infinity in the radial direction (see Fig.4.1). In the quasistatic approximation for weakly conducting media elaborated in sect.2.2 and for a given angular frequency ω, the potential in each layer must be a solution of the following differential equation.

$$\Delta\Phi_i(\omega, r, z) = -\frac{\rho_i(\omega, r, z)}{\varepsilon_0\epsilon_i} \ . \tag{4.1}$$

The time depending point charge distribution is

$$\rho(t, r, z) = \begin{cases} \rho_1(t, r, z) = Q \ \frac{\delta(r)}{2\pi r} \ \delta(z - q - vt) \ \Theta(z - q) \ \Theta(-z) & : \quad q < z < 0 \\ \rho_2(t, r, z) = 0 & : \quad 0 < z < p \end{cases} \tag{4.2}$$

where the two stepfunctions describe the sudden generation and annihilation of the charge in the interior of the condensor. It is assumed that the point charge is created in the vicinity of the cathode ($z = q$) and moves towards the surface of the conducting

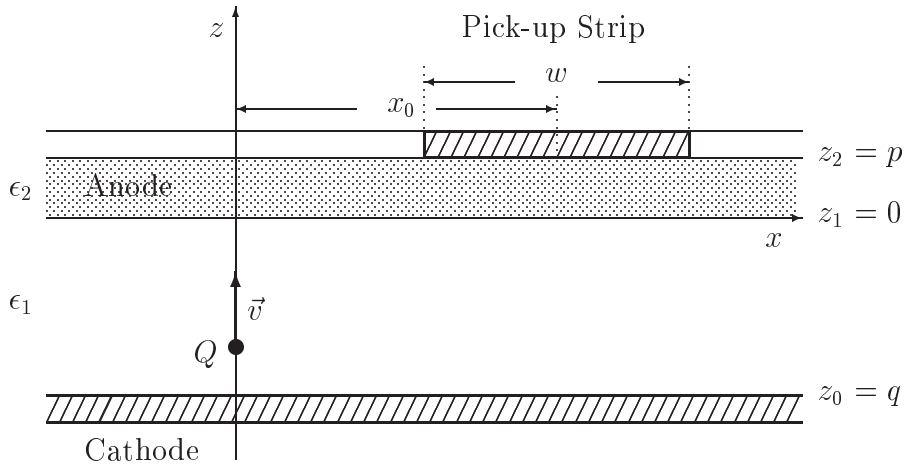

Figure 4.1: *A simple model for a Resistive Plate Chamber. Geometrical and electrical parameters used in this chapter are shown. Distance of the electrodes:* $D = p - q$*; thickness of the layer:* $d = p$*.*

layer, where it is annihilated ($z = 0$). Charge conservation requires there to be an other charge of opposite sign. In fact, the electron cloud is generated by ionisation. But the ions hardly move and induce a static field only, which is disregarded. The Fourier transform $\rho(\omega, r, z)$ of the point charge distribution (4.2) is given by :

$$\begin{aligned} \rho(\omega, r, z) &= \int_{-\infty}^{\infty} dt\ \rho(t, r, z)\ e^{i\omega t} = \\ &= \begin{cases} \rho_1(\omega, r, z) = \frac{Q}{v}\ \frac{\delta(r)}{2\pi r}\ e^{i\frac{\omega}{v}(z-q)}\ \Theta(z-q)\ \Theta(-z) & : \quad q < z < 0; \\ \rho_2(\omega, r, z) = 0 & : \quad 0 < z < p. \end{cases} \end{aligned} \tag{4.3}$$

The two layers are bounded in the z-direction by ideally conducting electrodes located at $z = p > 0$ and $z = q < 0$. This gives the boundary conditions:

$$\begin{aligned} \Phi_1\Big|_{z=q} &= 0\ , \\ \Phi_2\Big|_{z=p} &= 0\ . \end{aligned} \tag{4.4}$$

In the radial direction the potentials must fulfil a radiation condition:

$$\lim_{r\to\infty}\ r\ \frac{\partial \Phi_i}{\partial r} = 0\ . \tag{4.5}$$

At the interface between the two layers the potential must fulfil the following two continuity conditions:

$$\Phi_1\Big|_{z=0} = \Phi_2\Big|_{z=0} , \tag{4.6}$$

$$\epsilon_1 \frac{\partial \Phi_1}{\partial z}\Big|_{z=0} = \epsilon_2 \frac{\partial \Phi_2}{\partial z}\Big|_{z=0} . \tag{4.7}$$

The boundary value problem defined in eqs.(4.1) to (4.7) is solved with the help of an axially symmetric Green's function, which is the solution of the following differential equation:

$$\hat{L}\ G_{ij}(r,z;z') := \Big[\underbrace{\frac{1}{r}\frac{\partial}{\partial r}\Big(r\frac{\partial}{\partial r}\Big)}_{=:\ \Delta_r} + \frac{\partial^2}{\partial z^2} \Big]\ G_{ij}(r,z;z') = -\delta_{ij}\frac{\delta(r)}{2\pi r}\ \delta(z-z') . \tag{4.8}$$

In the two-layer problem under consideration the Green's function is expressed by 4 pieces; these depend on the positions of the source (index j) and observation points (index i) in the 2 layers. Inserting the following ansatz for the Green's function

$$G_{ij}(r,z;z') = \frac{1}{2\pi}\int_0^\infty d\rho\ \rho J_0(\rho r)\ g_{ij}(\rho,z;z') , \tag{4.9}$$

into eq.(4.8) yields a simpler differential equation for the reduced Green's function g_{ij}

$$\hat{L}_z\ g_{ij}(\rho,z;z') := \Big(\frac{\partial^2}{\partial z^2} - \rho^2\Big) g_{ij}(\rho,z;z') = -\delta_{ij}\delta(z-z') , \tag{4.10}$$

when the following integral represetation for Dirac's δ-distribution is used

$$\frac{\delta(r)}{r} = \int_0^\infty d\rho\ \rho J_0(\rho r) , \tag{4.11}$$

and if we take into account that the Bessel function $J_0(\rho r)$ is eigenfunction of the radial Laplacian Δ_r

$$\Delta_r\ J_0(\rho r) = -\rho^2 J_0(\rho r) . \tag{4.12}$$

The new funtions g_{ij} fulfil the same boundary conditions as ϕ_i.

$$g_{1j}\Big|_{z=p} = 0 , \tag{4.13}$$

$$g_{2j}\Big|_{z=q} = 0 . \tag{4.14}$$

We want to work with a Green's function g_{ij} satisfying the same continuity conditions as ϕ_i,

$$g_{1j}\Big|_{z=0} = g_{2j}\Big|_{z=0} , \tag{4.15}$$

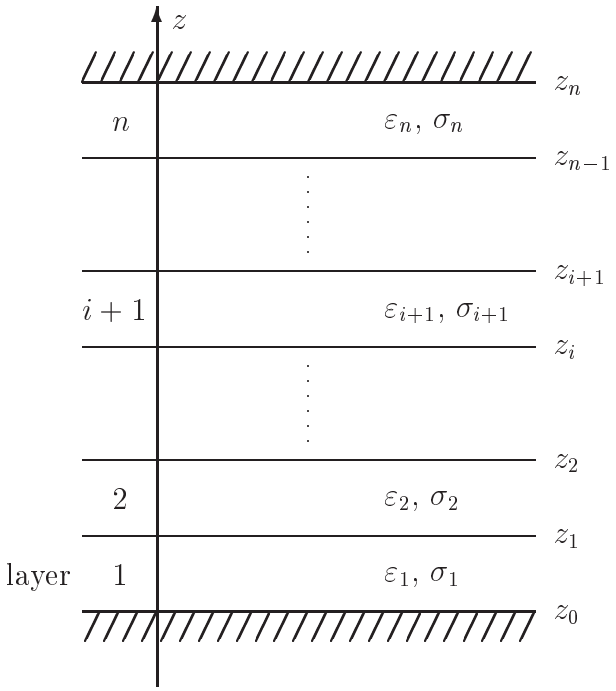

Figure 4.2: *A configuration consisting of n layers.*

$$\epsilon_1 \frac{\partial g_{1j}}{\partial z}\bigg|_{z=0} = \epsilon_2 \frac{\partial g_{2j}}{\partial z}\bigg|_{z=0} . \tag{4.16}$$

This requires the problem to be self-adjoint; this in turn necessitates a special treatment of the scalar product, elaborated in the next paragraph.

4.1.1 Selfadjointness and Scalar Product

For a multiple-layer problem, in which the parameters describing the properties of the media are piece-wise constant, the selfadjointness of the operators requires a special treatment. This property is very advantageous, since the Green's function is symmetric in the coordinates of the source and observation point only if the problem is posed such that it is self-adjoint. Otherwise it would be necessary to obtain a Green's function, which is a solution of a differential equation adjoint to the field equation. This entails that the continuity conditions for the Green's functions differ from those for the potential or field. All these problems can be avoided by defining the scalar product for any two solutions of the two-layer field equation in an appropriate way so that the whole problem is self-adjoint. How this new scalar product must be defined is shown for the more general problem with several layers.

A problem with n plane layers is considered as shown in Fig.4.2. Let $f(r,z)$ be a representative of the set Ω_n of functions consisting of n parts

$$f(r,z) = \begin{cases} f_1(r,z) & : \quad z_0 < z < z_1 \\ f_2(r,z) & : \quad z_1 < z < z_2 \\ \vdots & \quad \vdots \\ f_n(r,z) & : \quad z_{n-1} < z < z_n \end{cases} . \tag{4.17}$$

f_1 and f_n are supposed to fulfil the boundary conditions at the limits $z = z_0$ and $z = z_n$

$$\begin{aligned} f_1\Big|_{z=z_0} &= 0 \ , \\ f_n\Big|_{z=z_n} &= 0 \ . \end{aligned} \tag{4.18}$$

At each interface, separating two different layers, it is assumed that they satisfy the following continuity conditions:

$$\begin{aligned} f_i\Big|_{z=z_i} &= f_{i+1}\Big|_{z=z_i} \ , \\ \epsilon_i \frac{\partial f_i}{\partial z}\Big|_{z=z_i} &= \epsilon_{i+1} \frac{\partial f_{i+1}}{\partial z}\Big|_{z=z_i} \ , \qquad i = 1, \ldots, n-1 \ . \end{aligned} \tag{4.19}$$

And finally the functions $f_i(r,z)$ fulfil radiation conditions in each layer.

$$\lim_{r\to\infty} \ r \frac{\partial f_i}{\partial r} = 0 \ , \qquad i = 1, \ldots, n \ . \tag{4.20}$$

In addition, let Ω_n^z be the corresponding set of functions independent of r, so they are not required to fulfil the last radiation condition.

The potential $\phi(r,z) \in \Omega_n$ is solution of the differential equation

$$\hat{L} \ \phi(r,z) = -\xi(r,z) \ , \quad \text{or} \quad \hat{L} \ \phi_i(r,z) = -\xi_i(r,z) \ , \qquad i = 1, \ldots, n \ ; \tag{4.21}$$

with

$$\xi(r,z) = \begin{cases} \xi_1(r,z) = \frac{\rho_1(r,z)}{\varepsilon_0 \epsilon_1} & : \quad z_0 < z < z_1 \\ \xi_2(r,z) = \frac{\rho_2(r,z)}{\varepsilon_0 \epsilon_2} & : \quad z_1 < z < z_2 \\ \vdots & \quad \vdots \\ \xi_n(r,z) = \frac{\rho_n(r,z)}{\varepsilon_0 \epsilon_n} & : \quad z_{n-1} < z < z_n \end{cases} . \tag{4.22}$$

The differential equation in (4.21) is solved with the help of the Green's function $G_i(r,z;z') \in \Omega_n$

$$G_i(r,z;z') = \begin{cases} G_{i1}(r,z;z') & : \quad z_0 < z' < z_1 \\ G_{i2}(r,z;z') & : \quad z_1 < z' < z_2 \\ \vdots & \quad \vdots \\ G_{in}(r,z;z') & : \quad z_{n-1} < z' < z_n \end{cases} , \tag{4.23}$$

which is a solution of the following differential equation:

$$\hat{L}\ G_{ij}(r,z;z') = -\delta_{ij}\frac{\delta(r)}{2\pi r}\ \delta(z-z')\ . \tag{4.24}$$

In order to show the need for the new definition of the scalar product, at first the usual scalar product of two functions $A, B \in \Omega_n$ is defined as a sum over integrals, each extending over one layer.

$$\begin{aligned}(A_i,B_i) &:= 2\pi\int_0^\infty dr\ r\int_{z_{i-1}}^{z_i} dz\ A_iB_i\ ,\\ (A,B) &:= \sum_{i=1}^{n}(A_i,B_i)\ .\end{aligned} \tag{4.25}$$

It can be shown that with this sum over n layers the operator $\hat{L}$ (together with the continuity conditions (4.19)) is not self-adjoint. For, the formula corresponding to Green's theorem in layer i is:

$$\int_{z_{i-1}}^{z_i} dz\int_0^\infty dr\ rB_i\hat{L}A_i = \int_{z_{i-1}}^{z_i} dz\int_0^\infty dr\Big[B_i\ \frac{\partial}{\partial r}\Big(r\frac{\partial A_i}{\partial r}\Big) + rB_i\ \frac{\partial^2 A_i}{\partial z^2}\Big] =$$

$$\int_{z_{i-1}}^{z_i} dz\Big[B_i\ r\frac{\partial A_i}{\partial r}\Big]\Big|_{r=0}^{\infty} + \int_0^\infty dr\Big[rB_i\frac{\partial A_i}{\partial z}\Big]\Big|_{z_{i-1}}^{z_i} - \int_{z_{i-1}}^{z_i} dz\int_0^\infty dr\Big[r\frac{\partial B_i}{\partial r}\frac{\partial A_i}{\partial r} + r\frac{\partial B_i}{\partial z}\frac{\partial A_i}{\partial z}\Big] =$$

$$\int_{z_{i-1}}^{z_i} dz\underbrace{\Big[rB_i\frac{\partial A_i}{\partial r} - r\frac{\partial B_i}{\partial r}A_i\Big]\Big|_{r=0}^{\infty}}_{:=\ \mu_i} + \int_0^\infty drr\underbrace{\Big[B_i\frac{\partial A_i}{\partial z} - \frac{\partial B_i}{\partial z}A_i\Big]\Big|_{z_{i-1}}^{z_i}}_{:=\ \nu_i} + \int_{z_{i-1}}^{z_i} dz\int_0^\infty dr\ rA_i\hat{L}B_i$$

Analogous conversions can be done for all n layers. The terms μ_i become zero as both functions A and B are required to fulfil the radiation condition (4.20) in each layer.

$$\mu_i = \Big[rB_i\frac{\partial A_i}{\partial r} - r\frac{\partial B_i}{\partial r}A_i\Big]\Big|_{r=0}^{\infty} = 0\ . \tag{4.26}$$

Thus their sum from $i=1$ to n is zero. Moreover, the terms ν_0, ν_n vanish at the limits $z = z_0, z_n$ by the boundary conditions (4.18). However, even if the continuity conditions (4.19) at the interface $z = z_i$ between two neighbouring layers are taken into account, the sum of the terms ν_i does not vanish

$$\sum_{i=1}^{n}\nu_i = \sum_{i=1}^{n-1}\left\{\Big[B_i\frac{\partial A_i}{\partial z} - \frac{\partial B_i}{\partial z}A_i\Big]\Big|_{z=z_i} - \Big[B_{i+1}\frac{\partial A_{i+1}}{\partial z} - \frac{\partial B_{i+1}}{\partial z}A_{i+1}\Big]\Big|_{z=z_i}\right\} \neq 0\ , \tag{4.27}$$

because every summand in the second sum gives a value unequal to zero.

In contrast to eq.(4.25) a new kind of the scalar product is now introduced by the following definition (a corresponding scalar product for multiple-layer problems is also defined in [10]):

$$\begin{aligned}\langle A,B\rangle = \langle B,A\rangle \;&:=\; 2\pi\int_0^\infty dr\; r\Big[\sum_{i=0}^{n}\epsilon_i\int_{z_{i-1}}^{z_i} dz\; A_iB_i\Big] = \\ &=\; \sum_{i=1}^{n}\epsilon_i\;(A_i,B_i)\;. \end{aligned} \tag{4.28}$$

The corresponding new summand in eq.(4.27) now do become zero when the continuity conditions are inserted,

$$\epsilon_i\Big[B_i\frac{\partial A_i}{\partial z}-\frac{\partial B_i}{\partial z}A_i\Big]\Big|_{z=z_i}-\epsilon_{i+1}\Big[B_{i+1}\frac{\partial A_{i+1}}{\partial z}-\frac{\partial B_{i+1}}{\partial z}A_{i+1}\Big]\Big|_{z=z_i}=0\;, \tag{4.29}$$

and so the sum from $i=1$ to $n-1$ also vanishes. In this case the operator $\hat{L}$ (together with the continuity conditions(4.19)) is self-adjoint.

$$\langle A,\hat{L}B\rangle = \langle B,\hat{L}A\rangle\;. \tag{4.30}$$

The solution of the differential equation (4.21), (4.22) can be obtained if the general functions A and B are replaced by the potential $\phi(r,z)$ and the Green's function $G_i(r,z)$, respectively.

$$\begin{aligned}\langle\phi,\hat{L}G_i\rangle &= \langle G_i,\hat{L}\phi\rangle \\ \longrightarrow\quad \sum_{j=1}^{n}\epsilon_j\;(\phi_j,\hat{L}G_{ij}) &= \sum_{j=1}^{n}\epsilon_j\;(G_{ij},\hat{L}\phi_j)\end{aligned} \tag{4.31}$$

The expressions $\hat{L}G_{ij}$ and $\hat{L}\phi_j$ may be replaced by the r.h.s. of eq.(4.24) and (4.21). This gives

$$\begin{aligned}\sum_{j=1}^{n}\epsilon_j\delta_{ij}\Big(\phi_j,\frac{\delta(r)}{2\pi r}\;\delta(z-z')\Big) &= \sum_{j=1}^{n}\epsilon_j\;\Big(G_{ij},\frac{\rho_j}{\varepsilon_0\epsilon_j}\Big)\;, \\ \longrightarrow\quad \phi_i(r,z) &= \frac{1}{\varepsilon_0\epsilon_i}\sum_{j=1}^{n}\Big(G_{ij}(r,z;r',z'),\rho_j(r',z')\Big)\;.\end{aligned} \tag{4.32}$$

The definition of the scalar product, eq.(4.28), must be adhered to when the eigenfunction expansions are derived.

Now the definition introduced above is specialized to the case of two layers:

$$\langle A, B\rangle = \langle B, A\rangle := 2\pi \int_0^\infty dr\ r\Big[\epsilon_1 \int_q^0 dz\ A_1 B_1 + \epsilon_2 \int_0^p dz\ A_2 B_2\Big]\ . \tag{4.33}$$

And the corresponding definitions according to the reduced differential equation (4.10) are:

$$\begin{aligned}(a,b) = (b,a) \quad &= \quad (a_1,b_1) \ + \ (a_2,b_2) \ := \\ &:= \ \int_q^0 dz\ a_1 b_1 + \int_0^p dz\ a_2 b_2\ ; \\ \langle a,b\rangle = \langle b,a\rangle \quad &:= \ \epsilon_1 \int_q^0 dz\ a_1 b_1 + \epsilon_2 \int_0^p dz\ a_2 b_2\ .\end{aligned} \tag{4.34}$$

The potential $\phi_2(\omega, r, z)$ can be given, according to eq.(4.32) and (4.3):

$$\phi_2(\omega, r, z) = \frac{1}{\varepsilon_0 \epsilon_2}\Big(G_{21}(r, z; r', z'), \rho_1(\omega, r', z')\Big)\ . \tag{4.35}$$

4.1.2 Eigenfunction Expansion

Eigenfunctions

Each eigenfunction to the operator $\hat{L}_z$ consists of two pieces, each representing a particular solution in the appropriate layer.

$$Z(z,\lambda) = \begin{cases} Z_1(z,\lambda) & : \quad q < z < 0\ ; \\ Z_2(z,\lambda) & : \quad 0 < z < p\ . \end{cases} \tag{4.36}$$

An eigenfunction fulfils the following equation:

$$\hat{L}_z Z(\lambda) = -(\rho^2 + \lambda^2)\ Z(\lambda)\ . \tag{4.37}$$

For the eigenfunction expansion of the Green's function only eigenfunctions $Z(z,\lambda) \in \Omega_2^z$ must be taken into consideration.

Orthogonality

The new definition of the scalar product in (4.34) ensures the orthogonality of eigenfunctions $Z(\lambda)$ to the operator $\hat{L}_z$. Replacing the functions a and b in the following identity

$$\langle a, \hat{L}_z b\rangle = \langle b, \hat{L}_z a\rangle\ ; \quad a, b \in \Omega_2^z\ ,$$

by two eigenfunctions $Z(\lambda_k)$ and $Z(\lambda_l)$ with corresponding eigenvalues $-(\rho^2+\lambda_k^2)$ and $-(\rho^2+\lambda_l^2)$ yields according to eq.(4.37):

$$(\lambda_k^2-\lambda_l^2)\ \langle Z(\lambda_k), Z(\lambda_l)\rangle = 0\ .$$

The above equation is satisfied if either the first or the second factor vanishes. Thus for distinct eigenvalues λ_k and λ_l the following orthogonality relation can be found:

$$\langle Z(\lambda_k), Z(\lambda_l)\rangle = 0\ , \qquad \text{for } k\neq l\ . \tag{4.38}$$

The case $k=l$, which leads to the norm of $Z(\lambda_k)$ is considered separately in the paragraph after the next one.

Choice of an Appropriate Set of Eigenfunctions

A solution represented as

$$Z(z,\lambda) = \begin{cases} Z_1 = \frac{\sin[\lambda(z-q)]}{\sin\lambda q} & : \quad q<z<0\ ; \\ Z_2 = \frac{\sin[\lambda(z-p)]}{\sin\lambda p} & : \quad 0<z<p\ . \end{cases} \tag{4.39}$$

fulfils the differential equation (4.37), the boundary conditions (4.4) and the continuity condition (4.6). The remaining continuity condition (4.7)

$$\epsilon_1 \frac{\partial Z_1(\lambda)}{\partial z}\Big|_{z=0} = \epsilon_2 \frac{\partial Z_2(\lambda)}{\partial z}\Big|_{z=0}$$

leads to the following characteristic equation, which determines a discrete set of eigenvalues λ_n:

$$\epsilon_1 \sin\lambda_n p\ \cos\lambda_n q - \epsilon_2 \sin\lambda_n q\ \cos\lambda_n p = 0\ . \tag{4.40}$$

In the case under consideration, namely a gas gap and a weakly conducting dielectric layer, the values of the complex relative dielectric constants are

$$\epsilon_1 = 1\ , \qquad \epsilon_2 = \varepsilon + \frac{i\sigma}{\omega\varepsilon_0}\ .$$

The corresponding discrete set of eigenfunctions is:

$$Z(z,\lambda_n) = \begin{cases} Z_1 = \frac{\sin[\lambda_n(z-q)]}{\sin\lambda_n q} & : \quad q<z<0\ ; \\ Z_2 = \frac{\sin[\lambda_n(z-p)]}{\sin\lambda_n p} & : \quad 0<z<p\ . \end{cases} \tag{4.41}$$

Computing the Norm of the Eigenfunctions

An expression for the norm $\langle Z(\lambda), Z(\lambda)\rangle$ of an eigenfunction $Z(z,\lambda)$ is found in the following way: Two eigenfunctions, $Z(z,\lambda)$ and $\tilde{Z}(z,\tilde{\lambda})$, fulfil in layer 1 the following equations:

$$\begin{aligned} \frac{\partial^2 Z_1}{\partial z^2} &= -\lambda^2 Z_1 \ , \\ \frac{\partial^2 \tilde{Z}_1}{\partial z^2} &= -\tilde{\lambda}^2 \tilde{Z}_1 \ . \end{aligned}$$

Multiplying the first equation with $\tilde{Z}$ and the second one with Z, subtracting and integrating over z from $z = q$ to $z = 0$ gives:

$$\int_q^0 \left[\tilde{Z}_1 \frac{\partial^2 Z_1}{\partial z^2} - Z_1 \frac{\partial^2 \tilde{Z}_1}{\partial z^2}\right] dz = (\tilde{\lambda}^2 - \lambda^2) \int_q^0 Z_1 \tilde{Z}_1 \ dz \ .$$

Integrating by parts and inserting the boundary conditions (4.4) gives:

$$\frac{\left[\tilde{Z}_1 \frac{\partial}{\partial z} Z_1 - Z_1 \frac{\partial}{\partial z} \tilde{Z}_1\right]\Big|_{z=0}}{\tilde{\lambda}^2 - \lambda^2} = \int_q^0 Z_1 \tilde{Z}_1 \ dz \ .$$

When the eigenfunction $\tilde{Z}_1$ is made to tend towards the eigenfunction Z_1, then the eigenvalue $\tilde{\lambda}$ approaches the eigenvalue λ; so the ratio on the l.h.s of the last equation becomes indeterminate. Calculating the limit according to de l'Hospital's rule gives:

$$\begin{aligned} \int_q^0 Z_1^2(z,\lambda) \ dz &= \lim_{\tilde{\lambda}\to\lambda} \frac{\left[\tilde{Z}_1 \frac{\partial}{\partial z} Z_1 - Z_1 \frac{\partial}{\partial z} \tilde{Z}_1\right]\Big|_{z=0}}{\tilde{\lambda}^2 - \lambda^2} = \\ &= \frac{1}{2\lambda}\left[\frac{\partial}{\partial \lambda} Z_1\Big|_{z=0} \Big(\frac{\partial}{\partial z} Z_1\Big)\Big|_{z=0} - Z_1\Big|_{z=0} \frac{\partial}{\partial \lambda}\Big(\frac{\partial}{\partial z} Z_1\Big)\Big|_{z=0}\right] \ . \quad (4.42) \end{aligned}$$

An analogous integral over Z_2 must be extended from $z = 0$ to $z = p$. According to the definition (4.34) the norm is

$$\begin{aligned} \langle Z(\lambda), Z(\lambda)\rangle &= \frac{1}{2\lambda}\Bigg\{\epsilon_1\left[\frac{\partial}{\partial \lambda} Z_1\Big|_{z=0} \Big(\frac{\partial}{\partial z} Z_1\Big)\Big|_{z=0} - Z_1\Big|_{z=0} \ \frac{\partial}{\partial \lambda}\Big(\frac{\partial}{\partial z} Z_1\Big)\Big|_{z=0}\right] - \\ &\quad -\epsilon_2\left[\frac{\partial}{\partial \lambda} Z_2\Big|_{z=0} \Big(\frac{\partial}{\partial z} Z_2\Big)\Big|_{z=0} - Z_2\Big|_{z=0} \ \frac{\partial}{\partial \lambda}\Big(\frac{\partial}{\partial z} Z_2\Big)\Big|_{z=0}\right]\Bigg\} \ . \end{aligned} \quad (4.43)$$

With the help of

$$Z_i\Big|_{z=0} = -1; \qquad \frac{\partial}{\partial \lambda} Z_i\Big|_{z=0} = 0$$

we get from the general form (4.43) the following expression for the norm of an eigenfunction.

$$\begin{aligned}\langle Z(\lambda_n), Z(\lambda_n)\rangle &= -\frac{1}{2\lambda_n}\Big[\epsilon_1\,\frac{\partial}{\partial\lambda_n}\Big(\frac{\partial}{\partial z}Z_1\Big)\Big|_{z=0} - \epsilon_2\,\frac{\partial}{\partial\lambda_n}\Big(\frac{\partial}{\partial z}Z_2\Big)\Big|_{z=0}\Big] = \\ &= \frac{1}{2}\Big[\epsilon_1\Big(\frac{q}{\sin^2\lambda_n q} - \frac{\cot\lambda_n q}{\lambda_n}\Big) - \epsilon_2\Big(\frac{p}{\sin^2\lambda_n p} - \frac{\cot\lambda_n p}{\lambda_n}\Big)\Big]\ . \quad (4.44)\end{aligned}$$

The Green's Function

Because of the orthogonality relation (4.38) the eigenfunction expansion of the Green's function g_{ij} is given in the following way:

$$g_{ij}(z;z') = \sum_{n=1}^{\infty} \frac{Z_i(z,\lambda_n)Z_j(z',\lambda_n)}{\langle Z(\lambda_n), Z(\lambda_n)\rangle\ (\rho^2+\lambda_n^2)}\ . \quad (4.45)$$

The corresponding expression for the Green's function G_{ij} can be found by inserting the above equation (4.45) into eq.(4.9):

$$G_{ij}(r,z;z') = \frac{1}{2\pi}\sum_{n=1}^{\infty}\left[\frac{Z_i(z,\lambda_n)Z_j(z',\lambda_n)}{\langle Z(\lambda_n), Z(\lambda_n)\rangle}\int_0^{\infty} d\rho\ \frac{\rho J_0(\rho r)}{\rho^2+\lambda_n^2}\right]\ , \quad (4.46)$$

where the integral can be done to give:

$$\int_0^{\infty} d\rho\ \frac{\rho J_0(\rho r)}{\rho^2+\lambda_n^2} = K_0(\lambda_n r)\ . \quad (4.47)$$

The Green's function G_{21}, is needed for calculating the current on the plate bounding layer 2, which is induced by a point charge moving in layer 1. By inserting (4.41) and (4.44) into eq.(4.46) we get (with eq.(4.47))

$$G_{21}(r,z;z') = \frac{1}{\pi}\sum_{n=1}^{\infty}\Big[\frac{\sin[\lambda_n(z-p)]\sin[\lambda_n(z'-q)]}{N_n}\ K_0(\lambda_n r)\Big]\ , \quad (4.48)$$

with the denominator N_n given by

$$N_n(\omega) := \sin\lambda_n q\ \sin\lambda_n p\ \Big[\epsilon_1\Big(\frac{q}{\sin^2\lambda_n q} - \frac{\cot\lambda_n q}{\lambda_n}\Big) - \epsilon_2\Big(\frac{p}{\sin^2\lambda_n p} - \frac{\cot\lambda_n p}{\lambda_n}\Big)\Big]\ . \quad (4.49)$$

The scalar potential $\Phi_2(\omega,r,z)$ is found by folding the Green's function (4.46) with the charge distribution ρ_1 of (4.3), according to eq.(4.35).

$$\Phi_2(\omega,r,z) = \frac{Q}{2\pi\varepsilon_0\epsilon_2 v}\sum_{n=1}^{\infty}\Big[\frac{Z_2(z,\lambda_n)\Big(Z_1(z',\lambda_n), e^{i\frac{\omega}{v}(z'-q)}\Theta(z'-q)\Theta(-z')\Big)}{\langle Z(\lambda_n), Z(\lambda_n)\rangle}\ \times$$

$$\times\ K_0(\lambda_n r)\ \underbrace{\int_0^\infty dr''\ r''\frac{\delta(r'')}{r''}}_{=\ 1}\Big]\ , \tag{4.50}$$

where the scalar product $\Big(Z_1(z',\lambda_n), e^{i\frac{\omega}{v}(z'-q)}\Theta(z'-q)\Theta(-z')\Big)$ must be calculated according to the definition (4.34).

$$\begin{aligned}\Big(Z_1(z',\lambda_n), e^{i\frac{\omega}{v}(z'-q)}\Theta(z'-q)\Theta(-z')\Big) &= \int_q^0 dz'\ Z_1(z',\lambda_n)\ e^{i\frac{\omega}{v}(z'-q)} = \\ &= -\frac{1}{2}\frac{1}{\sin\lambda_n q}\Big[\frac{e^{i(\lambda_n-\frac{\omega}{v})q}-1}{\lambda_n-\frac{\omega}{v}}+\frac{e^{-i(\lambda_n+\frac{\omega}{v})q}-1}{\lambda_n+\frac{\omega}{v}}\Big]\ .\end{aligned} \tag{4.51}$$

Inserting (4.51) and (4.44) into (4.48) yields the final result for the frequency dependent potential.

$$\Phi_2(\omega,r,z) = -\frac{Q}{2\pi\varepsilon_0\epsilon_2 v}\sum_{n=1}^{\infty}\left\{\frac{\sin[\lambda_n(z-p)]}{N_n}\Big[\frac{e^{i(\lambda_n-\frac{\omega}{v})q}-1}{\lambda_n-\frac{\omega}{v}}+\frac{e^{-i(\lambda_n+\frac{\omega}{v})q}-1}{\lambda_n+\frac{\omega}{v}}\Big]K_0(\lambda_n r)\right\}\ . \tag{4.52}$$

The charge density on the anode is proportional to the normal derivative of the potential.

$$\begin{aligned}\eta(\omega,r) &= \varepsilon_0\epsilon_2\frac{\partial\phi_2(\omega,r,z)}{\partial z}\Big|_{z=p} = \\ &= -\frac{Q}{2\pi v}\sum_{n=1}^{\infty}\left\{\frac{\lambda_n}{N_n}\Big[\frac{e^{i(\lambda_n-\frac{\omega}{v})q}-1}{\lambda_n-\frac{\omega}{v}}+\frac{e^{-i(\lambda_n+\frac{\omega}{v})q}-1}{\lambda_n+\frac{\omega}{v}}\Big]K_0(\lambda_n r)\right\}\ .\end{aligned} \tag{4.53}$$

Its Fourier transformation gives the corresponding time depending charge density:

$$\eta(t,r) = \frac{1}{2\pi}\int_{-\infty}^{\infty}\eta(\omega,r)\ e^{-i\omega t}d\omega\ . \tag{4.54}$$

The integral over ω can be computed with the help of residues. Only the poles in ω of the square bracket in eq.(4.53) are taken into account:

$$\omega = \omega_n^{\pm} := \pm\lambda_n v\ . \tag{4.55}$$

In [4] these poles have been called the *motion poles*. There it was shown that the other poles gives only terms proportional to $\beta = v/c$, so that they can be neglected. Special care must be taken in the choice of the half plane in the complex ω-plane, where the original path of intgration is closed by a semi-circle. It turns out that the first term in the square bracket tends to zero in the upper half plane while the second vanishes in

the lower half plane as $|\omega|$ tends to infinity. The evaluation of the residues of the poles given in (4.55) yields the following series representation of the charge distribution, when the values $\epsilon_1 = 1$ and $\epsilon_2 = \varepsilon + \frac{i\sigma}{\omega\varepsilon_0}$ for the special case under consideration are inserted:

$$\eta(t,r) = -\frac{iQ}{2\pi}\sum_{n=1}^{\infty}\left[\lambda_n^+\frac{e^{-i\lambda_n^+ vt}}{N_n^+}K_0(\lambda_n^+ r) + \lambda_n^-\frac{e^{i\lambda_n^- vt}}{N_n^-}K_0(\lambda_n^- r)\right] . \tag{4.56}$$

$\lambda_n^\pm$ are the n-th roots of the transcendental equation (4.40), when ω is replaced by the pole $\omega_n^\pm$:

$$\sin\lambda_n p\ \cos\lambda_n q - (\varepsilon \pm \frac{i\sigma}{\lambda_n v\varepsilon_0})\sin\lambda_n q\ \cos\lambda_n p = 0\ ; \tag{4.57}$$

$N_n^\pm$ is defined by:

$$N_n^\pm = N_n(\omega_n^\pm)\ . \tag{4.58}$$

It turns out that it is advantageous not to use the expression given in eq.(4.49) for numerical calculations but an equivalent one obtained from the integral representation:

$$N_n^\pm = i\,\frac{\partial}{\partial\lambda_n}\left[\cos\lambda_n p\ \sin\lambda_n q - \frac{1}{\varepsilon \pm \frac{i\sigma}{\lambda_n v\varepsilon_0}}\ \sin\lambda_n p\ \cos\lambda_n q\right] . \tag{4.59}$$

The reason is that both terms in the round bracket of eq.(4.49) become very large for small values for λ_n. Thus their difference causes a significant round-off error.

Total Charge and Current

The total charge induced on the anode is given by:

$$q_T(t) = 2\pi\int_0^\infty dr\ r\ \eta(t,r) = -iQ\sum_{n=1}^{\infty}\left[\frac{1}{\lambda_n^+}\frac{e^{-i\lambda_n^+ vt}}{N_n^+} - \frac{1}{\lambda_n^-}\frac{e^{i\lambda_n^- vt}}{N_n^-}\right] . \tag{4.60}$$

And finally the total current is found by time derivation.

$$I_T(t) = \frac{dq_T(t)}{dt} = -Qv\sum_{n=1}^{\infty}\left[\frac{e^{-i\lambda_n^+ vt}}{N_n^+} + \frac{e^{i\lambda_n^- vt}}{N_n^-}\right] . \tag{4.61}$$

Charge and Current Induced on a Strip

Spatial integration of the charge density (4.56) over a strip extending to infinity in both directions of the y-axis and of width w in the x-direction yields an approximate

expression for the charge induced on an anode strip.

$$\begin{aligned} q_S(t) &= \int_{x_0-w/2}^{x_0+w/2} dx \int_{-\infty}^{\infty} dy\ \eta(t,r) = \\ &= -\frac{iQ}{2}\sum_{n=1}^{\infty}\frac{1}{\lambda_n^+}\frac{e^{-i\lambda_n^+ vt}}{N_n^+}\ \begin{cases} 2-e^{\lambda_n(x_0-w/2)}-e^{-\lambda_n(x_0+w/2)} & : \quad x_0 \le w/2; \\ e^{-\lambda_n(x_0-w/2)}-e^{-\lambda_n(x_0+w/2)} & : \quad x_0 \ge w/2. \end{cases} \end{aligned} \tag{4.62}$$

The above expression splits into two parts depending whether the trajectory of the moving charge lies directly below the strip or outside. The corresponding current is found by derivation w.r.t. time.

$$\begin{aligned} I_S(t) &= \frac{dq_S(t)}{dt} = \\ &= -\frac{Qv}{2}\sum_{n=1}^{\infty}\frac{e^{-i\lambda_n^+ vt}}{N_n^+}\ \begin{cases} 2-e^{\lambda_n(x_0-w/2)}-e^{-\lambda_n(x_0+w/2)} & : \quad x_0 \le w/2; \\ e^{-\lambda_n(x_0-w/2)}-e^{-\lambda_n(x_0+w/2)} & : \quad x_0 \ge w/2. \end{cases} \end{aligned} \tag{4.63}$$

4.1.3 Integral Representation

The calculation of the integral representation in the case of a weakly conducting dielectric layer starts with the expression for the Green's function G_{21}. It is derived in an analogous way as it will be done in the next paragraph, so we may present the result omitting the details:

$$G_{21}(r,z;r'=0,z') = \frac{\epsilon}{2\pi}\int_0^{\infty} d\lambda\ J_0(\lambda r)\ \frac{\sinh[\lambda(p-z)]\sinh[\lambda(q-z')]}{\epsilon\cosh\lambda p\sinh\lambda q-\cosh\lambda q\sinh\lambda p}\ , \tag{4.64}$$

with $\epsilon = \varepsilon + \frac{i\sigma}{\omega\varepsilon_0}$. The potential ϕ_2 is found by folding the Green's function G_{21} and the frequency dependent charge distribution ρ_1, given in eq.(4.3), according to (4.35).

$$\begin{aligned} \phi_2(\omega,r,z) &= \frac{1}{\varepsilon_0\epsilon}\Big(G_{21}(r,z;r`,z'),\rho_1(\omega,r',z')\Big) = \\ &= -\frac{iQ}{2\pi\varepsilon_0 v}\int_0^{\infty} d\lambda\ J_0(\lambda r)\ \frac{\sinh[\lambda(p-z)]\Big[\frac{e^{-(\lambda-i\frac{\omega}{v})q}-1}{i\lambda-\frac{\omega}{v}}+\frac{e^{(\lambda-i\frac{\omega}{v})q}-1}{i\lambda+\frac{\omega}{v}}\Big]}{\epsilon\cosh\lambda p\sinh\lambda q-\cosh\lambda q\sinh\lambda p}\ . \end{aligned} \tag{4.65}$$

The spatial integral can be done if it is interchanged with the λ-integration. The ferquency-dependent surface charge density on the anode is:

$$\begin{aligned}\eta(\omega,r) &= \varepsilon_0\epsilon\frac{\partial\phi_2(\omega,r,z)}{\partial z}\Big|_{z=0} = \\ &= -\frac{i\epsilon Q}{2\pi v}\int_0^\infty d\lambda\ J_0(\lambda r)\ \frac{\lambda\left[\frac{e^{-(\lambda-i\frac{\omega}{v})q}-1}{i\lambda-\frac{\omega}{v}}+\frac{e^{(\lambda-i\frac{\omega}{v})q}-1}{i\lambda+\frac{\omega}{v}}\right]}{\epsilon\cosh\lambda p\sinh\lambda q-\cosh\lambda q\sinh\lambda p}\ . \qquad (4.66)\end{aligned}$$

Fourier transformation yields the time-dependent surface charge density.

$$\begin{aligned}\eta(t,r) &= \frac{1}{2\pi}\int_{-\infty}^{+\infty}\eta(\omega,r)e^{-i\omega t}\ d\omega = \\ &= \frac{Q}{2\pi}\int_0^\infty d\lambda\ \lambda J_0(\lambda r)\left[\frac{e^{\lambda vt}}{\tilde{N}_n^+}-\frac{e^{-\lambda vt}}{\tilde{N}_n^-}\right]\ , \qquad (4.67)\end{aligned}$$

where the denominator $N_n^\pm$ stands for:

$$N_n^\pm := \cosh\lambda p\sinh\lambda q-\frac{1}{\varepsilon\pm\frac{\sigma}{\lambda v\varepsilon_0}}\cosh\lambda q\sinh\lambda p\ . \qquad (4.68)$$

As it is described in Chapter 3, the Bessel function $J_0(\lambda r)$ may be replaced by $\frac{1}{2}H_0^{(1)}$ if the integration over λ runs from $-\infty$ to ∞. Now the integral can be evaluated by Cauchy's residue theorem. The result so obtained is equivalent to eq.(4.56).

$$\eta(t,r)=-\frac{i\pi Q}{4}\sum_{n=1}^\infty\left\{\tilde{\lambda}_n^+\frac{e^{\tilde{\lambda}_n^+vt}}{[\frac{\partial}{\partial\lambda}\tilde{N}_n^+]_{\lambda=\tilde{\lambda}_n^+}}\ H_0^{(1)}(\tilde{\lambda}_n^+r)-\tilde{\lambda}_n^-\frac{e^{-\tilde{\lambda}_n^-vt}}{[\frac{\partial}{\partial\lambda}\tilde{N}_n^-]_{\lambda=\tilde{\lambda}_n^-}}\ H_0^{(1)}(\tilde{\lambda}_n^-r)\right\}\ . \qquad (4.69)$$

$\tilde{\lambda}_n^\pm$ is the n-th zero of $\tilde{N}_n^\pm$ in the upper half-plane of the complex λ-plane.

4.2 Quasi-Static Approximation for an Isolating Dielectric Layer

4.2.1 Eigenfunction Expansion

In the simpler case of an isolating layer the potential must be a solution of the differential equation

$$\Delta\phi_i(r,z;z')=-\frac{\rho_i(r,z;z')}{\varepsilon_0\varepsilon_i}\ , \qquad (4.70)$$

as it has been elaborated in sect.2.1. If the point charge distribution

$$\rho(r,z;z') = \begin{cases} \rho_1(r,z;z') = Q\ \frac{\delta(r)}{2\pi r}\ \delta(z-z')\ \Theta(z-q)\ \Theta(-z) & : \quad q<z<0 \\ \rho_2(r,z;z') = 0 & : \quad 0<z<p \end{cases} \tag{4.71}$$

is inserted into the general form of the solution (4.35), it follows that, in this case, the solution is proportional to the Green's function G_{21}, given in eq.(4.48).

$$\begin{aligned} \Phi_2(r,z;z') &= \frac{Q}{\varepsilon_0\varepsilon_2}\ G_{21}(r,z;z') = \\ &= \frac{Q}{\pi\varepsilon_0\varepsilon_2}\sum_{n=1}^{\infty}\Big[\frac{\sin[\lambda_n(z-p)]\sin[\lambda_n(z'-q)]}{N_n}\ K_0(\lambda_n r)\Big]\ . \end{aligned} \tag{4.72}$$

The complex dielectric constants ϵ_i in the denominator N_n and the characteristic equation (4.40) may be replaced by the real one, ε_i. The charge density on the anode is proportional to the normal derivative of the potential.

$$\eta(r;z') = \varepsilon_0\varepsilon_2\ \frac{\partial\Phi_2}{\partial z}\Big|_{z=p} = \frac{Q}{\pi}\sum_{n=1}^{\infty}\Big[\frac{\lambda_n\ \sin[\lambda_n(z'-q)]}{N_n}\ K_0(\lambda_n r)\Big]\ . \tag{4.73}$$

In the following discussion the general dielectric constants are replaced by the special values for the case under consideration, $\varepsilon_1 = 1$ and $\varepsilon_2 = \varepsilon$.

Total Charge and Current

Integrating the surface charge density over the whole plate gives the total charge:

$$q_T(z') = 2\pi\int_0^{\infty} dr\ r\ \eta(r;z') = 2Q\sum_{n=1}^{\infty}\frac{\sin[\lambda_n(z'-q)]}{\lambda_n N_n}\ . \tag{4.74}$$

Finally, the current flowing through the whole electrode is obtained by inserting $z' = z_0 + vt$ and deriving the total charge w.r.t. time:

$$I_T(z') = \frac{dq_T(z')}{dt} = v\ \frac{dq_T(z')}{dz'} = 2Qv\sum_{n=1}^{\infty}\ \frac{\cos[\lambda_n(z'-q)]}{N_n}\ . \tag{4.75}$$

Charge and Current Induced on a Strip

The charge flowing through a strip of width w having a transversal distance x_0 from the trajectory of Q (cf. Fig.4.1) is given by :

$$q_S(z') = \int_{x_0-w/2}^{x_0+w/2} dx \int_{-\infty}^{\infty} dy\ \eta(r;z') =$$

$$= \varepsilon Q \sum_{n=1}^{\infty} \frac{\sin[\lambda_n(z'-q)]}{\lambda_n N_n} \begin{cases} 2 - e^{\lambda_n(x_0-w/2)} - e^{-\lambda_n(x_0+w/2)} & : \quad x_0 \leq w/2; \\ e^{-\lambda_n(x_0-w/2)} - e^{-\lambda_n(x_0+w/2)} & : \quad x_0 \geq w/2. \end{cases} \tag{4.76}$$

And the corresponding current is:

$$\begin{aligned} I_S(z') &= \frac{dq_S(z')}{dt} = v\,\frac{dq_S(z')}{dz'} = \\ &= \varepsilon Q v \sum_{n=1}^{\infty} \frac{\cos[\lambda_n(z'-q)]}{N_n} \begin{cases} 2 - e^{\lambda_n(x_0-w/2)} - e^{-\lambda_n(x_0+w/2)} & : \quad x_0 \leq w/2; \\ e^{-\lambda_n(x_0-w/2)} - e^{-\lambda_n(x_0+w/2)} & : \quad x_0 \geq w/2. \end{cases} \end{aligned} \tag{4.77}$$

4.2.2 Integral Representation

To find the integral representation we follow the same procedure as presented in Chapter 3 for the simple case of an empty plane condensor. In order to receive a closed expression for the total charge and current flowing through the whole plate it turns out to be convenient to insert the following new ansatz for the Green's function

$$G_{ij}(x,y,z;z') = \frac{1}{2\pi} \int_{-\infty}^{+\infty} dk_x\, dk_y e^{i(k_x x + k_y y)} g_{ij}(\kappa, z; z') \;, \tag{4.78}$$

with

$$\kappa^2 = k_x^2 + k_y^2 \;, \tag{4.79}$$

into the differential equation (4.8). This yields the identical differential equation for the reduced Green's function g_{ij} as given in (4.10):

$$\left(\frac{\partial^2}{\partial z^2} - \kappa^2\right) g_{ij}(z;z') = -\delta_{ij}\delta(z-z') \;, \tag{4.80}$$

if the integral representation of the δ-distribution is used:

$$\delta(x)\delta(y) = \frac{1}{2\pi} \int_{-\infty}^{+\infty} dx \int_{-\infty}^{+\infty} dy\; e^{i(k_x x + k_y y)} \;. \tag{4.81}$$

The new funtions g_{ij} again fulfil the same boundary conditions,

$$g_{1j}\Big|_{z=q} = 0 \;, \tag{4.82}$$

$$g_{2j}\Big|_{z=p} = 0 \;, \tag{4.83}$$

and the same continuity conditions as the Green's function G_{ij}.

$$g_{1j}\Big|_{z=0} = g_{2j}\Big|_{z=0} , \tag{4.84}$$

$$\varepsilon_1 \frac{\partial g_{1j}}{\partial z}\Big|_{z=0} = \varepsilon_2 \frac{\partial g_{2j}}{\partial z}\Big|_{z=0} , \tag{4.85}$$

The reduced Green's function may be assumed to have the following form:

$$g_{ii} = \frac{e^{-\kappa|z-z'|}}{\kappa} + \bar{g}_{ii} , \tag{4.86}$$

$$g_{12} = e \cdot \sinh[\kappa(z-q)] , \tag{4.87}$$

$$g_{21} = f \cdot \sinh[\kappa(z-p)] , \tag{4.88}$$

$$\bar{g}_{11} = a \cdot e^{\kappa z} + b \cdot e^{-\kappa z} , \tag{4.89}$$

$$\bar{g}_{22} = c \cdot e^{\kappa z} + d \cdot e^{-\kappa z} . \tag{4.90}$$

The first term of g_{ii} satisfies the differential equation (4.80), but does not fulfil the boundary and continuity conditions (4.82) to (4.85). The functions $\bar{g}_{ii}$, g_{12} and g_{21} are solutions of the corresponding homogenous equation and ensure that the combination with g_{ii} fit the conditions (4.82) to (4.85). The coefficients a to f can be determined by solving the sytem of inhomogenous equations created by inserting the expressions (4.86) to (4.90) into the eqs.(4.82) to (4.85). The solutions can be reinserted and yield the final result for the reduced Green's function g_{ij}. Here only the functions g_{12} and g_{21} are shown.

$$g_{21} = \frac{\varepsilon_2 \sinh[\kappa(z-p)] \sinh[\kappa(z'-q)]}{\kappa[\varepsilon_1 \cosh(\kappa q)\sinh(\kappa p) - \varepsilon_2 \cosh(\kappa p)\sinh(\kappa q)]} , \tag{4.91}$$

$$g_{12} = \frac{\varepsilon_1 \sinh[\kappa(z-q)] \sinh[\kappa(z'-p)]}{\kappa[\varepsilon_1 \cosh(\kappa q)\sinh(\kappa p) - \varepsilon_2 \cosh(\kappa p)\sinh(\kappa q)]} . \tag{4.92}$$

The Green's function G_{21} is with $D = p - q$, $z_0 = z' - q$, $d = p$, $\varepsilon_1 = 1$ and $\varepsilon_2 = \varepsilon$:

$$G_{21}(x,y,z;z') = \frac{\varepsilon}{2\pi^2} \int_{-\infty}^{+\infty} dk_x \int_{-\infty}^{+\infty} dk_y \frac{1}{\kappa} \frac{\sinh[\kappa(D-z)]\sinh(\kappa z_0)\ e^{i(k_x x + k_y y)}}{(1+\varepsilon)\sinh(\kappa D) + (\varepsilon - 1)\sinh[\kappa(D-2d)]} \tag{4.93}$$

The charge density is according to (4.72):

$$\begin{aligned} \eta(x,y;z_0) &= \varepsilon_0 \varepsilon \frac{\partial G_{21}}{\partial z}\Big|_{z=D} = \\ &= -\frac{\varepsilon Q}{2\pi^2} \int_{-\infty}^{+\infty} dk_x \int_{-\infty}^{+\infty} dk_y \frac{\sinh(\kappa z_0)\ e^{i(k_x x + k_y y)}}{(\varepsilon+1)\sinh(\kappa D) + (\varepsilon-1)\sinh[\kappa(D-2d)]} \end{aligned} \tag{4.94}$$

Total Charge and Current

To get the total charge flowing through the anode the integral must be performed over the whole plane. This yields a simple expression linear in z_0.

$$q_T(z_0) = \int_{-\infty}^{+\infty} dx \int_{-\infty}^{+\infty} dy\ \eta(x,y;z_0) = -\frac{\varepsilon Q z_0}{\varepsilon(D-d)+d}\ . \tag{4.95}$$

Thus the total current proportional to the derivative of q_T w.r.t. z_0 is constant.

$$I_T(z_0) = \frac{dq(z_0)}{dt} = v\frac{dq(z_0)}{dz_0} = -\frac{\varepsilon Q v}{\varepsilon(D-d)+d}\ . \tag{4.96}$$

Charge and Current Induced on an Anode Strip

The charge induced on the anode strip is:

$$\begin{aligned} q_S(z_0) &= \int_{-\infty}^{+\infty} dy \int_{x_0-w/2}^{x_0+w/2} dx\ \eta(x,y;z_0) = \\ &= -\frac{2Q\varepsilon}{\pi}\int_0^{\infty}\frac{dk_x}{k_x}\ \frac{\sin(k_x w/2)\cos(k_x x_0)\sinh(k_x z_0)}{(\varepsilon+1)\sinh(k_x D)+(\varepsilon-1)\sinh[k_x(d-2d)]}\ . \end{aligned} \tag{4.97}$$

The expression for the current is found by derivation w.r.t. z_0, and with the substitution $k_x = \frac{\zeta}{D}$.

$$\begin{aligned} I_S(z_0) &= \frac{dq_S}{dt} = v\ \frac{dq_S}{dz_0} = \\ &= -\frac{Qv}{\pi D}\int_0^{\infty} d\zeta\ \ \sin(\zeta\frac{w}{2D})\cos(\zeta\frac{x_0}{D})\frac{\cosh(\zeta\frac{z_0}{D})}{\sinh\zeta}\ f(\varepsilon,\frac{d}{D},\zeta) \end{aligned} \tag{4.98}$$

with

$$f(\varepsilon,\frac{d}{D},\zeta) = \frac{2\varepsilon}{(\varepsilon+1)+(\varepsilon-1)\frac{\sinh[\zeta(1-2d/D)]}{\sinh\zeta}} = \frac{2\varepsilon}{\varepsilon+1}\sum_{n=0}^{\infty}\left[\frac{\varepsilon-1}{\varepsilon+1}\right]^n\left[\frac{\sinh[\zeta(1-2d/D)]}{\sinh\zeta}\right]^n . \tag{4.99}$$

The factor $f(\varepsilon, d/D, \zeta)$ accounts for the dielectric layer. If the relative dielectric layer $\varepsilon = 1$ then $f(\varepsilon, d/D, \zeta) = 1$. In that case the integral (4.98) can be evaluated analytically to give:

$$\frac{I_S D}{Qv} = \frac{1}{2}\ \frac{\sinh[\frac{\pi(x_0-w/2)}{D}]}{\cos[\frac{\pi z_0}{D}]+\cosh[\frac{\pi(x_0-w/2)}{D}]} - \frac{1}{2}\ \frac{\sinh[\frac{\pi(x_0+w/2)}{D}]}{\cos[\frac{\pi z_0}{D}]+\cosh[\frac{\pi(x_0+w/2)}{D}]} \tag{4.100}$$

Of course this coincides with the result (3.15) of Chapter 3. If the factor f is not constant then the integral in (4.98) must be evaluated by more elaborate methods described in the next paragraph.

Evaluation of the Current Integral

The factor $f(\varepsilon, d/D, \zeta)$ is constant if either $\varepsilon = 1$ or $d = D/2$. In all other cases the integral (4.98) must be evaluated numerically or by series expansion which are again evaluated numerically. All analytical (symbolic) and numeric computations are done in *Mathematica*, [17]. The integral (4.98) is an infinite integral with an oscillating integrand. So in some cases the routine **NIntegrate**[] of *Mathematica* fails, even if the Option **Method** $\rightarrow$ **Oscillatory** is used. It was found more expedient to insert the series given in formula (4.99) into eq.(4.98) and to integrate term by term. The expression for the current (4.98) is rewritten as:

$$\begin{aligned} \frac{I_S D}{Qv} &= \mathcal{J}_{00}(D, x_0, z_0) + \frac{\varepsilon - 1}{\varepsilon + 1}\, \mathcal{J}_{00}(D, x_0, z_0) + \\ &+ \sum_{n=1}^{\infty} \left[\frac{\varepsilon - 1}{\varepsilon + 1}\right]^n \left[\mathcal{J}_n\Big(\frac{x_0 - w/2}{D}, \frac{z_0}{D}, 1 - \frac{2d}{D}\Big) - \mathcal{J}_n\Big(\frac{x_0 + w/2}{D}, \frac{z_0}{D}, 1 - \frac{2d}{D}\Big)\right] . \end{aligned} \tag{4.101}$$

The first term in the first line gives the contribution for a point charge in an empty condensor. The second term together with the sum in the second line gives a relatively small correction due to the dielectric layer. The integrals

$$\mathcal{J}_n(a, b, c) := \frac{1}{2\pi} \int_0^{\infty} d\zeta \frac{\sin(\zeta a) \cosh(\zeta b) \sinh^n(\zeta c)}{\sinh^{n+1} \zeta} , \quad 0 \le b < 1;\ 0 \le c < 1 , \tag{4.102}$$

can be done analytically in *Mathematica*. This is described and results are listed in the appendix A. In the cases for which evaluations were done this was performed in the following way: The analytic expressions were used up to $n = 6$ as **NIntegrate**[] had still troubles to evaluate them. These gave sufficient accuracy as could be checked by summing 6 further terms in which the integrals were done by **NIntegrate**; for $n > 6$ this command performed without problems. The numeric integrations run into severe trouble for $a = 0$; the obvious value 0 must be inserted by a branching command.

Chapter 5

The Method of Images

The method of images is another technique to solve the electrostatic two-layer problem investigated in the preceding chapters. In addition to the series and integral representation described in Chapter 4 it offers a third way to calculate the current flowing through an anode strip. The advantage of this new representation given by a triple sum is the simplicity of the summand and the avoidance of convergence problems in the vicinity of the edge of the strip.

5.1 The Basic Idea

The method of images is used in electrostatic boundary value problems dealing with conducting surfaces or boundaries along which the potential is held constant. These boundaries are either closed finite simply-connected surfaces or extend towards infinity such that the whole space is separated into two complementary subspaces. Charges, in our case point charges, are located in that part we are interested in. Under favourable circumstances the reaction fields induced by the boundaries may be expressed by fields due to image charges, whose locations, signs and values are chosen such that the total field (due to both the orignal and the image charges) fulfils all the boundary conditions. All the image charges must lie outside the subspace wherein the source charge is located.

5.2 Image Techniques for Two-Layer Problems

When the boundary is a plane surface it is even possible to treat two-layer problems by the method of images (cf.[12]). We consider a point charge Q located in a half-space 1 with relative dielectric constant ε_1; that of the complimentary half-space 2 is ε_2. It

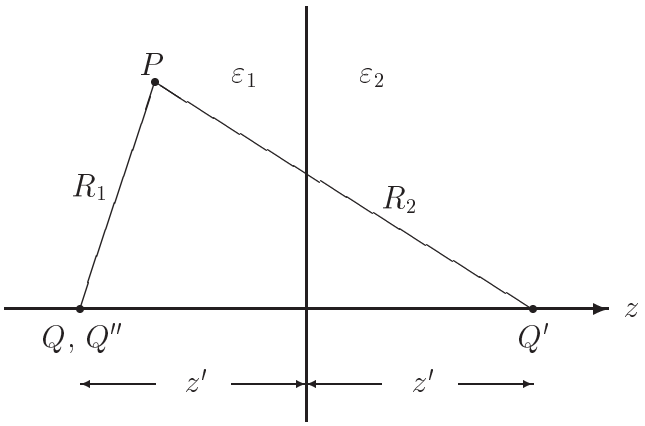

Figure 5.1: *The method of images for a two-layer problem.*

can be shown that the potential in 1 may be expressed by the potentials of the original charge Q and that of an image charge Q', whose position is found by reflection at the interface separating 1 from 2 (see Fig.5.1). So the total potential in that half-space is:

$$\Phi = \frac{1}{4\pi\varepsilon_0\varepsilon_1}\Big(\frac{Q}{R_1} + \frac{Q'}{R_2}\Big), \qquad z < 0 \ . \tag{5.1}$$

The potential in half-space (2) is determined by the point charge Q'' located at the same place as Q.

$$\Phi = \frac{1}{4\pi\varepsilon_0\varepsilon_2}\ \frac{Q''}{R_2}, \qquad z > 0 \ . \tag{5.2}$$

The values of the two image charges Q' and Q'' are functions of the two relative dielectric constants ε_1 and ε_2 .

$$Q' \ = \ -\underbrace{\frac{2\varepsilon_2}{\varepsilon_2 + \varepsilon_1}}_{=:\ \alpha}\ Q \ , \tag{5.3}$$

$$Q'' \ = \ -\underbrace{\frac{\varepsilon_2 - \varepsilon_1}{\varepsilon_2 + \varepsilon_1}}_{=:\ \beta}\ Q \ . \tag{5.4}$$

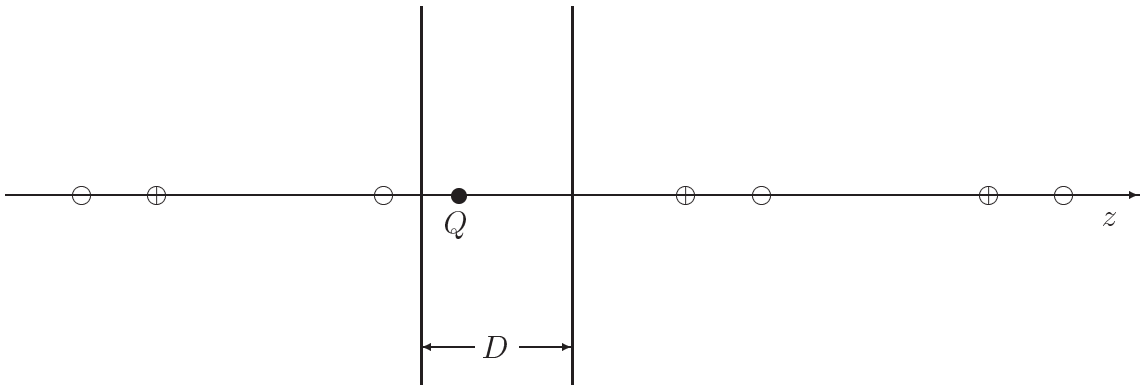

Figure 5.2: *The positions of the images ($\oplus$- and $\ominus$-branch) for an empty plane condensor.*

5.3 Point Charge in an Empty Plane Condensor

5.3.1 Computation of the Positions and the Values of the Image Charges

The source charge and the pertinent subspace lie between the two plane electrodes. All the image charges are located outside both electrodes. They are found by reflecting the oringal charge at the two electrodes; then each image is reflected at the other electrode, and so on. Thus one gets two branches of images labeled by $\oplus$ and $\ominus$, respectively; each depends on the position of the electrode at which the first reflection was done. Here the discussion is limited to the series of images located to the right of the plate at the right hand side (see Fig.5.2). Closed expressions for their positions are given by:

$$\begin{aligned} \oplus: &\quad 2bk + z &\quad k = 0, 1, 2, \dots\ , \\ \ominus: &\quad 2b(k+1) + z &\quad k = 0, 1, 2, \dots\ . \end{aligned}$$

The value of the image charges of the $\oplus$-branch is Q, that of the $\ominus$-branch $-Q$. Of course, ananlogous considerations apply to the images located to the left of the left condensor plate.

It is not reasonable to compute the total charge induced by the charge Q on the plate to the right by summing up all the partial charges induced on this plate by all the images. We consider a conducting plane located at $z = 0$ perpendicular to the z-axis (Fig.5.3). An arbitrary image charge q (at $z = z'$) and its companion $-q$ (at $z = -z'$) generate the following field at a point of the plate having distance r from the z-axis.

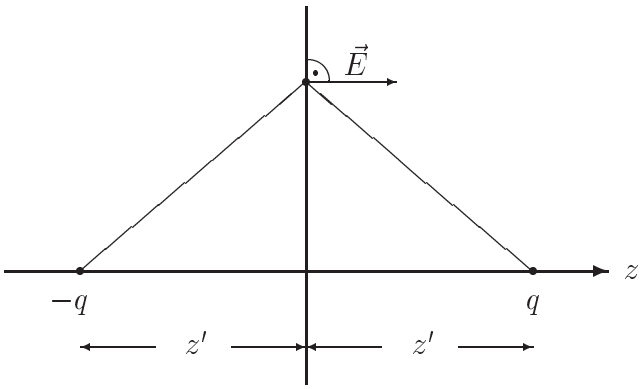

Figure 5.3: *The electric field induced on a condensor electrode by an arbitrary point charge and its image.*

$$\vec{E}(r,z') = E_z(r,z')\ \vec{e}_z = \frac{q}{2\pi\varepsilon_0}\ \frac{z'}{(r^2+z'^2)^{3/2}}\ \vec{e}_z \tag{5.5}$$

The corresponding surface charge density is proprotional to the normal ($= z$)-component of the electric field. Integrating this density over the whole plate gives:

$$\eta = \varepsilon_0 E_z = \frac{q}{2\pi}\ \frac{z'}{(r^2+z'^2)^{3/2}}\ , \quad 2\pi\int_0^\infty \eta\ r\ dr = 2\pi q\ . \tag{5.6}$$

We see that the induced total charge does not depend on the position z' of the image charges, and, if summed up, yields a wrong result. But this difficulty can be avoided: At first one computes the charge (or the current) induced on a strip as just described; thereafter the wanted total charge (or current) is found by making the width of the strip to tend to infinity.

5.3.2 Computation of the Current through a Strip of the Condensor Electrode

The same array as in Fig.5.3 is considered. The electric field or more precisely the surface charge density is integrated over a strip of infinite length in the y-direction. For this, the following infinite integral over y is evaluated:

$$\int_{-\infty}^{\infty}\eta\ dy = \frac{q}{2\pi}\int_{-\infty}^{\infty}\frac{z'}{(r^2+z'^2)^{3/2}}\ dy = \frac{q}{\pi}\ \frac{z'}{x^2+z'^2}\ , \quad \text{with} \quad r^2 = x^2+y^2\ . \tag{5.7}$$

The result is integrated over x:

$$\frac{q}{\pi}\int \frac{z'}{x^2+z'^2}\,dx = \frac{q}{\pi}\,\arctan\Big(\frac{x}{z'}\Big); \qquad \frac{q}{\pi}\,\frac{\partial}{\partial z'}\Big[\arctan\Big(\frac{x}{z'}\Big)\Big] = -\frac{q}{\pi}\,\frac{x}{x^2+z'^2}\ . \quad (5.8)$$

In order to obtain the current, the charge must be derived w.r.t. time, so w.r.t. z'. These expressions can be summed after the positions z' have been replaced with the distances from the plate at the right listed in (5.5). The two series (denoted by $S^{\oplus}$ and $S^{\ominus}$) so obtained are convergent.

$$S^{\oplus} = \sum_{k=0}^{\infty} \frac{x}{[2Dk+z]^2+x^2} = \frac{i}{4D}\Big[\psi\Big(\frac{z-ix}{2D}\Big) - \psi\Big(\frac{z+ix}{2D}\Big)\Big]\ , \quad (5.9)$$

$$S^{\ominus} = \sum_{k=0}^{\infty} \frac{x}{[2D(k+1)-z]^2+x^2} = \frac{i}{4D}\Big[\psi\Big(1+\frac{z-ix}{2D}\Big) - \psi\Big(1+\frac{z+ix}{2D}\Big)\Big]\ . \quad (5.10)$$

The function ψ on the r.h.s of the last equations is Euler's ψ-function. Particular attention must be paid to the direction of the motion of the image charges, so to the sign of the current. Let as assume the source charge $Q > 0$ and moves along the z-axis in the positive sense. Then the motion of the image charges belonging to the first branch is along the negative direction. Since their charge $-Q < 0$, the resulting current is positive. The direction of motion, the sign of the charge, so also the current are positive for the images of the second branch. Of course, analogous remarks apply for a negative source charge, a negative direction of its motion respectively. Thus the two series must be added to give the total current.

It is not surprising that the above series, in particular the sum give a closed expression for the case of an empty plane condensor:

$$\frac{Qv}{\pi}(S^{\oplus}+S^{\ominus}) = -\frac{Qv}{2D}\,\frac{\sinh(\pi x/D)}{\cos(\pi z'/D)-\cosh(\pi x/D)}\ . \quad (5.11)$$

As in (5.8) only the indefinite integral over x has been done, now the limits $x_0 + w/2$ and $x_0 - w/2$ must be inserted to yield the final result:

$$\frac{I_S D}{Qv} = \frac{1}{2}\,\frac{\sinh[\frac{\pi(x_0-w/2)}{D}]}{\cos[\frac{\pi z'}{D}]-\cosh[\frac{\pi(x_0-w/2)}{D}]} - \frac{1}{2}\,\frac{\sinh[\frac{\pi(x_0+w/2)}{D}]}{\cos[\frac{\pi z'}{D}]-\cosh[\frac{\pi(x_0+w/2)}{D}]}\ . \quad (5.12)$$

The result turns into expression (3.15) of Chapter 3 when z is replaced by $D - z_0$. This is possible if we take into account that z and z_0 denote the distance from the point charge to the anode and cathode, respectively. This is the same result as given in [7] and [8] apart for a small numerical slip correted here ($\frac{1}{2}$ in place of $\frac{1}{4}$ in front of the fractions).

As indicated above, the current induced on the whole electrode can be obtained through the limit in which the width of the strip tends to infinity.

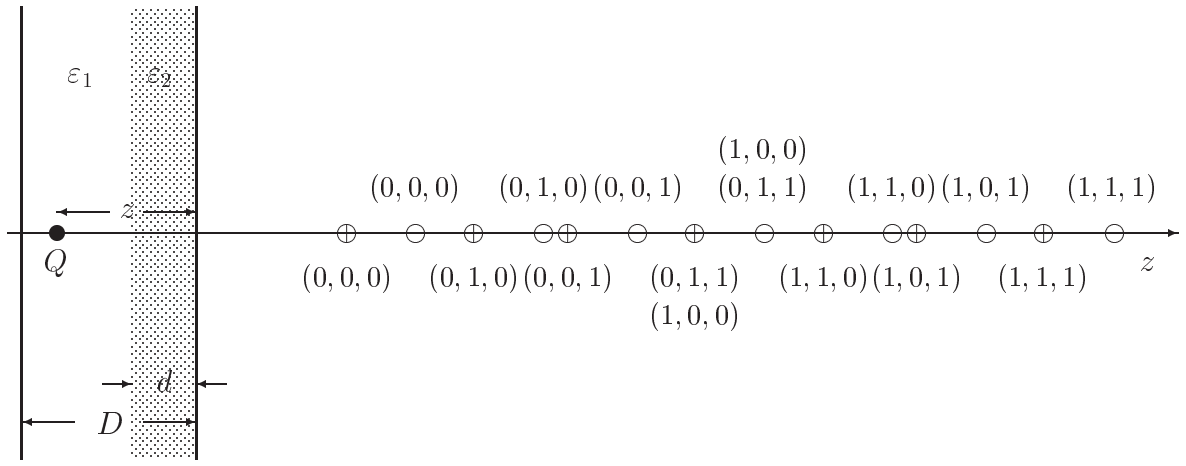

Figure 5.4: *The positions of the images ($\oplus$- and $\ominus$-branch) for a two-layer plane condensor. The images q are labeled by the triple (k,l,m), ($\oplus \ldots$ lower line, $\ominus \ldots$ upper line).*

5.4 Point Charge in a Plane Condensor with Two Layers

The method of images can be applied to a plane condensor containing two parallel isolating layers with different dielectric constants.

5.4.1 Positions and Values of the Image Charges

The subspace under consideration consists of two isolating dielectric layers (ε_1, ε_2) bounded by the two conducting plates (Fig.5.4). The detailed derivation is again limited to the images located to the right of the right hand plate of the condensor. As above we get two branches of images. According to the rules of reflection at conducting planes and by (5.1) to (5.4) an arbitrary image q produces 3 new images on the right hand side in different ways:

	Position of image	Value of image
1	Reflection on the left plate + reflection at the right plate	$\gamma\ q$
2	Charge q in domain 2 induces an image q' by reflection on the interface done according to (5.3) + reflection at the right plate	$-\beta\ q$
3	Image of q w.r.t. the right plate (if it exists) in the domain 1 induces an image q''at the same position according to (5.4) + reflection at the left plate + reflection at the right plate	$+\beta\ q$

$$\beta = \frac{\varepsilon_2 - \varepsilon_1}{\varepsilon_2 + \varepsilon_1} \quad \gamma = \frac{4\ \varepsilon_1\varepsilon_2}{(\varepsilon_2 + \varepsilon_1)^2}.$$

Table: *Position and value of the 3 daughter images of q.*

With the help of the recurrences given in the table above closed expressions for the positions and values of all images to the right of the right hand plate can be computed. The corresponding formulae are given below for the branch $\oplus$. Those for the branch $\ominus$ (and all following corresponding expressions for $\ominus$) are obtained by the replacement rule $z \to 2D - z$. The positions of the images located to the right of the plate at right are:

$$2[D(k+m) + d(l-m)] + z, \qquad k, l, m = 0, 1, 2, \ldots\ . \tag{5.13}$$

The values of these images are:

$$\alpha\ (-1)^l\ \gamma^k\ \beta^{l+m}\ Q \tag{5.14}$$

with

$$\alpha = \frac{2\varepsilon_2}{\varepsilon_1 + \varepsilon_2}, \qquad \underbrace{\beta = \frac{\varepsilon_2 - \varepsilon_1}{\varepsilon_1 + \varepsilon_2}, \qquad \gamma = \frac{4\ \varepsilon_1\varepsilon_2}{(\varepsilon_1 + \varepsilon_2)^2}}_{\gamma + \beta^2 = 1}\ . \tag{5.15}$$

The running subscripts k, l, m are related to the 3 lines of the entries in the center column of the table above.

5.4.2 Frequency of Images Labelled by a Number Triple (k, l, m)

A given image charge labelled by a number triple (k, l, m) may be reached from the very first image $(0, 0, 0)$ at several different ways by increasing the 3 numbers in varying sequences. If there are no additional rules to satisfy, then the number of different sequences would be the multinomial coefficient

$$\left(\begin{array}{c} n \\ k,\ l,\ m \end{array} \right) = \frac{n!}{k!\ l!\ m!}\ , \quad n = k + l + m\ . \tag{5.16}$$

But according to the results of sect. 5.2 there is one restriction: Increasing m by 1 must not be followed by increasing l by 1. A more detailed investigation shows that the occurences are given by:

$$\sum_{i=0}^{Min[l,m]} (-1)^i \begin{pmatrix} n-i \\ k,\ l-i,\ m-i,\ i \end{pmatrix} \tag{5.17}$$

with $n = k + l + m$. The polynominal coefficient can be transformed in the following way:

$$\begin{pmatrix} n-i \\ k,\ l-i,\ m-i,\ i \end{pmatrix} = \begin{pmatrix} n-i \\ i \end{pmatrix} \begin{pmatrix} n-2i \\ k,\ l-i,\ m-i \end{pmatrix} . \tag{5.18}$$

5.4.3 Current through a Strip of an Electrode of the Two-Layer Condensor

The expression $S^{\oplus}$ (corresponding to (5.9)) in the case of the two layer problem is a triple sum over (k, l, m) :

$$\begin{aligned} S^{\oplus}(D,d;x,z) &= \sum_{n=0}^{\infty} \sum_{k=0}^{n} \gamma^k \beta^{n-k} \sum_{l=0}^{n-k} \frac{(-1)^l\ x}{\{2[D(n-l)+d(k-n+2l)]+z\}^2+x^2} \times \\ &\quad \times \sum_{i=0}^{Min[l,n-k-l]} (-1)^i \begin{pmatrix} n-i \\ k,\ l-i,\ n-k-l-i,\ i \end{pmatrix} \end{aligned} \tag{5.19}$$

The sum in this form is most suitable for the numerical evaluation with a sufficiently large limit for n. For further calculation it is rewritten with $s := n - i$, and rule (5.18) is used:

$$\begin{aligned} S^{\oplus}(D,d;x,z) &= \sum_{s=0}^{\infty} \sum_{i=0}^{s} (-1)^i \begin{pmatrix} s \\ i \end{pmatrix} \times \\ &\quad \times \sum_{\substack{k,\,l-i,\,m-i \\ k+l+m=n}} \begin{pmatrix} s-i \\ k,\ l-i,\ m-i \end{pmatrix} \frac{(-1)^l\ \gamma^k\ \beta^{l+m}\ x}{\{2[D(k+m)+d(l-m)]+z\}^2+x^2} \end{aligned} \tag{5.20}$$

The last sum includes all triples k, l, m which sum up to a fixed n. In contrast to the simple case of the empty plane condensor it is not possible to find closed expressions for this problem.

5.4.4 Convergence of the Series

The convergence of the series is assured if the moduli of the two quantities β and γ are smaller than unity. This is indeed the case:

$$|\beta| = \left|\frac{\varepsilon_2 - \varepsilon_1}{\varepsilon_2 + \varepsilon_1}\right| < 1 \ , \tag{5.21}$$

as both ε_1 and ε_2 are positive, and

$$|\gamma| = \left|\frac{4\ \varepsilon_2\varepsilon_1}{(\varepsilon_2 + \varepsilon_1)^2}\right| < 1 \ , \tag{5.22}$$

because γ is the square of the geometric mean over the arithmetic mean of the two relative dielectric constants ε_1 and ε_2. To satisfy the last inequality the case $\varepsilon_1 = \varepsilon_2$ must be excluded.

5.4.5 Transformation to the Integral Representation

The above series may be recast with the help of the following Mellin transform M_σ:

$$\Gamma(\sigma)\ b^{-\sigma} = \int_0^\infty dt\ t^{\sigma-1}e^{-bt} \ =: \ M_\sigma[e^{-bt}] \ . \tag{5.23}$$

Before performing the transformation according to (5.23) it is convenient to decompose the denominator of $S^{\oplus}$ into partial fractions.

$$\frac{x}{\{2[\ ]+z\}^2 + x^2} = \frac{i}{2}\left\{\frac{1}{2[\ ]+z+ix} - \frac{1}{2[\ ]+z-ix}\right\} = -Im\Big[\frac{1}{2[\ ]+z+ix}\Big] \ . \tag{5.24}$$

[ ] is a shorthand symbol for the square bracket in the denominator of $S^{\oplus}$. Now the expression on the l.h.s of (5.24) are replaced by the fraction on the very right hand side. The new series are denoted by $S^{\oplus}_{Im}$ and $S^{\ominus}_{Im}$, respectively. The lower index shall be a mnemonic, that only their imaginary part is relevant according to (5.24). The Mellin tranform is used for $\sigma = 1$, which entails $\Gamma(1) = 1$.

$$\begin{aligned} S^{\oplus}_{Im} \ &= \ \int_0^\infty dt\ \sum_{s=0}^{\infty}\sum_{i=0}^{s}(-1)^i \begin{pmatrix} s \\ i \end{pmatrix} \sum_{\substack{k,l-i,m-i \\ k+l+m=n}} \begin{pmatrix} s-i \\ k,\ l-i,\ m-i \end{pmatrix} \gamma^k\ (-\beta)^l\ \beta^m\ \times \\ &\qquad\qquad \times\ e^{-\{2[D(m+k)+d(l-m)]+z+ix\}t} \\ &= \ \int_0^\infty dt\ e^{-(z+ix)t}\sum_{s=0}^{\infty}\sum_{i=0}^{s}(-1)^i \begin{pmatrix} s \\ i \end{pmatrix}\Big(-\beta^2 e^{-2Dt}\Big)^i\ \times \end{aligned}$$

$$\times \underbrace{\sum_{\substack{k,\,l-i,\,m-i \\ k+l+m=n}} \binom{s-i}{k,\ l-i,\ m-i} \Big(\gamma e^{-2Dt}\Big)^k \Big(-\beta e^{-2dt}\Big)^l \Big(\beta e^{-2(D-d)t}\Big)^m}_{= \left[\gamma e^{-2Dt} + \beta\left(e^{-2(D-d)t} - e^{-2dt}\right)\right]^{s-i}}$$

The interchange of the sum and the integral is justified by the absolute convergence of the former. The sum over i can also be done to give:

$$\Big[\underbrace{(\gamma+\beta^2)}_{=\,1} e^{-2Dt} + \beta\big(e^{-2(D-d)t} - e^{-2dt}\big)\Big]^s$$

So we get the following integral representation in place of (5.21):

$$S^{\oplus}_{Im} = \int_0^\infty dt\ e^{-(z+ix)t} \sum_{s=0}^{\infty} \Big[e^{-2Dt} + \beta\big(e^{-2(D-d)t} - e^{-2dt}\big)\Big]^s \tag{5.25}$$

$$= \int_0^\infty dt\ \frac{e^{-(z+ix)t}}{1 - e^{-2Dt} - \beta\big(e^{-2(D-d)t} - e^{-2dt}\big)} \tag{5.26}$$

5.4.6 Current through an Anode Strip

To get the current flowing through an anode strip both expressions $S^{\oplus}$ and $S^{\ominus}$ are summed and appropriate boundary values for x are inserted. $S^{\ominus}$ can be obtained from $S^{\oplus}$, as already mentioned, by the replacement $z \to 2D - z$.

$$I_S(D,d,x_0,z,w) = \frac{Qv\alpha}{\pi}\Big[S^{\oplus}(D,d,x,z) + S^{\ominus}(D,d,x,z)\Big]\Big|_{x=x_0-\frac{w}{2}}^{x=x_0+\frac{w}{2}} = \tag{5.27}$$

$$= -\frac{Qv\alpha}{\pi}\, Im\Big[\Big[S^{\oplus}_{Im}(D,d,x,z) + S^{\ominus}_{Im}(D,d,x,z)\Big]\Big|_{x=x_0-\frac{w}{2}}^{x=x_0+\frac{w}{2}}\Big] \tag{5.28}$$

5.4.7 A Closed Expression for the Half-Filled Condensor

A simple closed expression can be found for the special case $D = 2d$ (*half-filled condensor*). The last term of the denominator in (5.25) vanishes and the remaining integral can be evaluated after interchanging sum and integral. The sum of the resulting series can be transformed in the corresponding expressions $S^{\oplus}$ and $S^{\ominus}$ by following the rule (5.24) in opposite direction. The sum of the latter leads to a simple closed form:

$$S^{\oplus} + S^{\ominus} = \sum_{s=0}^{\infty}\Big[\frac{x}{(2Ds+z)^2 + x^2} + \frac{x}{(2Ds+z)^2 - x^2}\Big] = \frac{\pi}{2D}\ \frac{\sinh(\pi x/D)}{\cosh(\pi x/D) - \cos(\pi z/D)} \tag{5.29}$$

Finally the current is:

$$\frac{I_S D}{Qv} = \frac{\alpha}{2}\,\frac{\sinh[\frac{\pi(x_0-w/2)}{D}]}{\cos[\frac{\pi z'}{D}]-\cosh[\frac{\pi(x_0-w/2)}{D}]} - \frac{\alpha}{2}\,\frac{\sinh[\frac{\pi(x_0+w/2)}{D}]}{\cos[\frac{\pi z'}{D}]-\cosh[\frac{\pi(x_0+w/2)}{D}]}\ . \tag{5.30}$$

It is remarkable that this result is identical to (5.12) exept for a factor α, which depends on the two relative dielectric constants ε_1 and ε_2.

5.4.8 Approximation for a Very Thin Dielectric Layer

An approximate closed expression for the current can be given when the dielectric layer is very thin as compared to the gas gap, which implies that $d \ll D$. The variable of integration is changed, $\tau = 2dt$ in (5.26):

$$\begin{aligned} S^{\oplus}_{Im} &= \frac{1}{2d}\int_0^\infty d\tau \frac{e^{-\frac{z+ix}{2d}\tau}}{1-\underbrace{e^{-\frac{D}{d}\tau}}_{\approx\ 0} - \beta(\underbrace{e^{-(\frac{D}{d}-1)\tau}}_{\approx\ 0} - e^{-\tau})} \approx \\ &\approx \frac{1}{2d}\int_0^\infty d\tau \frac{e^{-\frac{z+ix}{2d}\tau}}{1+\beta\ e^{-\tau}} = \\ &= \frac{1}{2d}\ \Phi\Big(-\beta,\ 1,\ \frac{z+ix}{2d}\Big)\ . \end{aligned} \tag{5.31}$$

The function just given is Lerch's Φ-function defined as ([17]; [19], §9.55):

$$\Phi(z,s,a) = \sum_{k=0}^{\infty} \frac{z^k}{(a+k)^s}\ , \qquad |z|<1\ . \tag{5.32}$$

The approximation for $S^{\oplus}_{Im}$ together with (5.28) yields

$$\frac{I_S D}{Qv} = -\frac{\alpha D}{2\pi d}\ Im\left[\left[\Phi\Big(-\beta,\ 1,\ \frac{z+ix}{2d}\Big) + \Phi\Big(-\beta,\ 1,\ 1-\frac{z-ix}{2d}\Big)\right]\Big|_{x=x_0-\frac{w}{2}}^{x=x_0+\frac{w}{2}}\right]\ . \tag{5.33}$$

The condition for the parameter z, given in eq.(5.32), is satisfied according to (5.21).

The approximation for a very thin layer, given as a closed expression in eq.(5.33), produces quite satisfactory results for the case that the point charge is not too far away from the plane of the anode strips, what is verified in Fig.5.5 with the help of an example.

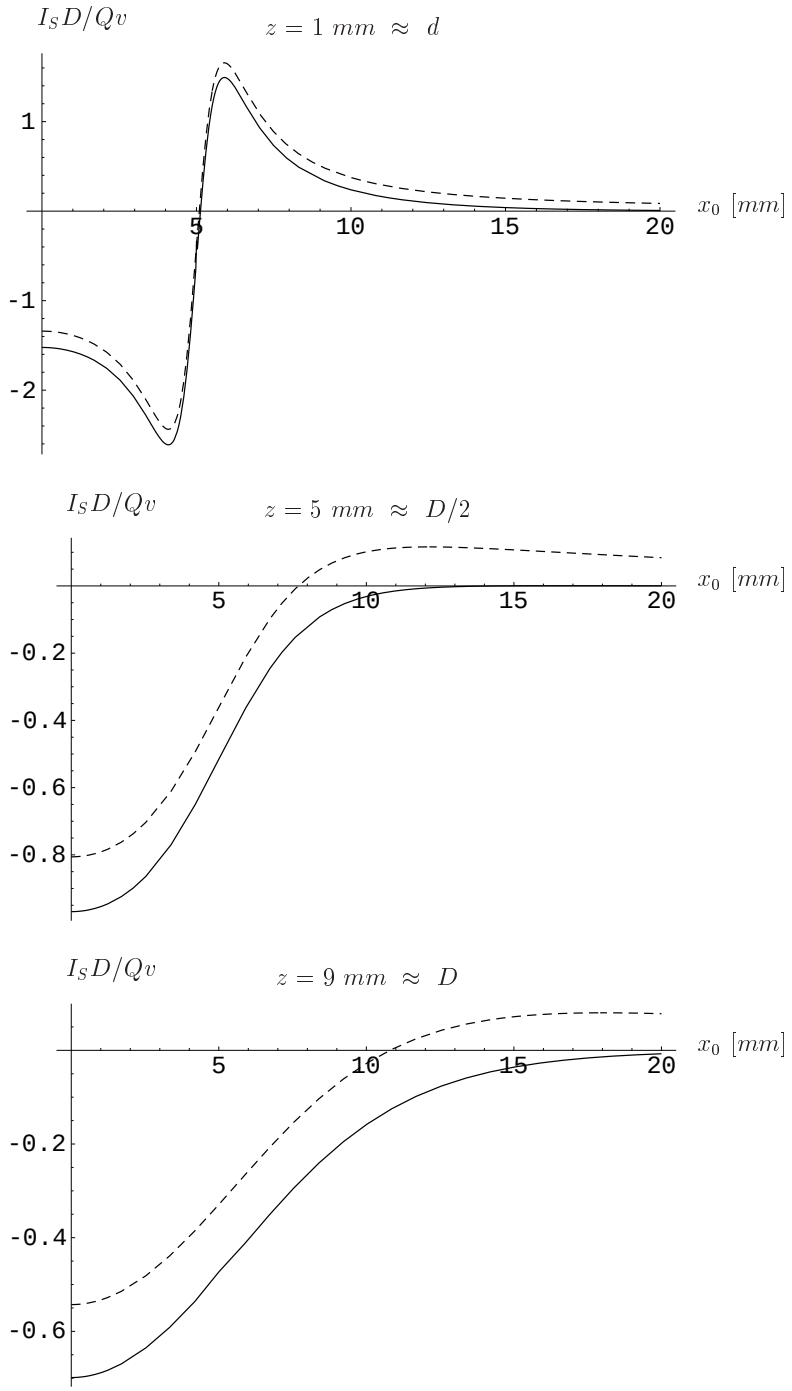

Figure 5.5: *Current I_S through an anode strip calculated with eq.(4.77) for the quasistatic model with an isolating layer (continous lines) and computed with the closed form given in eq.(5.33) as an approximation for the case of an very thin dielectric layer (dashed lines). The instantaneous longitudinal distance z of the charge from the plane of the anode strips is indicated in the head of each drawing. In the uppermost the charge is near to the plane of the anode strips; in the lowest drawing it is very near to the cathode. The drawing in the middle correponds to a position halfway between cathode and anode strips. $D = 10\ mm$, $d = 0.4\ mm$, $\varepsilon = 4$.*

Chapter 6

Two-Dimensional Models and Conformal Maps

In this chapter the influence of the gap separating two anode strips on the field distribution and on the signals is investigated. It is advantageous to use two-dimensional models corresponding to the three-dimensional configuration treated in the previous chapters so that complex field representations and the method of conformal maps may be applied. The properties of complex analytic functions are used to represent solutions of the potential equation fulfilling certain boundary conditions in a simple geometry. The powerful method of conformal maps is used to obtain solutions of Poisson's equation with more complicated boundaries. This procedure is based on the invariance of the Laplacian and of point charge distributions under a conformal transformation performed with the help of analytic functions. In other words: At first a solution is obtained for a configuration, whose boundary has a very simple shape. This solution can be transformed into the wanted solution of a complicated configuration under scrutiny provided one can find an analytic function, which maps the boundary (or electrodes) of the real configuration into that (or those) of the simple problem. Another advantage of the complex field representation is the simple expression for the electric flux passing through a piece of a curve.

6.1 Complex Field Representations

The two rectangular coordinates x, y are combined to a complex coordinate:

$$z := x + iy$$

The properties of complex analytic functions offer a powerful method to solve two-dimensional problems. From the Cauchy-Riemann eqations it follows that both the real

and the imaginary part of an analytic function $u+iv = f(z)$ solve the Laplace equation in a regular point.

$$\Delta u(z) = 0 \ ; \qquad \Delta v(z) = 0 \ . \tag{6.1}$$

So the solution of the two-dimensional potential equation may be expressed by the real or imaginary part of a complex function $\Psi(z)$analytic in the domain under consideration, which function is called the complex potential for obvious reasons.

$$\Phi(x,y) = Re[\Psi(z)] \ . \tag{6.2}$$

The set of curves $Re[\Psi(z)] = const.$ represents the equipotentials, the orthogonal set $Im[\Psi(z)] = const.$ the electric field lines. The singularities of the complex potential correspond to the sources, i.e. to the electric charges. The complex expression for the field is found from the complex potential by a derivation:

$$\vec{E} = E_x + iE_y = -\Big(\frac{d\Psi}{dz}\Big)^* \ . \tag{6.3}$$

The electric flux passing through a piece of a curve between the points z_1 and z_2 may be easily obtained from the imaginary part of the complex potential.

$$\begin{aligned} \int_{z_1}^{z_2} \vec{E}\cdot d\vec{n} &= \int_{z_1}^{z_2} \Big[-\frac{\partial Re[\psi]}{\partial x}\, dy + \frac{\partial Re[\psi]}{\partial y}\, dx\Big] = \\ &= \int_{z_1}^{z_2} \Big[-\frac{\partial Im[\psi]}{\partial y}\, dy - \frac{\partial Im[\psi]}{\partial x}\, dx\Big] = Im[\Psi(z_1) - \Psi(z_2)] \ . \end{aligned} \tag{6.4}$$

In going from the first to the second line above the Cauchy-Riemann equations were used. The total charge q induced on such a piece of a conducting boundary is found from the electric flux, i.e. from the complex potential at the end points.

$$q = -\varepsilon_0\varepsilon \int_{z_1}^{z_2} \vec{E}\cdot d\vec{n} = \varepsilon_0\varepsilon \ Im[\Psi(z_2) - \Psi(z_1)] \ . \tag{6.5}$$

All formulae given up to now are related to the static field due to a point charge at rest. We are interested in the current induced on a strip of the boundary by a point charge moving with constant speed towards the conducting boundary on a normal to it. In the frame of the quasi-static approximation the motion of the charge is taken into account by inserting its time-dependent position $z_0(t)$ for the source point coordinate of the complex potential.The current induced in the strip between the points z_1 and z_2 is then:

$$I = \frac{dq}{dt} = \varepsilon_0\varepsilon \ Im\Big[\frac{d}{dt}[\Psi(z_2) - \Psi(z_1)]\Big] \ . \tag{6.6}$$

As we are dealing with point charges as sources, the time-dependent complex potential $\Psi(t)$ is proportional to a complex Green's function $G(z, z_0(t))$. z_0 is the time-dependent position of the point charge: $z_0 = vt + z_{00}$. z_{00} and v are the initial position and the velocity of the charge.

6.2 Conformal Maps

The essential part of our task is to determine a complex Green's function $G(z, z_0)$ such that

$$\Phi(x, y) = \frac{Q}{\varepsilon_0 \varepsilon} \, G(z, z_0) \; . \tag{6.7}$$

This task is performed by a comformal map. A holomorphic function $w = u + iv = f(z)$, which maps the z-plane onto the complex w-plane, transforms the Laplacian of the z-plane into that of the w-plane in the following way:

$$\Delta_w = \frac{1}{|f'(z)|^2} \, \Delta_z \; . \tag{6.8}$$

The potential of a charge distribution in a domain with constant dielectric constant ε is a solution of Poisson's equation:

$$\varepsilon_0 \varepsilon \; \Delta_w \Phi(u, v) = \varepsilon_0 \varepsilon \Big[\frac{\partial^2}{\partial u^2} + \frac{\partial^2}{\partial v^2} \Big] \Phi(u, v) = \rho_w \; . \tag{6.9}$$

The corresponding equation in the z-plane is:

$$\varepsilon_0 \varepsilon \; \Delta_z \Phi(x, y) \;\; = \;\; \Big[\frac{\partial^2}{\partial x^2} + \frac{\partial^2}{\partial y^2} \Big] \Phi(x, y) = |f'(z)|^2 \rho_w(u(x, y), v(x, y)) \; . \tag{6.10}$$

A more detailed investigation [14] shows that the charge density describing a point charge is not changed by a conformal map.

$$Q \; \delta(u - u_0) \delta(v - v_0) \iff Q \; \delta(x - x_0) \delta(y - y_0) \; . \tag{6.11}$$

Let us assume we know a holomorphic function $G_1(w, w_0)$ (w_0 position of the charge), whose real part is the electric potential due to a point charge located in a configuration with a simple boundary (e.g. a plane condensor) in the w-plane. We need the potential for a point charge located in a configuration with a boundary having another shape, the real boundary, (in the z-plane). If we succed in finding a holomorphic function $w(z)$ mapping the simple boundary into the real one, then the wanted potential is the real part of the following function.

$$G(z, z_0) = G_1(w(z), w(z_0)) \; . \tag{6.12}$$

6.3 Models Describing a Plane Condensor with a Gap

In this section 4 two-dimensional models for a plane condensor with a gap in one electrode are compared and used to investigate fields and signals in RPC's. Of course, point

charges in the two-dimensional models correspond to line charges in the real three-dimensional world. In all models the motion is perpendicular to the plane metallic boundaries.

1. A point charge is moving towards a continuous metallic plate of infinite extent.
2. A point charge is moving between two parallel continuous metallic plates.
3. A point charge is moving towards two coplanar metallic semi-infinite metallic plates separated by a gap.
4. A point charge is moving in a plane condensor, whose one electrode has a gap.

The last model of the four just listed matches best the geometry of a RPC. The gap separating two coplanar electrodes corresponds to the gap separating two anode strips. On the other hand, its solution is the most complicated one and requires the largest effort. One cannot expect that the solutions obtained from these two-dimensional models match those of the corresponding three-dimensional models, so of the real problem. But one can get insights how the presence of the gap influences the strength of the signal.

6.3.1 A Continuous Conducting Plate

A point charge Q is located at $z_0 = x_0 + iy_0$ above the ideally conducting plate $y = 0$ (see Fig.6.1). The complex Green's function is [13] :

$$G(z, z_0) = \frac{1}{2\pi} \log \frac{\sinh(z - z_0)}{\sinh(z - z_0^*)} \ . \tag{6.13}$$

A moving charge, $z_0 = -ivt = iy_0$, induces a current I_S calculated according to (6.6) flowing through a strip between $x_1 = -w/2$ and $x_2 = w/2$ of the infinite plate $y = 0$:

$$\frac{I_S D}{Qv} = \frac{D}{\pi}\left[\frac{x_0 - w/2}{(x_0 - w/2)^2 + y_0^2} - \frac{x_0 + w/2}{(x_0 + w/2)^2 + y_0^2}\right] \ . \tag{6.14}$$

The current assumes an extreme if the charge is above the strip and is sufficiently near to it (cf. Figs.6.6, 6.7). This extreme occurs at

$$x_1 = \sqrt{y_0^2 + (w/2)^2 - 2y_0\sqrt{y_0^2 + (w/2)^2}} \ , \tag{6.15}$$

provided the vertical position is within the limits:

$$0 < y_0 < w/(2\sqrt{3}) \ .$$

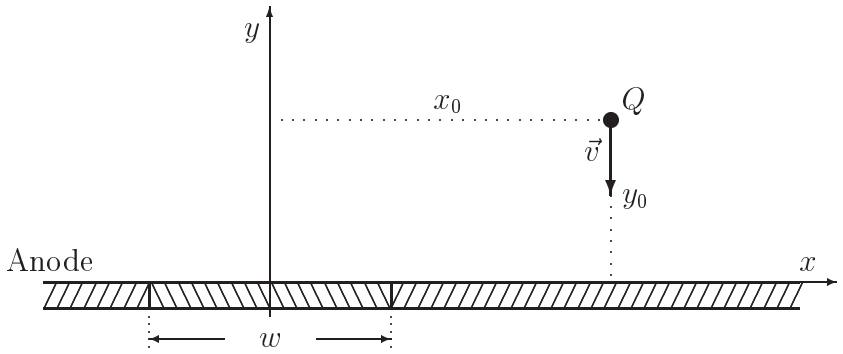

Figure 6.1: *Geometry of a (line) charge above a conducting plane.*

Another extreme of the current occurs at

$$x_2 = \sqrt{y_0^2 + (w/2)^2 + 2y_0\sqrt{y_0^2 + (w/2)^2}} \ . \tag{6.16}$$

This extreme is not subject to a restriction as is x_1. However, it is located in the space outside the strip, in which domain there is the gap separating the two strips. In this area the present model, which uses a continuous sheet for the anode, will not represent a good approximation. The more realistic models containing a real gap may still show such an extreme but it is much smaller if it is present at all.

6.3.2 Plane Condensor

The charge is at the same position as above. The two conducting plates lie at $y = 0$ and $y = D$ (see Fig.6.2). The complex Green's function is:

$$G(z, z_0) = \frac{1}{2\pi} \log \frac{\sinh[\frac{\pi(z-z_0)}{D}]}{\sinh[\frac{\pi(z-z_0^*)}{D}]} \ . \tag{6.17}$$

The motion of the charge and the strip are the same as above. The expression for the current

$$\frac{I_S D}{Qv} = \frac{1}{2} \frac{\sinh[\frac{\pi(x_0-w/2)}{D}]}{\cosh[\frac{\pi(x_0-w/2)}{D}] - \cos[\frac{\pi y_0}{D}]} - \frac{1}{2} \frac{\sinh[\frac{\pi(x_0+w/2)}{D}]}{\cosh[\frac{\pi(x_0+w/2)}{D}] - \cos[\frac{\pi y_0}{D}]} \ . \tag{6.18}$$

flowing through the strip found in this two-dimensional model is the same as that obtained above from the three-dimensional model, eq.(3.15). The different signs in the denominators result from different choices of the position of the electrode on which the current is induced. Here this electrode is at $z = 0$, in references [7], [8] as well as in (3.15) it is at $z = D$.

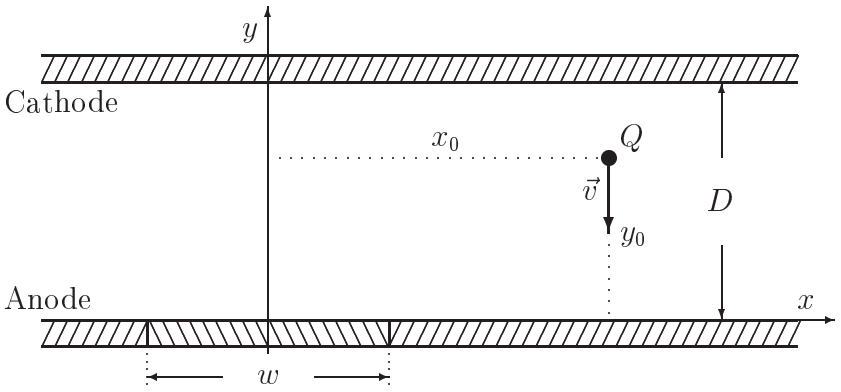

Figure 6.2: *Geometry of a (line) charge in a plane condensor.*

6.3.3 Two Coplanar Semi-Infinite Conducting Plates Separated by a Gap

We consider an infinite conducting plane, $y = 0$, having a gap extending from $x = -g/2$ and $x = g/2$. The anode strip is the part of the plane extending from $x = -g/2$ to $x = -g/2 + w$ (cf. Fig.6.4). The position of the charge is again the same as above. This configuration is mapped to an infinite plane condensor, whose plates are located at $V = \pm\pi/2$ in the $W = U + iV$-plane, by the following function (see Fig.6.3):

$$W(z) = i \arcsin\left(\frac{2z}{g}\right) . \tag{6.19}$$

The complex Green's function for the plane condensor is

$$G_1(W, W_0) = \frac{1}{2\pi} \log \frac{\sinh[(W - W_0)/2]}{\sinh[(W - W_0^* + i\pi)/2]} . \tag{6.20}$$

and that for the two coplanar semi-infinite conducting plates separated by a gap is

$$G(z, z_0) = G_1\left(i \arcsin\left(\frac{2z}{g}\right), i \arcsin\left(\frac{2z_0}{g}\right)\right) . \tag{6.21}$$

The current flowing through an anode strip is induced by a charge, which moves towards the plane of the plates as given above. It is

$$\begin{aligned} 2\pi \frac{I_S}{Qv} = & - \frac{x_0 - g/2}{(x_0 - g/2)^2 + y_0^2} - \frac{w - y_0 + g/2}{(w - x_0 + g/2)^2 + y_0^2} - \\ & - Im\left[\frac{\sqrt{g^2/4 - (w + g/2)^2}}{i\sqrt{g^2/4 + z_0^2}\,(z_0^* - (w + g/2))}\right] . \end{aligned} \tag{6.22}$$

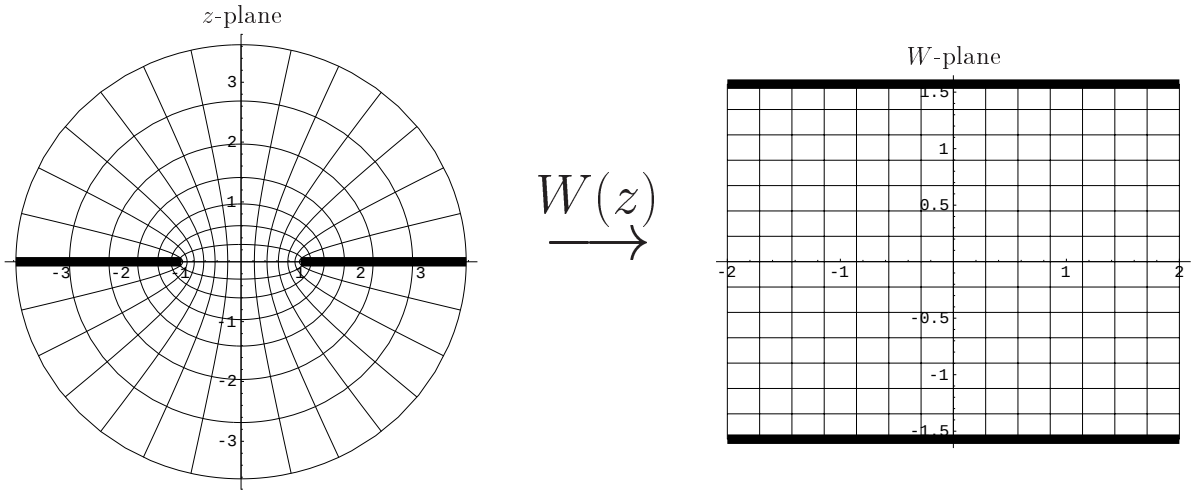

Figure 6.3: *The function* $W(z) = i \arcsin(2z/g)$ *maps the set of equipotentials and the orthogonal set of electric field lines on the corresponding sets of lines of an infinite plane condensor. The thick lines are the ideally conducting electrodes; the plates of the plane condensor are located at* $\pm i\pi/2$ *in the* W*-plane.* ($g = 2$)

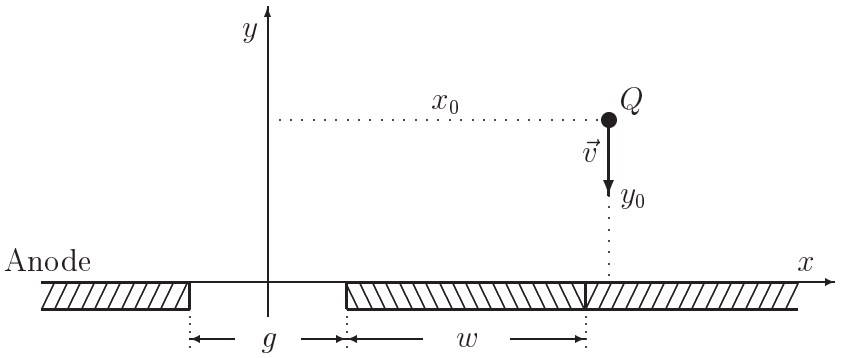

Figure 6.4: *Geometry of a (line) charge above a split infinite electrode.*

6.3.4 A Plane Condensor with a Continuous and a Split Electrode

The boundaries of this model consist of a continuous conducting plate located at $y = D$ and a split conducting plate at $y = 0, |x| > g/2$, Fig.6.5. The position of the line charge is at $z_0 = z_0 + iy_0$. In this case one starts from a continuous plate, whose halves have opposite potentials of the same magnitude. We call this a "flat condensor". The corresponding Green's function is:

$$G_1(W, W_0) = \frac{1}{2\pi} \log \frac{W - W_0}{W - W_0^*} \ . \tag{6.23}$$

The plane condensor with a gap represented in the z-plane is mapped conformally onto a "flat condensor" in the w-plane by the following function:

$$z(W) = \frac{D}{\pi} \left[\frac{(p-1)^2}{p} \left(\frac{1}{2} - \frac{1}{W+1} \right) + \log(W) \right] \ . \tag{6.24}$$

The parameter p is a root of the following transcendental equation:

$$\frac{D}{\pi} \left[\frac{p^2 - 1}{2p} + \log(W) \right] = \frac{g}{2} \ . \tag{6.25}$$

The wanted Green's function $G(z, z_0)$ for the condensor in the z-plane is again given by eq.(6.12). There is a difficulty hampering the use of this model: The function $W(z)$, which is the inverse to $z(W)$ introduced in eq.(6.24), is needed. It is impossible to find an analytic expression for this inverse function; so it can be computed numerically only. This requirement renders this model much more cumbersome than the three preceeding ones. The current flowing through a strip of width w adjacent to the left (right) edge of the gap is:

$$\frac{I_S D}{Q v} = \mp Im \left[\frac{\partial}{\partial y_0} G(iD \mp w \mp g/2, iD - z_0) - \frac{\partial}{\partial y_0} G(iD \mp g/2, iD - z_0) \right] \ . \tag{6.26}$$

6.4 Comparison of the Four Models

In Figs.6.6, 6.7 the results of the four models are compared. They show the current I_S flowing through an anode strip induced by a charge Q moving towards the anode on a straight trajectory perpendicular to the electrodes. x_0 gives the transverse distance of the trajectory from a perpendicular passing through the center line of the strip under consideration. Half of this strip is shown at the bottom of each figure, then follows the

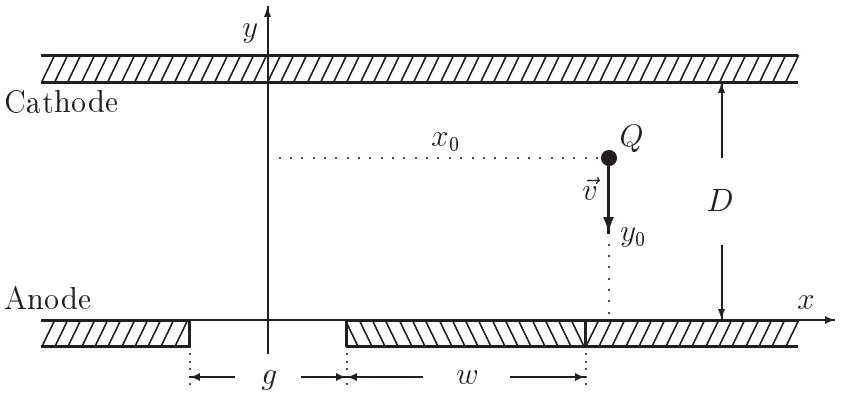

Figure 6.5: *Geometry of a (line) charge in a plane condensor with a split electrode.*

gap; at the right there is a larger portion of the next strip. All the curves give the current flowing through the left strip. y_0 is the instantaneous distance from the anode as shown in Figs.6.1 to 6.5. Of course, we must recall that in the conformal maps the left (right) electrodes extend to $-\infty$ (∞); the finite width of the strip is simulated by integrating in eq.(6.6) over an area A of width w. This approximation does not appear to be serious as the signal strength falls to low values over a length of magnitude w.

If the charge is above the anode strip and near to it (the uppermost drawing in Fig.6.6 and 6.7) all four models give roughly the same signal strength. There is a miminum, whose position is almost the same as given by all 4 models. Large difference occur in the gap domain. Models without a gap give a maximum, which must be regarded as spurious as it is not turning up in models including the gap. The latter show a maximum (at about $x_0 = 8$ mm) when the charge is moving under the edge of the next strip. For values of x_0 beyond that maximum the signal tapers of quite fast as shown by all 4 models.

When the charge is moving far from the anode and near the real or virtual position of the cathode the latter, if present, doubles the signal strength. The influence of the gap is small (the lowest drawing in Fig.6.6 and 6.7). The signal tapers of with increasing transverse distance x_0 for the models with anode and cathode, while it changes sign and then stays nonzero for a certain range for models with an anode only. When the charge is moving halfway in the gas gap (the middle drawing in Fig.6.6 and 6.7) the gap separating the strips still exercises a certain influence while the cathode, if present, enhances the signal though by a factor less than 2. Again the lack of the cathode gives a change of sign, which must be regarded as spurious as it does not occur when the cathode is present.

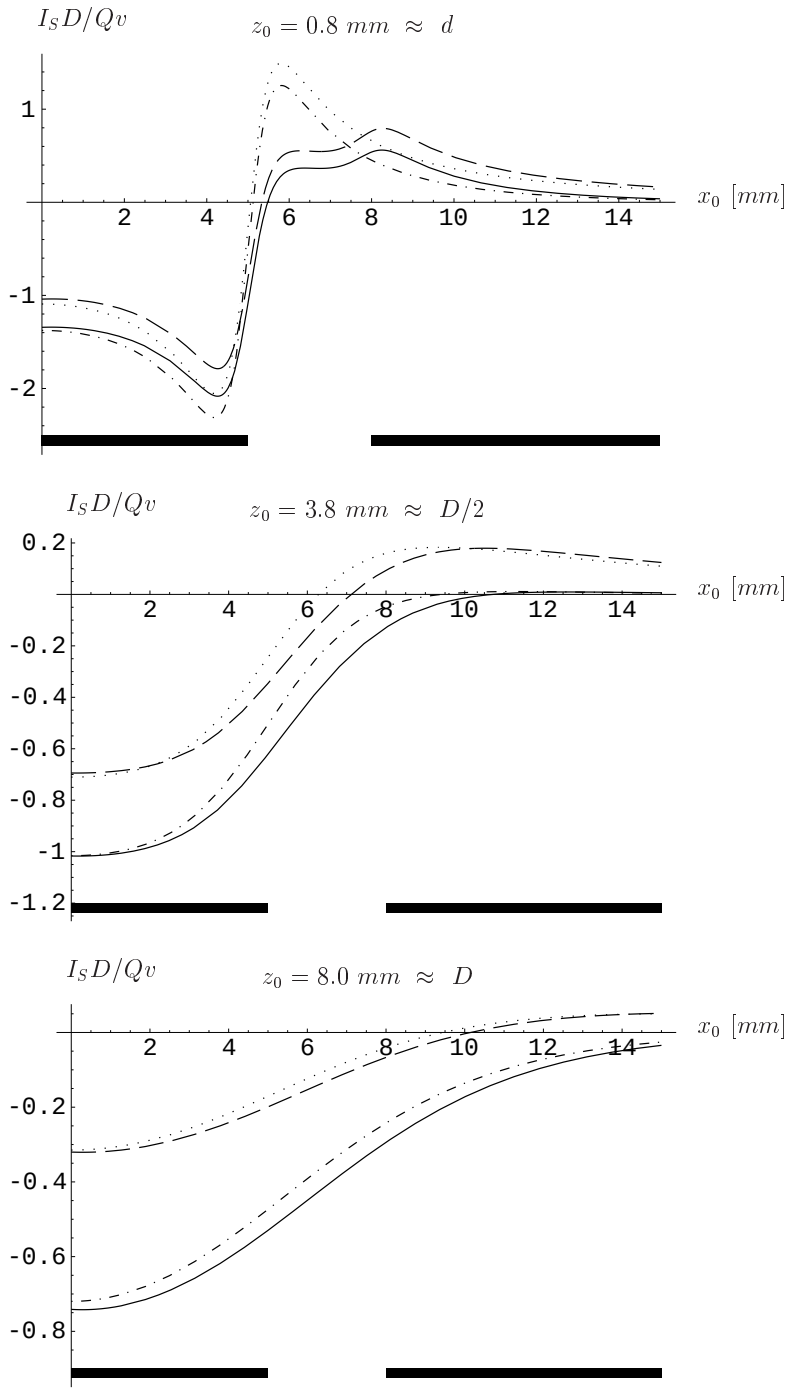

Figure 6.6: *Current I_S through an anode strip, whose center is at $z_0 = 0$, of a RPC due to a (line) charge Q moving with velocity $v = 5 \cdot 10^4\ m/s$ on a perpendicular to the electrodes versus distance x_0 of this trajectory from strip center. $D = 8.8\ mm$ is distance of the two electrodes. $w = 10\ mm$ is width of strips; $g = 3\ mm$ that of gap between strips. Instantaneous longitudinal coordinate of charge z_0 is indicated in the head of each drawing. In the uppermost the charge is near to the plane of the anode strips; if there is a dielectric it is just at the interface separating this from the gas gap. In the lowest drawing it very near to the cathode. The drawing in the middle correponds to a position halfway between cathode and anode strips. Different types of lines give results of different models. "——" model 6.3.4, Fig.6.5, consisting of a continuous and a split electrode; "– – –" model 6.3.3, Fig.6.4, with just one split electrode; "·····" model 6.3.1, Fig.6.1, a simple full electrode; "– · – · –" model 6.3.2, Fig.6.2, an infinite plane condensor.*

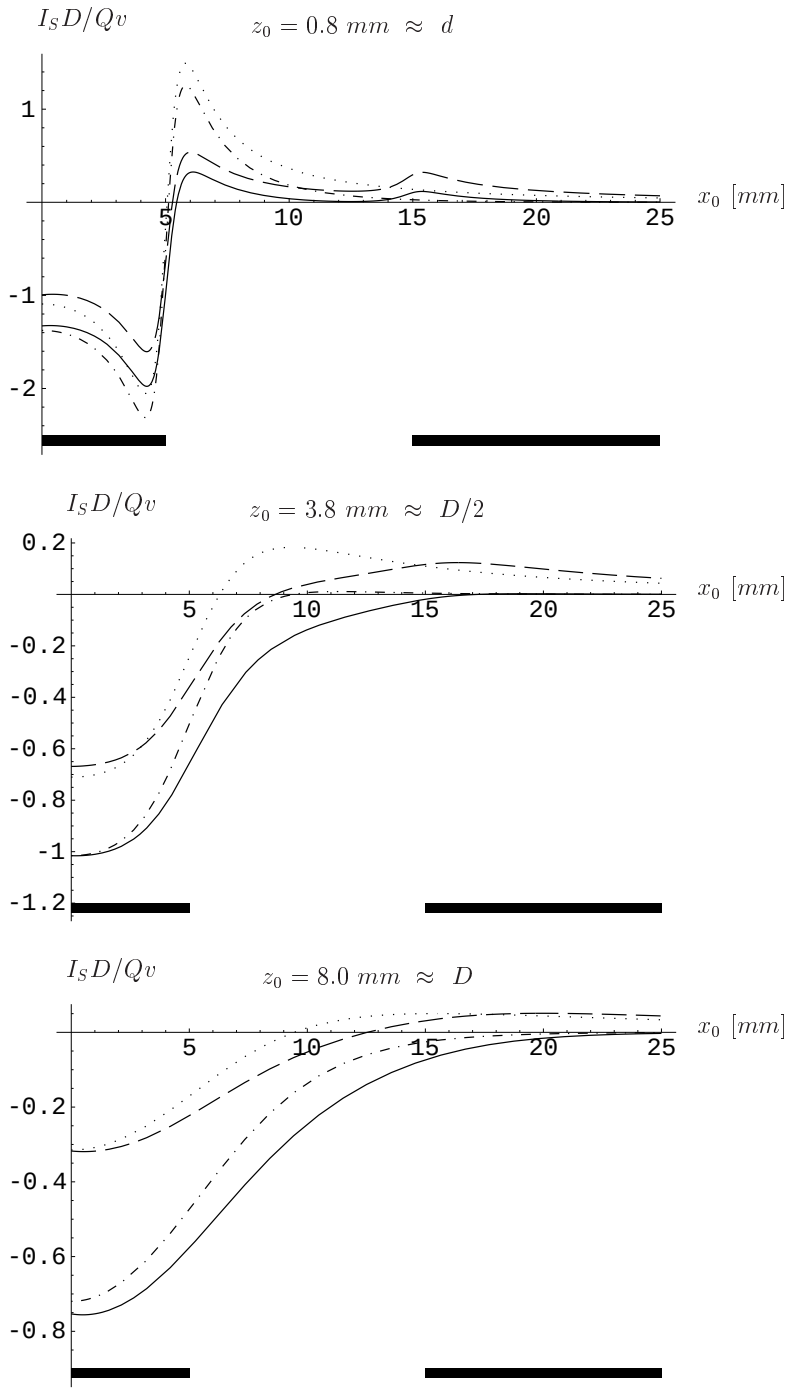

Figure 6.7: *Current I_S through an anode strip, whose center is at $z_0 = 0$, of a RPC due to a (line) charge Q moving with velocity $v = 5 \cdot 10^4\ m/s$ on a perpendicular to the electrodes versus distance x_0 of this trajectory from strip center. $D = 8.8\ mm$ is distance of the two electrodes. $w = 10\ mm$ is width of strips; $g = 10\ mm$ that of gap between strips. Instantaneous longitudinal coordinate of charge z_0 is indicated in the head of each drawing. In the uppermost the charge is near to the plane of the anode strips; if there is a dielectric it is just at the interface separating this from the gas gap. In the lowest drawing it very near to the cathode. The drawing in the middle correponds to a position halfway between cathode and anode strips. Different types of lines give results of different models. "——" model 6.3.4, Fig.6.5, consisting of a continuous and a split electrode; "– – –" model 6.3.3, Fig.6.4, with just one split electrode; "·····" model 6.3.1, Fig.6.1, a simple full electrode; "– · – · –" model 6.3.2, Fig.6.2, an infinite plane condensor.*

Chapter 7

The Dynamical Model

A method to solve this model which comprises the solution of the full time-dependent Maxwell equations (at least at the beginning) may be described as follows: The Green's tensor of the electromagnetic field fulfilling the appropriate boundary conditions is set up; it is multiplied by the electric current corresponding to the moving charge (distribution) and integrated over all time. This gives the electric field within the condensor. The surface current density is proportional to the electric field component normal to the electrodes of the plane condensor. Integrating the current density over the whole electrode gives the total charge; its time derivative the wanted current. However, there is a simpler way to find the wanted quantities avoiding the cumbersome treatment of the Green's tensor. This is possible because the source current has a particular simple shape.

7.1 Basic Equations

One starts from the Maxwell equations for time-harmonic fields (the time-dependence $e^{-i\omega t}$ is omitted in some of the equations below):

$$\nabla \times \vec{E} = i\omega \vec{B} \ , \tag{7.1}$$

$$\nabla \times \vec{H} = \vec{j} - i\omega\varepsilon_0 \epsilon \vec{E} \ , \tag{7.2}$$

$$\nabla \cdot \vec{B} = 0 \ , \tag{7.3}$$

$$\nabla \cdot \vec{E} = 0 \ . \tag{7.4}$$

The complex relative dielectric constant depends on the real relative dielectric constant and on the conductivity σ of the homogeneous medium.

$$\epsilon = \varepsilon + \frac{i\sigma}{\varepsilon_0 \omega} \tag{7.5}$$

From eq.(7.3) it is seen that a vector potential $\vec{A}$ with the following properties exists

$$\vec{B} = \nabla \times \vec{A} \; . \tag{7.6}$$

The electric field $\vec{E}$ is found from eq.(7.1) with a scalar potential Φ

$$\vec{E} = i\omega\vec{A} - \nabla\Phi \; . \tag{7.7}$$

This gives with (7.2)

$$\Delta\vec{A} + k^2\vec{A} = -\mu_0\vec{j} + \nabla\Big(\nabla\vec{A} - i\,\frac{k^2}{\omega}\phi\Big) \; , \tag{7.8}$$

with the complex wave number k defined as

$$k^2 = \omega^2\varepsilon_0\epsilon\mu_0 \; , \tag{7.9}$$

and from (7.4) one gets the final result:

$$i\omega\nabla\vec{A} - \Delta\Phi = \frac{\rho}{\varepsilon_0\epsilon} \; . \tag{7.10}$$

The vector potential $\vec{A}$ introduced in (7.6) is not unique. Inspection of this equation shows that an arbitrary gradient field may be added to $\vec{A}$ without changing the corresponding magnetic induction $\vec{B}$. So there is the freedom to chose a gauge of the vector potential in an arbitrary way. The above equations simplify considerably by choosing the Lorentz gauge.

$$\nabla\cdot\vec{A} - i\,\frac{k^2}{\omega}\,\Phi = 0 \; . \tag{7.11}$$

Inserting (7.11) into (7.7) shows that the electic field is only a function of the vector potential $\vec{A}$:

$$\vec{E} \;=\; i\omega\Big(\vec{A} \;+\; \frac{1}{k^2}\nabla\nabla\cdot\vec{A}\Big). \tag{7.12}$$

Inserting (7.11) into (7.8) give an equation relating $\vec{A}$ to the source current $\vec{j}$:

$$\Delta\vec{A} + k^2\vec{A} = -\mu_0\vec{j} \; . \tag{7.13}$$

The boundary conditions for the electric field lead to the corresponding conditions for the vector potential

$$\vec{e}_z \times \vec{E} = 0 \; , \quad \Longrightarrow \quad \vec{e}_z \times \Big(\vec{A} + \frac{1}{k^2}\nabla\nabla\cdot\vec{A}\Big) = 0 \; . \tag{7.14}$$

Up to now the fact that the interior of the condensor consists of two parallel layers has not been taken into account. Such a procedure is possible as the parameters characterizing the media are constant in each layer. The fields must fulfil continuity conditions across the interface separating the media; from these the corresponding continuity conditions for the vector potential are obtained.

$$\begin{aligned}
\vec{E} \;:\quad & \vec{e}_z \times \left(\vec{A}_1 + \tfrac{1}{k^2}\nabla\nabla\cdot\vec{A}_1\right) &=\quad & \vec{e}_z \times \left(\vec{A}_2 + \frac{1}{k^2}\nabla\nabla\cdot\vec{A}_2\right) , \\
\vec{B} \;:\; \vec{e}_z \times \nabla \times & \left(\vec{A}_1 + \tfrac{1}{k^2}\nabla\nabla\cdot\vec{A}_1\right) &=\; \vec{e}_z \times \nabla \times & \left(\vec{A}_2 + \frac{1}{k^2}\nabla\nabla\cdot\vec{A}_2\right) .
\end{aligned} \tag{7.15}$$

In addition the Sommerfeld radiation condition must be fullfilled at infinity:

$$\lim_{r\to\infty}\; r\Big(\frac{\partial\vec{A}}{\partial r} - ik\vec{A}\Big) = 0 \; . \tag{7.16}$$

The time-dependent current due to the moving charge consisting of two parts is:

$$\begin{aligned}
\vec{j}(t,r,z) &= \vec{e}_z \; j(t,r,z) = \\
&= \vec{e}_z \cdot \begin{cases} j_1(t,r,z) = Qv \; \frac{\delta(r)}{2\pi r} \; \delta(z-q-vt) \; \Theta(z-q) \; \Theta(-z) & : \quad q < z < 0 \\ j_2(t,r,z) = 0 & : \quad 0 < z < p \end{cases} ,
\end{aligned} \tag{7.17}$$

whose Fourier transform is given by:

$$\begin{aligned}
\vec{j}(\omega,r,z) &= \vec{e}_z \; j(\omega,r,z) = \int_{-\infty}^{\infty} \vec{j}(t,r,z) \; e^{i\omega t} \; dt = \\
&= \vec{e}_z \cdot \begin{cases} j_1(\omega,r,z) = Qv \; \frac{\delta(r)}{2\pi r} \; \Theta(z-q) \; \Theta(-z) \; e^{i\frac{\omega}{v}(z-q)} & : \quad q < z < 0 \\ j_2(\omega,r,z) = 0 & : \quad 0 < z < p \end{cases} .
\end{aligned} \tag{7.18}$$

It is assumed that the charge Q is generated just in front of the electrode confining the gas gap, $z = q$, and moves up to the interface of the dielectric layer, $z = 0$. Charge conservation requires an equal charge of opposite sign to arise at the same time at the same spot. It is tacitly assumed that this second charge does not move so that its static field does not contribute to the time-varying signal. The only non-zero component of the source current is along the z-axis. The same applies to the vector potential $\vec{A} = \vec{e}_z A$, which thus is a solution of the following scalar differential equation:

$$\Delta A_i(\omega,r,z) + k_i^2 A_i(\omega,r,z) = -\mu_0 j_i(\omega,r,z) \; , \quad i = 1,2 \; . \tag{7.19}$$

The boundary and continuity conditions (7.14) to (7.15) may be simplified accordingly, where also the cylindrical symmetry is taken into account:

$$\left.\frac{\partial A_1}{\partial z}\right|_{z=q} = 0 \ , \tag{7.20}$$

$$\left.\frac{\partial A_2}{\partial z}\right|_{z=p} = 0 \ ; \tag{7.21}$$

$$\left.A_1\right|_{z=0} = \left.A_2\right|_{z=0} \ , \tag{7.22}$$

$$\left.\frac{1}{\epsilon_1}\frac{\partial A_1}{\partial z}\right|_{z=0} = \left.\frac{1}{\epsilon_2}\frac{\partial A_2}{\partial z}\right|_{z=0} \ . \tag{7.23}$$

The boundary value problem defined in eqs.(7.18) to (7.23) is solved with the help of an axially symmetric Green's function, which is the solution of the following differential equation:

$$\hat{L}_i \ G_{ij}(r,z;z') = \Big[\frac{1}{r}\ \frac{\partial}{\partial r}\Big(r\frac{\partial}{\partial r}\Big) + \frac{\partial^2}{\partial z^2} + k_i^2\Big]\ G_{ij}(r,z;z') = -\delta_{ij}\frac{\delta(r)}{2\pi r}\ \delta(z-z') \ . \tag{7.24}$$

Again, the Green's function of this two-layer problem consists of 4 pieces dependent on the position of the source (index $j = 1,2$) and the point of observation (index $i = 1,2$). In contrast to the quasi-static approximation of chapter 4 the operator $\hat{L}_i$ must have an index i because of the additional term k_i^2. The same ansatz for the Green's function as it has been used in the former chapters

$$G_{ij}(r,z;z') = \frac{1}{2\pi}\int_0^\infty d\rho\ \rho J_0(\rho r)\ g_{ij}(\rho,z;z') \ , \tag{7.25}$$

yields the following differential equation for the reduced Green's function g_{ij}

$$\hat{L}_i^z \ g_{ij}(\rho,z;z') := \Big(\frac{\partial^2}{\partial z^2} + k_i^2 - \rho^2\Big)\ g_{ij}(\rho,z;z') = -\delta_{ij}\delta(z-z') \ , \tag{7.26}$$

when it is inserted into eq.(7.24). In order to simplify notation in the following paragraphs let Λ_2 be the set of functions consisting of two parts corresponding to the two layers, which satisfy the boundary and continuity conditions (7.20) to (7.23) and the radiation condition (7.16); and let Λ_2^z be the set of functions independent of r, which are supposed to fulfil the boundary and continuity conditions (7.20) to (7.23). The requirement of selfadjointness of the operator $\hat{L}$ consisting of two parts each extending over the range of one layer only

$$\hat{L} = \begin{cases} \hat{L}_1 & : \quad q < z < 0 \\ \hat{L}_2 & : \quad 0 < z < p \end{cases} \ , \tag{7.27}$$

together with the boundary and continuity conditions, necessitates a special treatment of the scalar product.

7.2 Selfadjointness

As was also done in the quasi-static treatment of the two-layer problem in Chapter 4 care must be exercised to define a scalar product such that one gets self-adjoint operators. With two arbitrary functions $A, B \in \Lambda_2$ the expression corresponding to Green's theorem valid in layer 1 reads as:

$$\int_0^p dz \int_0^\infty dr\ rB_1\hat{L}A_1 = \int_0^p dz \int_0^\infty dr \Big[B_1 \frac{\partial}{\partial r}\Big(r\frac{\partial A_i}{\partial r}\Big) + rB_1\frac{\partial^2 A_1}{\partial z^2} + rk_1^2 B_1 A_1\Big] =$$

$$\int_0^p dz \Big[B_1 r\frac{\partial A_1}{\partial r}\Big]\Big|_{r=0}^\infty + \int_{r=0}^\infty dr \Big[rB_1\frac{\partial A_1}{\partial z}\Big]\Big|_0^p - \int_0^p dz \int_0^\infty dr\ r\Big[\frac{\partial B_1}{\partial r}\frac{\partial A_1}{\partial r} + \frac{\partial B_1}{\partial z}\frac{\partial A_1}{\partial z} - k_1^2 B_1 A_1\Big] =$$

$$\int_0^p dz \underbrace{\Big[rB_1\frac{\partial A_1}{\partial r} - r\frac{\partial B_1}{\partial r}A_1\Big]\Big|_{r=0}^\infty}_{:=\ \mu_1} + \int_0^\infty drr \underbrace{\Big[B_1\frac{\partial A_1}{\partial z} - \frac{\partial B_1}{\partial z}A_1\Big]\Big|_0^p}_{:=\ \nu_1} + \int_0^p dz \int_0^\infty dr\ rA_1\hat{L}B_1$$

Analogous transformations can be done in layer 2. The terms μ_i are zero in view of the radiation condition (7.16) prescribed for A_1 and B_1.

$$\begin{aligned}\mu_1 &= \Big[r\Big(B_1\frac{\partial A_1}{\partial r} - ik_1A_1B_1 + ik_1A_1B_1 - A_1\frac{\partial B_1}{\partial r}\Big)\Big]\Big|_0^\infty = \\ &= \Big[B_1 r\Big(\frac{\partial A_1}{\partial r} - ik_1A_1\Big) - A_1 r\Big(\frac{\partial B_1}{\partial r} - ik_1B_1\Big)\Big]\Big|_0^\infty = 0\ .\end{aligned}$$

However the terms ν_1 and the corresponding one, ν_2, to be calculated for layer 2 do not cancel each other:

$$\nu_1 + \nu_2 = \Big[B_1\frac{\partial A_1}{\partial z} - \frac{\partial B_1}{\partial z}A_1\Big]\Big|_{z=0} - \Big[B_2\frac{\partial A_2}{\partial z} - \frac{\partial B_2}{\partial z}A_2\Big]\Big|_{z=0} \neq 0\ .$$

As in Chapter 4 a new definition of the scalar product is adopted to circumvent the problem. As all the considerations and transformations have been described there we do not repeat all details. A scalar product defined as

$$\langle A, B\rangle = \langle B, A\rangle := \int_0^\infty dr\ r\Big[\frac{1}{\epsilon_1}\int_q^0 A_1B_1\ dz + \frac{1}{\epsilon_2}\int_0^p A_2B_2\ dz\Big]\ , \tag{7.28}$$

leads to the following expression corresponding to the terms ν_i :

$$\nu_1 + \nu_2 = \frac{1}{\epsilon_1}\Big[B_1\frac{\partial A_1}{\partial z} - \frac{\partial B_1}{\partial z}A_1\Big]\Big|_{z=0} - \frac{1}{\epsilon_2}\Big[B_2\frac{\partial A_2}{\partial z} - \frac{\partial B_2}{\partial z}A_2\Big]\Big|_{z=0} = 0\ ,$$

which adds up to zero after the boundary and continuity conditions have been applied. So in this case the operator $\hat{L}$ is self-adjoint:

$$\langle A, \hat{L}B\rangle = \langle B, \hat{L}A\rangle\ . \tag{7.29}$$

One must adopt the new definition of the scalar product just introduced in (7.28), too, when deriving the wanted eigenfunction expansion.

Now the general functions A and B are replaced by the vector potential $A \in \Lambda_2$ and the Green's function $G_{ij} \in \Lambda_2$ in eq.(7.29):

$$\begin{aligned} \langle A, \hat{L} G_i \rangle &= \langle G_i, \hat{L} A \rangle \\ \longrightarrow \quad \sum_{j=1}^{2} \frac{1}{\epsilon_j} \, (A_j, \hat{L}_j G_{ij}) &= \sum_{j=1}^{2} \frac{1}{\epsilon_j} \, (G_{ij}, \hat{L}_j A_j) \; , \end{aligned} \tag{7.30}$$

where the round bracket denotes the usual scalar product defined in Chapter 4, eq.(4.25). The expressions $\hat{L}_j G_{ij}$ and $\hat{L}_j A_j$ may be replaced by the r.h.s. of eq.(7.24) and (7.19). This gives

$$\begin{aligned} \sum_{j=1}^{2} \frac{\delta_{ij}}{\epsilon_j} \Big(A_j, \frac{\delta(r)}{2\pi r} \, \delta(z - z') \Big) &= \sum_{j=1}^{2} \frac{\mu_0}{\epsilon_j} \Big(G_{ij}, j_j \Big) \; , \\ \longrightarrow \quad A_i(\omega, r, z) &= \mu_0 \epsilon_i \sum_{j=1}^{2} \frac{1}{\epsilon_j} \Big(G_{ij}(r, z; r', z'), j_j(\omega, r', z') \Big) \; . \end{aligned} \tag{7.31}$$

For the case under consideration a simpler expression follows from the general form above:

$$A_2(\omega, r, z) = \mu_0 \frac{\epsilon_2}{\epsilon_1} \Big(G_{21}(r, z; r', z'), j_1(\omega, r', z') \Big) \; . \tag{7.32}$$

7.3 Eigenfunction Expansion

7.3.1 Eigenfunctions

Each eigenfunction to the operator $\hat{L}^z$, defined in eq.(7.26), consists of two pieces, each representing a particular solution in the appropriate layer.

$$Z(z) = \begin{cases} Z_1(z) & : \quad q < z < 0 \; ; \\ Z_2(z) & : \quad 0 < z < p \; . \end{cases} \tag{7.33}$$

An eigenfunction fulfils the following equation:

$$\hat{L}^z Z = (k_1^2 - \rho^2 - \lambda_1^2) Z = (k_2^2 - \rho^2 - \lambda_2^2) Z \; , \tag{7.34}$$

from which it follows:

$$\varrho^2 := k_1^2 - \lambda_1^2 = k_2^2 - \lambda_2^2 \; . \tag{7.35}$$

For the eigenfunction expansion of the Green's function only eigenfunctions $Z(z) \in \Lambda_2^z$ must be taken into account. As it has been shown in Chapter 4, the identity (7.29) guarantees orthogonality for each pair of distinct eigenfunctions.

7.3.2 Choice of an Appropriate Set of Eigenfunctions

The two pieces of the function operator are assumed as:

$$Z(z,\varrho) = \begin{cases} Z_1 = \frac{\cos[\lambda_1(z-q)]}{\cos\lambda_1 q} & : \quad q < z < 0 \ ; \\ Z_2 = \frac{\cos[\lambda_2(z-p)]}{\cos\lambda_2 p} & : \quad 0 < z < p \ . \end{cases} \tag{7.36}$$

It fulfils the differential equation (7.34), the boundary conditions (7.20), (7.21), and the continuity condition (7.22). The last condition to be met is (7.23), leading to

$$\frac{1}{\epsilon_1}\frac{\partial Z_1(z,\varrho)}{\partial z}\Big|_{z=0} = \frac{1}{\epsilon_2}\frac{\partial Z_2(z,\varrho)}{\partial z}\Big|_{z=0} \ ,$$

or

$$\epsilon_2\lambda_{1n}\sin\lambda_{1n}q \ \cos\lambda_{2n}p = \epsilon_1\lambda_{2n}\sin\lambda_{2n}p \ \cos\lambda_{1n}q \ . \tag{7.37}$$

Equation (7.35) is evaluated with (7.9) to give:

$$\omega^2\varepsilon_0\mu_0(\epsilon_1-\epsilon_2) = \lambda_{1n}^2 - \lambda_{2n}^2 \ . \tag{7.38}$$

Eqs.(7.37) and (7.38) are the characteristic equations determining the discrete pairs $\{\lambda_{1n},\lambda_{2n}\}$ of eigenvalues, where the general dielectric constants ϵ_1 and ϵ_2 may be replaced by the special values:

$$\epsilon_1 = 1 \ , \quad \epsilon_2 = \varepsilon + \frac{i\sigma}{\omega\varepsilon_0} \ .$$

This yields a discrete set of eigenfunctions:

$$Z(z,\varrho_n) = \begin{cases} Z_1 = \frac{\cos[\lambda_{1n}(z-q)]}{\cos\lambda_{1n}q} & : \quad q < z < 0 \ ; \\ Z_2 = \frac{\cos[\lambda_{2n}(z-p)]}{\cos\lambda_{2n}p} & : \quad 0 < z < p \ . \end{cases} \tag{7.39}$$

7.3.3 Normalization of the Eigenfunctions

The expression for the norm $\langle Z(\varrho), Z(\varrho)\rangle$ of an eigenfunction $Z(z,\varrho)$ is found from that for the inner product of two eigenfunctions $Z(z,\varrho)$ and $\tilde{Z}(z,\tilde{\varrho})$ in an analogous way, as it has been performed in Chapter 4. In layer 1 the eigenfunction fulfil the following equations:

$$\frac{\partial^2 Z_1}{\partial z^2} = -\lambda_1^2 Z_1 \ , \quad \frac{\partial^2 \tilde{Z}_1}{\partial z^2} = -\tilde{\lambda}_1^2 \tilde{Z}_1 \ .$$

Multiplying the first equation with $\tilde{Z}_1$ and the second one with Z_1, subtracting one from the other and integrating over z from $z = q$ to $z = 0$ gives:

$$\int_q^0 \Big[\tilde{Z}_1\frac{\partial^2 Z_1}{\partial z^2} - Z_1\frac{\partial^2 \tilde{Z}_1}{\partial z^2}\Big] \ dz = (\tilde{\lambda}_1^2 - \lambda_1^2)\int_q^0 Z_1\tilde{Z}_1 \ dz \ .$$

An integration by parts and use of the boundary condition (7.20) yields:

$$\frac{\left[\tilde{Z}_1 \frac{\partial}{\partial z} Z_1 - Z_1 \frac{\partial}{\partial z} \tilde{Z}_1\right]\Big|_{z=0}}{\tilde{\lambda}_1^2 - \lambda_1^2} = \int_q^0 Z_1 \tilde{Z}_1 \, dz \ .$$

Making tend the eigenfunction $\tilde{Z}_1$ towards Z_1 entails the same behaviour for the two corresponding eigenvalues; the ratio on the r.h.s. of the last equation becomes indeterminate. Applying de l'Hospital's rule gives:

$$\begin{aligned} \int_q^0 Z_1^2(z,\lambda) \, dz &= \lim_{\tilde{\lambda}_1 \to \lambda_1} \frac{\left[\tilde{Z}_1 \frac{\partial}{\partial z} Z_1 - Z_1 \frac{\partial}{\partial z} \tilde{Z}_1\right]\Big|_{z=0}}{\tilde{\lambda}_1^2 - \lambda_1^2} = \\ &= \frac{1}{2\lambda_1}\left[\frac{\partial}{\partial \lambda_1} Z_1\Big|_{z=0} \Big(\frac{\partial}{\partial z} Z_1\Big)\Big|_{z=0} - Z_1\Big|_{z=0} \frac{\partial}{\partial \lambda_1}\Big(\frac{\partial}{\partial z} Z_1\Big)\Big|_{z=0}\right] \end{aligned} \quad (7.40)$$

A corresponding calculation must be extended over two Z_2's from $z = 0$ to $z = p$. The norm is according to the definition (7.28):

$$\begin{aligned} \langle Z(\varrho), Z(\varrho)\rangle &= \frac{1}{2}\Bigg\{ \frac{1}{\epsilon_1 \lambda_1}\left[\frac{\partial}{\partial \lambda_1} Z_1\Big|_{z=0} \Big(\frac{\partial}{\partial z} Z_1\Big)\Big|_{z=0} - Z_1\Big|_{z=0} \frac{\partial}{\partial \lambda_1}\Big(\frac{\partial}{\partial z} Z_1\Big)\Big|_{z=0}\right] - \\ &\quad - \frac{1}{\epsilon_2 \lambda_2}\left[\frac{\partial}{\partial \lambda_2} Z_2\Big|_{z=0} \Big(\frac{\partial}{\partial z} Z_2\Big)\Big|_{z=0} - Z_2\Big|_{z=0} \frac{\partial}{\partial \lambda_2}\Big(\frac{\partial}{\partial z} Z_2\Big)\Big|_{z=0}\right]\Bigg\} \ . \end{aligned} \quad (7.41)$$

The functions $Z(z, \varrho_n)$ defined in eq.(7.39) have the following properties:

$$\begin{aligned} Z_i(z,\lambda_{in})\Big|_{z=0} &= 1 \ , \quad i = 1,2 \ ; \\ \frac{\partial Z_i(z,\lambda_{in})}{\partial \lambda_{in}}\Big|_{z=0} &= 0 \ , \quad i = 1,2 \ . \\ \frac{\partial}{\partial \lambda_{1n}}\Big(\frac{\partial Z_1(z,\lambda_{1n})}{\partial z}\Big)\Big|_{z=0} &= -\frac{q}{\cos^2 \lambda_{1n} q} - \frac{\tan \lambda_{1n} q}{\lambda_{1n}} \ ; \\ \frac{\partial}{\partial \lambda_{2n}}\Big(\frac{\partial Z_2(z,\lambda_{2n})}{\partial z}\Big)\Big|_{z=0} &= -\frac{p}{\cos^2 \lambda_{2n} p} - \frac{\tan \lambda_{2n} p}{\lambda_{2n}} \ . \end{aligned}$$

Inserting all these results in the above expression for the norm we get the following final expression for it:

$$\begin{aligned} \langle Z(\varrho_n), Z(\varrho_n)\rangle &= \frac{1}{2}\left[\frac{1}{\epsilon_1 \lambda_{1n}} \frac{\partial}{\partial \lambda_{1n}}\Big(\frac{\partial Z_1(z,\lambda_{1n})}{\partial z}\Big)\Big|_{z=0} - \frac{1}{\epsilon_2 \lambda_{2n}} \frac{\partial}{\partial \lambda_{2n}}\Big(\frac{\partial Z_2(z,\lambda_{2n})}{\partial z}\Big)\Big|_{z=0}\right] = \\ &= \frac{1}{2}\left[\frac{1}{\epsilon_1}\Big(\frac{q}{\cos^2 \lambda_{1n} q} + \frac{\tan \lambda_{1n} q}{\lambda_{1n}}\Big) - \frac{1}{\epsilon_2}\Big(\frac{p}{\cos^2 \lambda_{2n} p} + \frac{\tan \lambda_{2n} p}{\lambda_{2n}}\Big)\right] \ . \end{aligned} \quad (7.42)$$

7.3.4 Green's Function

As mentioned above, the new definition of the scalar product ensures orthogonality for each pair of eigenfunctions $Z(z,\varrho_k)$ and $Z(z,\varrho_l)$, with $k \neq l$. Thus the reduced Green's function g_{ij}, given in the spectral representation, is:

$$g_{ij}(z;z') = \sum_{n=1}^{\infty} \frac{Z_i(z,\lambda_n) Z_j(z',\lambda_n)}{\langle Z(\lambda_n), Z(\lambda_n)\rangle \ (\rho^2 - \varrho_n^2)} \ . \tag{7.43}$$

And finally the wanted eigenfunction expansion for the Green's function G_{ij} is found by inserting this expression into the r.h.s. of eq.(7.25).

$$G_{ij}(r,z;z') = \frac{1}{2\pi} \sum_{n=1}^{\infty} \left[\frac{Z_i(z,\lambda_{in}) Z_j(z',\lambda_{jn})}{\langle Z(\varrho_n), Z(\varrho_n)\rangle} \int_0^{\infty} d\rho \ \frac{\rho J_0(\rho r)}{\rho^2 - \varrho_n^2} \right] \ , \tag{7.44}$$

where the integral can be done:

$$\int_0^{\infty} d\rho \ \frac{\rho J_0(\rho r)}{\rho^2 - \varrho_n^2} = K_0(i\varrho_n r) \ . \tag{7.45}$$

The (one-component vector) potential A_2 in layer 2 due to a charge moving in layer 1 is obtained by folding the Green's function $G_{21}(r,z;z')$ with the only non-zero current component $j_1(\omega,r,z)$, eq.(7.18), according to eq.(7.32):

$$\begin{aligned} A_2(\omega,r,z) \ &= \ Q \frac{\mu_0 \epsilon_2}{4\pi^2 \epsilon_1} \sum_{n=1}^{\infty} \left[\frac{Z_2(z,\lambda_{2n}) \Big(Z_1(z',\lambda_{1n}), e^{i\frac{\omega}{v}(z'-q)} \Theta(z'-q)\Theta(-z') \Big)}{\langle Z(\varrho_n), Z(\varrho_n)\rangle} \ \times \right. \\ &\left. \times \ K_0(i\varrho_n r) \underbrace{\int_0^{\infty} dr'' \ r'' \frac{\delta(r'')}{r''}}_{=\ 1} \right] \ , \end{aligned} \tag{7.46}$$

where the scalar product $\Big(Z_1(z',\lambda_{1n}), e^{i\frac{\omega}{v}(z'-q)} \Theta(z-q)\Theta(-z) \Big)$ must be calculated according to the definition (4.25).

$$\begin{aligned} \Big(Z_1(z',\lambda_{1n}), e^{i\frac{\omega}{v}(z'-q)} \Theta(z'-q)\Theta(-z') \Big) \ &= \ \int_q^0 dz \ Z_1(z',\lambda_{1n}) \ e^{i\frac{\omega}{v}(z-q)} = \\ &= \ -\frac{i}{2} \ \frac{1}{\cos \lambda_{1n} q} \left[\frac{e^{i(\lambda_{1n} - \frac{\omega}{v})q} - 1}{\lambda_{1n} - \frac{\omega}{v}} - \frac{e^{-i(\lambda_{1n} + \frac{\omega}{v})q} - 1}{\lambda_{1n} + \frac{\omega}{v}} \right] \ . \end{aligned} \tag{7.47}$$

Inserting eqs.(7.47), (7.42) into expression (7.46) gives the following final result for the vector potential:

$$A_2(\omega,r,z) = -\frac{i\mu_0 Q}{2\pi}\sum_{n=1}^{\infty}\left\{\frac{\cos[\lambda_{2n}(z-p)]}{N_n}\left[\frac{e^{i(\lambda_{1n}-\frac{\omega}{v})q}}{\lambda_{1n}-\frac{\omega}{v}} - \frac{e^{-i(\lambda_{1n}+\frac{\omega}{v})q}}{\lambda_{1n}+\frac{\omega}{v}}\right]K_0(i\varrho_n r)\right\}\ , \quad (7.48)$$

with the denominator

$$N_n(\omega) = \cos\lambda_{2n}p\ \cos\lambda_{1n}q\left[\frac{\epsilon_1}{\epsilon_2}\Big(\frac{p}{\cos^2\lambda_{2n}p}+\frac{\tan\lambda_{2n}p}{\lambda_{2n}}\Big)-\Big(\frac{q}{\cos^2\lambda_{1n}q}+\frac{\tan\lambda_{1n}q}{\lambda_{1n}}\Big)\right]\ . \quad (7.49)$$

The electric field component normal to the electrodes is found from eqs.(7.14) with $\vec{A} = \vec{e_z}A$ and $\mu_0\omega/k_2^2 = 1/(\omega\varepsilon_0\epsilon_2)$:

$$E_2(\omega,r,z) = -\frac{Q}{2\pi\omega\varepsilon_0\epsilon_2}\sum_{n=1}^{\infty}\left\{\frac{\varrho_n^2}{N_n(\omega)}\cos[\lambda_{2n}(z-p)]\left[\frac{e^{i(\lambda_{1n}-\frac{\omega}{v})}}{\lambda_{1n}-\frac{\omega}{v}} - \frac{e^{-i(\lambda_{1n}+\frac{\omega}{v})}}{\lambda_{1n}+\frac{\omega}{v}}\right]K_0(i\varrho_n r)\right\}\ ; \quad (7.50)$$

The surface charge density on the anode is proportional to the normal (z-) component of the electric field:

$$\eta(\omega,r) = -\varepsilon_0\epsilon_2\ E_2(\omega,r,z=p) = \frac{Q}{2\pi\omega}\sum_{n=1}^{\infty}\left\{\frac{\varrho_n^2}{N_n(\omega)}\left[\frac{e^{i(\lambda_{1n}-\frac{\omega}{v})}}{\lambda_{1n}-\frac{\omega}{v}} - \frac{e^{-i(\lambda_{1n}+\frac{\omega}{v})}}{\lambda_{1n}+\frac{\omega}{v}}\right]K_0(i\varrho_n r)\right\}\ . \quad (7.51)$$

The time-dependent charge density is found by performing the inverse Fourier transform:

$$\eta(t,r) = \frac{1}{2\pi}\int_{-\infty}^{\infty}\eta(\omega,r)\ e^{-i\omega t}\ d\omega\ ,$$

which is evaluated by Cauchy's residue theorem. Note that the path of integration for term 1 in the square backet of eq.(7.51) is closed by a semi-circle in the upper complex ω-halfplane, that for term 2 by a semi-circle in the lower complex ω-halfplane. Only the poles located at

$$\omega = \omega_n^{\pm} := \pm\lambda_{1n}v \quad (7.52)$$

are taken into account; the poles resulting from the zeros of the function $N_n(\omega)$ are neglected as before (cf.[4]).

$$\eta(t,r) = \frac{iQ}{2\pi}\sum_{n=1}^{\infty}\Big[\frac{\varrho_n^{+2}}{\lambda_{1n}^{+}}\frac{e^{-i\lambda_{1n}^{+}vt}}{N_n^{+}}\ K_0(i\varrho_n^{+}r) - \frac{\varrho_n^{-2}}{\lambda_{1n}^{-}}\frac{e^{i\lambda_{1n}^{-}vt}}{N_n^{-}}\ K_0(i\varrho_n^{-}r)\Big]\ . \quad (7.53)$$

$\lambda_{1n}^{\pm}$, $\lambda_{2n}^{\pm}$ are the solutions of the system of characteristic equations resulting from (7.37) and (7.38) after $\omega_n^{\pm}$ from eq.(7.52) has been inserted. The same substitutions must also be done in the expresssions for ϱ_n, eq.(7.35), and the denominator, eq.(7.49):

$$(\varrho_n^{\pm})^2 = k_1^2 - (\lambda_{1n}^{\pm})^2 = k_2^2 - (\lambda_{2n}^{\pm})^2\ ; \quad (7.54)$$

$$N_n^{\pm} = N_n(\omega^{\pm})\ . \quad (7.55)$$

As it has already been mentioned in Chapter 4, it is convenient for numerical calculations to use a different but equivalent expression for $N_n^{\pm}$ as it is given in eq.(7.49). It has the following form and can be obtained from the integral representation:

$$N_n^{\pm} = i\ \frac{\partial}{\partial \lambda_{1n}} \left[\cos\lambda_{2n} p\ \sin\lambda_{1n} q - \frac{1}{\varepsilon \pm \frac{i\sigma}{\lambda_{1n} v \varepsilon_0}}\ \sin\lambda_{2n} p\ \cos\lambda_{1n} q \right] . \tag{7.56}$$

7.3.5 Current on Whole Electrode

Integrating the surface charge density over the whole electrode gives the following expression for the total charge:

$$q_T(t) = 2\pi \int_0^{\infty} dr\ r\ \eta(t,r) = -iQ \sum_{n=1}^{\infty} \left[\frac{1}{\lambda_{1n}^+}\ \frac{e^{-i\lambda_{1n}^+ vt}}{N_n^+} - \frac{1}{\lambda_{1n}^-}\ \frac{e^{i\lambda_{1n}^- vt}}{N_n^-} \right] . \tag{7.57}$$

Here the integral

$$\int_0^{\infty} dr\ r\ K_0(i\varrho_n r) = -\frac{1}{\varrho_n^2}$$

has been used. Deriving this expression w.r.t. time gives the induced current on the anode:

$$I_T(t) = \frac{dq_T(t)}{dt} = -Qv \sum_{n=1}^{\infty} \left[\frac{e^{-i\lambda_{1n}^+ vt}}{N_n^+} + \frac{e^{i\lambda_{1n}^- vt}}{N_n^-} \right] . \tag{7.58}$$

7.3.6 Current through a Strip

The charge on a strip is obtained by integrating the surface charge density (7.53) over the area of the strip:

$$\begin{aligned} q_S(t) &= \int_{x_0 - w/2}^{x_0 + w/2} dx \int_{-\infty}^{\infty} dy\ \eta(t,r) = \\ &= \frac{iQ}{2} \sum_{n=1}^{\infty} \left[\frac{1}{\lambda_{1n}^+}\ \frac{e^{-i\lambda_{1n}^+ vt}}{N_n^+}\ B_+ - \frac{1}{\lambda_{1n}^-}\ \frac{e^{i\lambda_{1n}^- vt}}{N_n^-}\ B_- \right] , \end{aligned} \tag{7.59}$$

where B_+ and B_- are abbreviations for the following expressions:

$$B_{\pm} := \begin{cases} 2 - e^{i\varrho_n^{\pm}(x_0 - \frac{w}{2})} - e^{-i\varrho_n^{\pm}(x_0 + \frac{w}{2})} & : \quad |x_0| \le \frac{w}{2} \\ e^{-i\varrho_n^{\pm}(x_0 - \frac{w}{2})} - e^{-i\varrho_n^{\pm}(x_0 + \frac{w}{2})} & : \quad |x_0| \ge \frac{w}{2} \end{cases} .$$

Then the current through the anode strip is:

$$I_S(t) = \frac{dq_S(t)}{dt} = \frac{Qv}{2} \sum_{n=1}^{\infty} \left[\frac{e^{-i\lambda_{1n}^+ vt}}{N_n^+}\ B_+ + \frac{e^{i\lambda_{1n}^- vt}}{N_n^-}\ B_- \right] . \tag{7.60}$$

Chapter 8

Numerical Evaluations

It is in the nature of things that the numerical calculation of the current flowing through an anode strip is the less cumbersome the simpler the used model is. Thus it is convenient to investigate the ranges of geometrical and electrical parameters, where a more complicate model can be well approximated by a simpler one.

8.1 When May the Dynamical Model Be Replaced by the Quasi-Static Approximation for Weakly Conducting Layers

To work out the difference between the complicated dynamical model and the quasi-static model for a weakly conducting layer we evaluate the z_0 dependent total current I_T induced on the whole electrode for a few significant conductivities σ using the results from both models. For the numerical computation we want to use the series representation for the total current given in eq.(4.61) and (7.58). But there is a problem: the series' are not convergent (see Fig.8.2). One possibility to avoid this difficulty is to start with the expressions for the corresponding total charges q_T, eq.(4.60) and (7.57). In this case the series' are convergent because there is an additional convergence generating factor (eigenvalue) in the denominator and the sign of the nominator alternates. So the z_0 dependent total charge are found by performing the sum of eq.(4.60) and (7.57) with sufficiently large limits. The derivation w.r.t z_0 can be done numerically and yields an expression which is proportional to the wanted total current. But there is another more suitable method of proceeding.

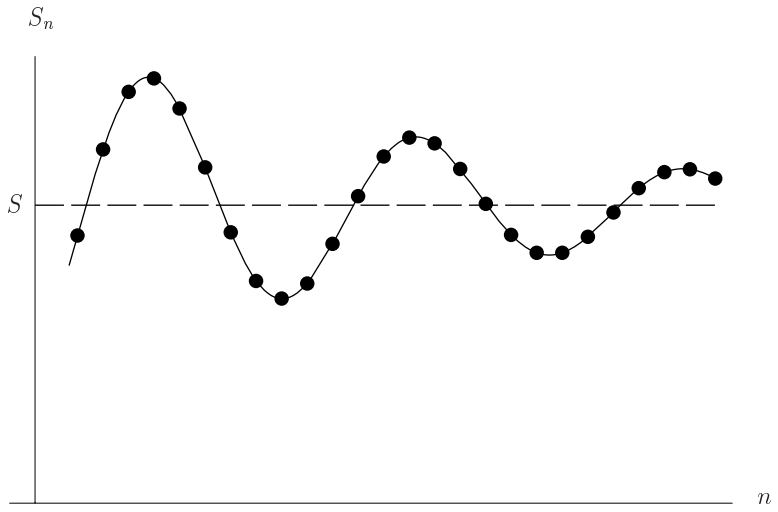

Figure 8.1: *A mathematical transient.*

8.1.1 Convergence Generation by a Shanks' Transform

The method consists of applying the Shanks' transformation to the series representation for the total current. Shanks' transformation ([20], [21], [22]) is based on the assumption that a sequence of partial sums S_n $(n = 1, 2, \ldots)$ can be thought of as representing a "mathematical transient" of the form

$$S_n = S + \sum_{k=1}^{K} a_k q_k^n \ . \tag{8.1}$$

Such a transient is depicted in Fig.8.1. If $|q_k| < 1$, then clearly

$$S = \lim_{n \to \infty} S_n \ .$$

The assumed form (8.1) implies that the sequence of partial sums satisfies a $(K+1)$th order finite difference equation. It can be shown that the repeated application of the transform extracts the base S (i.e., the constant solution of the finite difference equation) of the mathematical transient. These higher order Shanks' transforms are efficiently computed by means of following algorithm:

$$e_{s+1} = e_{s-1}(S_{n+1}) + \frac{1}{e_s(S_{n+1}) - e_s(S_n)} \ , \qquad s = 1, 2, \ldots \tag{8.2}$$

where

$$e_0(S_n) = S_n \ , \quad e_1(S_n) = \frac{1}{[e_0(S_{n+1}) - e_0(S_n)]} \ .$$

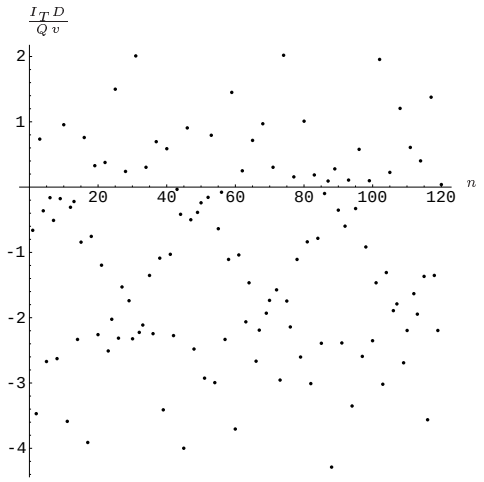

Figure 8.2: *The first* 120 *partial sums obtained from the series representation (7.58) for the following special parameters:* $D = 10\ mm$, $d = 1.4\ mm$, $\varepsilon = 3.5$, $\sigma = 7.5\ 10^{-4}\ S/m$, $v = 5\ 10^4\ m/s$, $z_0 = 3.5\ mm$.

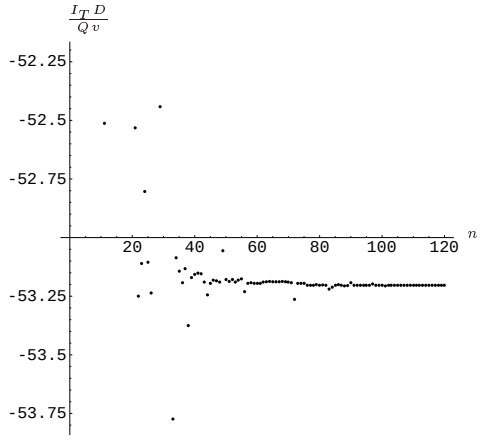

Figure 8.3: *The results of applying the first through the* 60*th-order Shanks' transform to the sequence of partial sums shown in the left picture.* n *denotes the number of partial sums which are involved.*

Only the even-order terms $e_{2r}(S_n)$ are Shanks' transforms of order r approximating S; the odd-order terms are merely intermediate auxiliary quantities. In Fig.8.3 a representative example for the results of applying the first through the 60th-order Shanks' transforms to the sequence of partial sums $S_0, S_1, \ldots, S_{120}$, Fig.8.2, obtained from the series representation of the total current given in eq.(7.58), are shown.

The sequence of partial sums is obviously not convergent, but convergence is generated after applying Shanks' transformation. As it can be seen clearly in Fig.8.3 there is a dramatic improvement of convergence by increasing the order of transformation.

This method was performed successfully to obtain the Figs.8.4 and 8.5. The left picture shows the z_0 dependence of the total current for a few significant values of the conductivity σ found from the dynamical model; and the right picture shows the same but is computed with the quasi-static approximation for weakly conducting media. As you can see by comparison, the quasistatic approximation is a reasonable substitution applicable for the whole range of conductivity we are interested in. A more detailed investigation has shown that the velocity v has a much higher impact on the validity of this approximation, but it holds for values $v < 10^6\ m/s$.

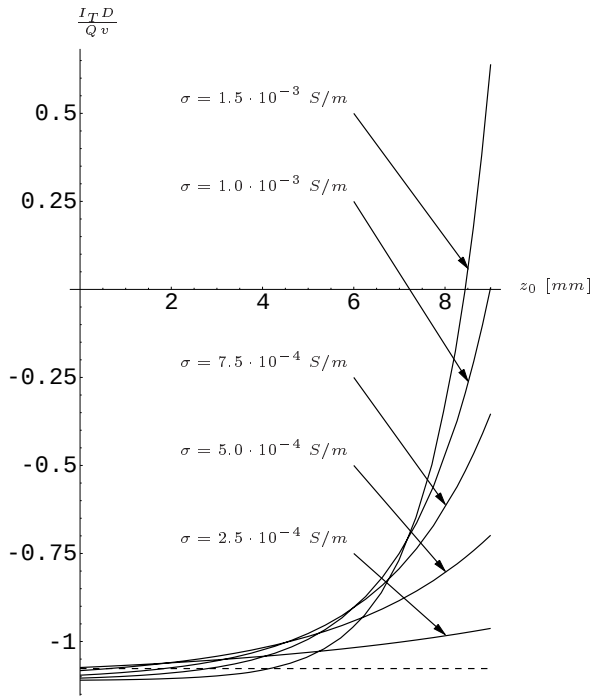

Figure 8.4: *The total current I_T on the anode in dependence on the position z_0 of the slowly moving ($v = 5 \cdot 10^4$ m/s) charge obtained from the dynamical model, eq.(7.58). $D = 10$ mm, $d = 1$ mm, $\varepsilon = 3.5$*

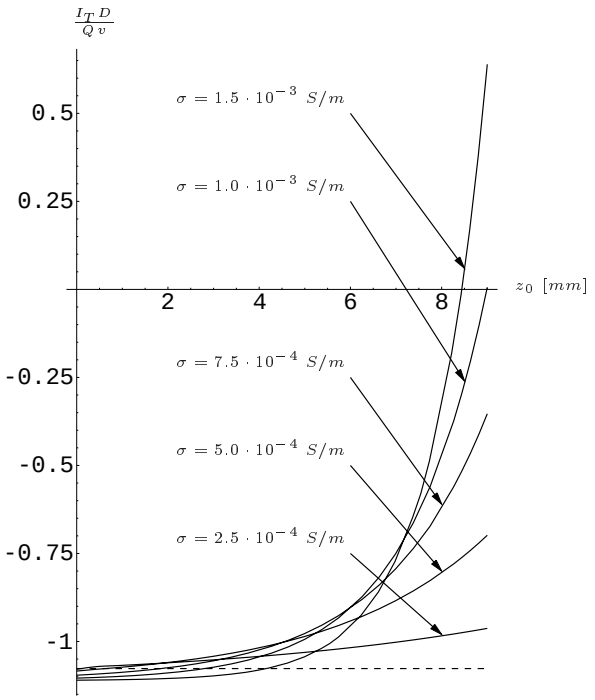

Figure 8.5: *The same, but calculated with the quasistatic approximation for a weakly conducting layer. The dashed line shows the constant total current for the case of an isolating layer given in eq.(4.61).*

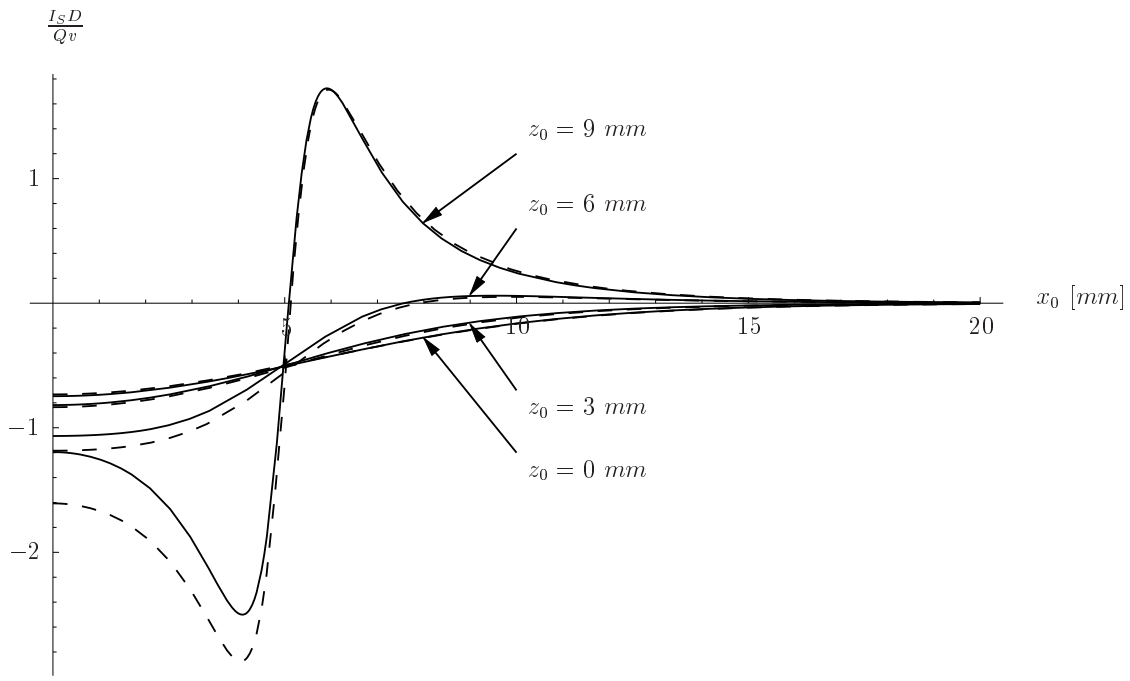

Figure 8.6: *The current flowing through an anode strip, width* $w = 10$ *mm, in dependence on the position* x_0 *for 4 distinct values of* z_0*. The dashed lines correspond to the case* $\sigma = 0$ *and the continuous lines to the case* $\sigma = 5 \cdot 10^{-4}$ *S/m.* $D = 10$ *mm,* $d = 1$ *mm,* $\varepsilon = 3.5$*,* $v = 5 \cdot 10^4$ *m/s.*

8.2 Influence of the Conductivity on the Signal

To investigate the influence of the conductivity on the current I_S induced on an anode strip we compare the results obtained from the quasistatic approximation for a conducting layer, eq.(4.63), and for an isolating layer, eq.(4.77). In the case that the trajectory of the moving charge lies in the region outside the anode strip ($x_0 \geq w/2$), the convergence is ensured by the two exponential functions $e^{\pm\lambda_n(x_0 \mp w/2)}$. The additional constant term 2 after the brace of eq.(4.63) and (4.77) for the case $x_0 \leq w/2$ yields an additional term to the current on the strip, which is not convergent. But this problem can be simply circumvented, because this term is proportional to the corresponding expression for the total current I_T, which can be calculated by applying Shanks' transformation described in the last section in the case of an weakly conducting layer; and for the case of an isolating layer it can be replaced by the closed expression for the total current, given in eq.(4.96).

Fig.8.6 shows the x_0-dependent current on an anode strip for 4 values of the position of the point charge z_0, and Fig.8.7 shows the dependence of the current on x_0 for 4 fixed

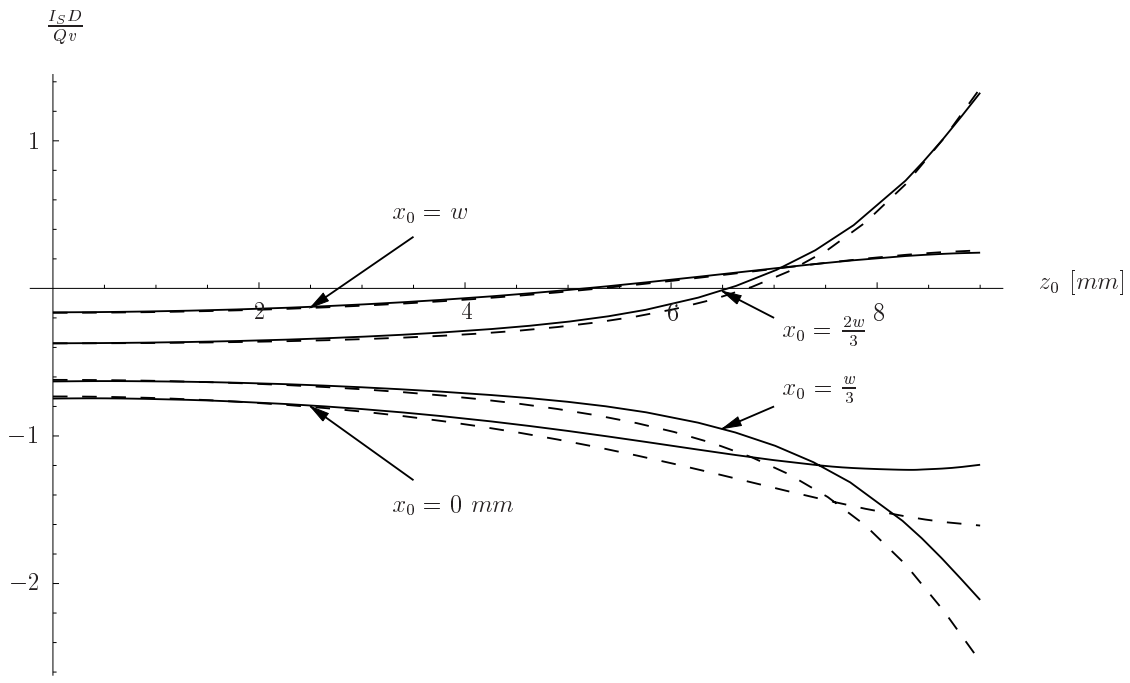

Figure 8.7: *The current flowing through an anode strip, width* $w = 10$ mm*, in dependence on the position* z_0 *for 4 distinct values of* x_0*. The dashed lines correspond to the case* $\sigma = 0$ *and the continuous lines to the case* $\sigma = 5 \cdot 10^{-4}$ S/m*.* $D = 10$ mm*,* $d = 1$ mm*,* $\varepsilon = 3.5$*,* $v = 5 \cdot 10^4$ m/s*.*

values for z_0. The dashed lines are obtained from the case of an isolating layer ($\varepsilon = 3.5$); and the continous lines are found for a weakly conducting layer ($\sigma = 5 \cdot 10^{-4}$ S/m). The conclusion of this investigation can be summarized by a simple statement: For most cases the impact of a conductivity $\sigma \neq 0$, in the range of values we are interested in, say $0 \leq \sigma \leq 10^{-3}$ S/m, is hardly noticeable, except if the charge is in the vicinity of the center line of an anode strip.

8.3 Influence of the Dielectric Constant on the Signal

Finally, we study the influence of the dielectric constant ε on the induced current. For this purpose we show the Figs.8.8 and 8.9, which are computed by performing eq.(4.77) and (3.15).

The influence of the dielectric constant ε seems to be similar to the effect of a scaling

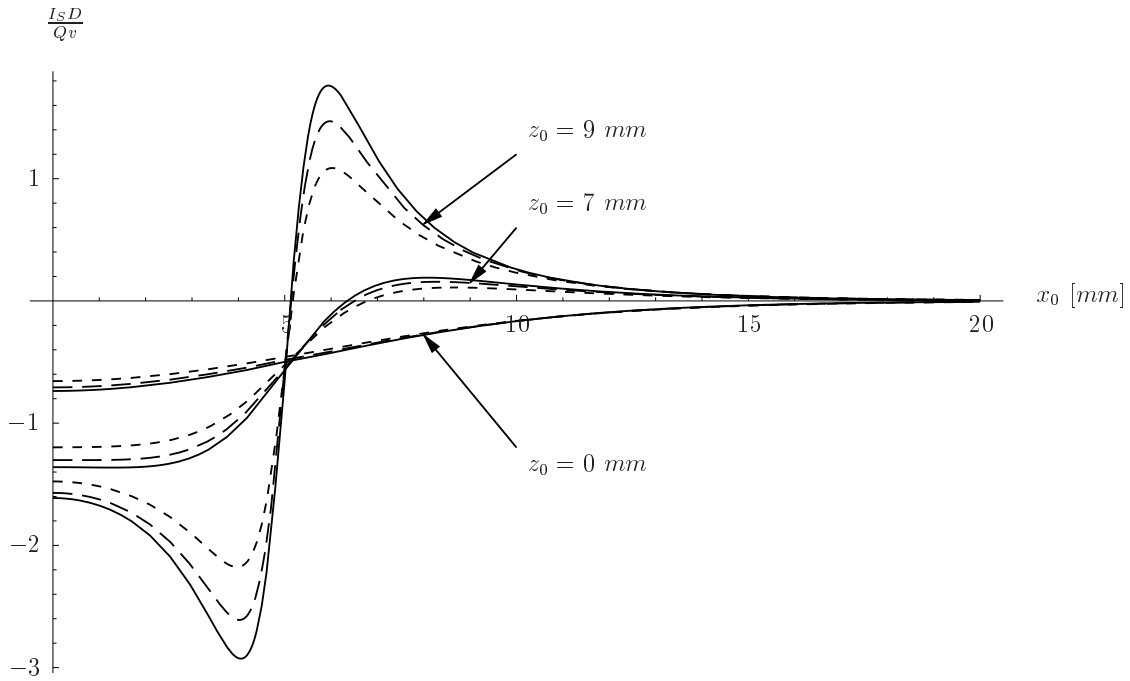

Figure 8.8: *The current flowing through an anode strip, width* $w = 10$ mm*, in dependence on the position* x_0 *for 3 distinct values of* z_0*. The dashed lines (smaller dashes), the dashed lines (longer dashes) and the continuous lines correspond to the cases* $\varepsilon = 1$*,* $\varepsilon = 2$ *and* $\varepsilon = 4$*, respectively.* $D = 10$ mm*,* $d = 1$ mm*,* $\sigma = 0$*,* $v = 5 \cdot 10^4$ m/s*.*

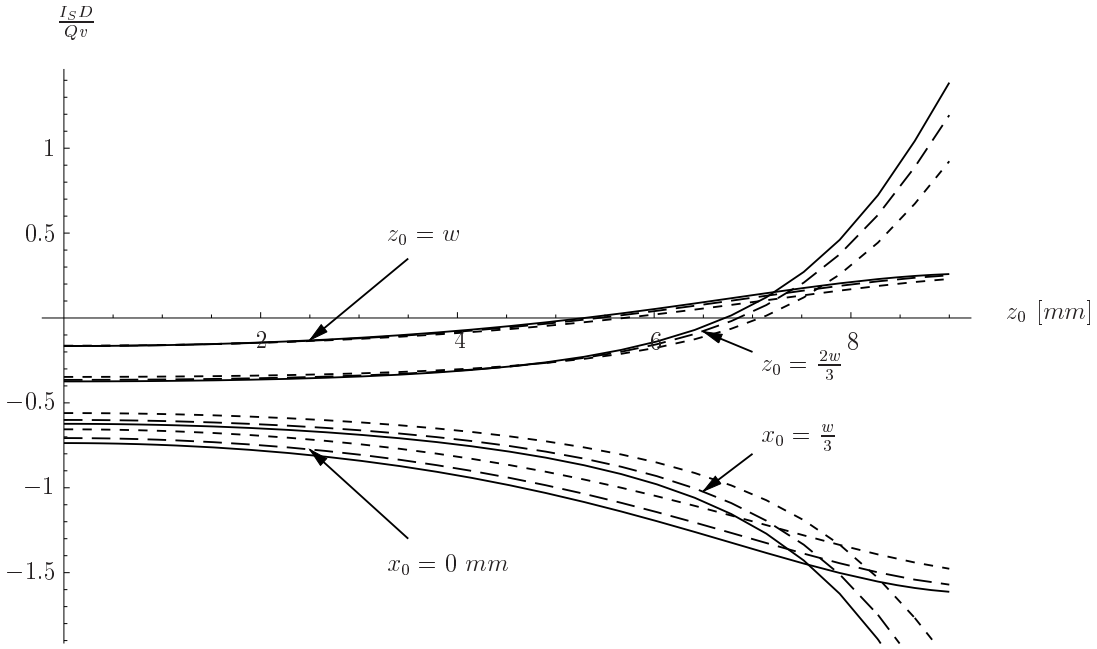

Figure 8.9: *The current flowing through an anode strip, width* $w = 10\ mm$*, in dependence on the position* z_0 *for 4 distinct values of* x_0*. The dashed lines (smaller dashes), the dashed lines (longer dashes) and the continuous lines correspond to the cases* $\varepsilon = 1$*,* $\varepsilon = 2$ *and* $\varepsilon = 4$*, respectively.* $D = 10\ mm$*,* $d = 1\ mm$*,* $\sigma = 0$*,* $v = 5 \cdot 10^4\ m/s$*.*

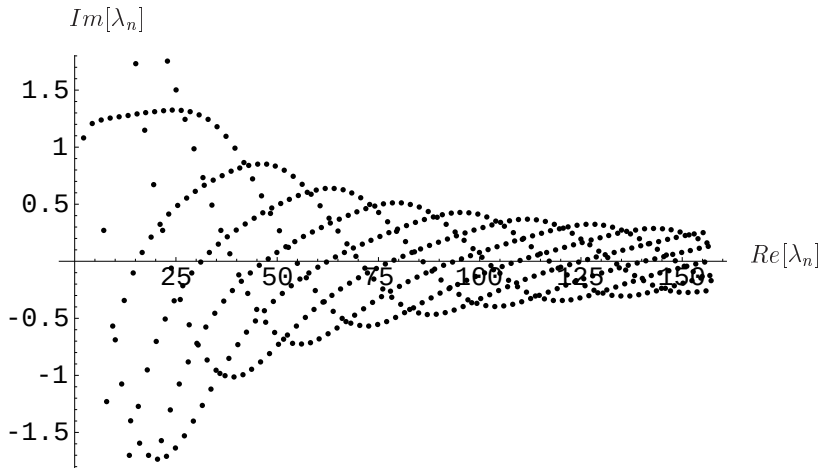

Figure 8.10: *Typical arrangement of eigenvalues λ_n in the complex λ-plane ($n = 1, 2, \ldots, 500$). $D = 10\ mm$, $d = 2.83\ mm$, $\varepsilon = 3.5$, $\sigma = 1.5 \cdot 10^{-3}\ S/m$, $v = 5 \cdot 10^4\ m/s$.*

factor, which appears explicitly as $\alpha = 2\varepsilon/(1+\varepsilon)$ in the closed form for the induced current in the case of a half filled condensor, eq.(5.30).

8.4 Computation of the Eigenvalues

To computate the pairs λ_{1n}, λ_{2n} of eigenvalues we must solve both characteristic equations (7.37) and (7.38) simultaneously. The appropriate command in *Mathematica* is **FindRoot**[] for this purpose, which requires the additional input of at least one starting value, which can be found successively in the following way. The purely real eigenvalues λ_n in the case of an isolating layer can be calculated without difficulty. Now these values can be applyed successfully as starting values to obtain the generally complex eigenvalues needed for the quasi-static approximatin for a weakly conducting layer; and finally these complex eigenvalues are suitable starting points for evaluating the wanted pairs of eigenvalues λ_{1n}, λ_{2n} for the dynamical model. A typical example for the arrangement of eigenvalues λ_n in the complex λ-plane are depicted in Fig.8.10.

Chapter 9

Conclusions

As it can be seen by comparison of the Figs.8.4 and 8.5 the quasistatic approximation for weakly conducting media, elaborated in Chapter 4, eq.(4.63), is a very satisfactory approximation for the more general dynamical model, Chapter 7, eq.(7.60). It seems to be applicable to all ranges of geometrical and electrical parameters, we are interested in, say $0 \leq \sigma \leq 10^{-3}\ S/m$.

The influence of the weak conductivity of the dielectric layer is negligible as long as the point charge is not in the vicinity of the center line of the anode strips (see. Figs.8.6, 8.7). Thus the simpler formulae (4.77) may be useful.

The impact of the dielectric on the signal is shown in Figs.8.8 and 8.9, which compare the results of the calculations according to eq.(4.77) and the simple formula for an empty plane condensor, given in eq.(3.15). At least in the case $\varepsilon = 2$ the influence is quite small. Of course, the dielectric will change the static electric field strength prevailing in the gas gap, so influence the development and velocity of the electron avalanche. But these effects are not included in our approach as we assume the value of the charge and the velocity as given. For the special case of a half-filled condensor a closed form for the current can be given, eq.(5.30); an approximate expression in closed form, eq.(5.33), is found for the case of a dielectric layer very thin as compared to the distance of the electrodes.

The influence of the gap between two neighbouring anode strips is investigated in Chapter 6 by 4 two-dimensional models. It turns out that the models described in Chapter 4, 5 and 7, which do not take the gap into consideration, give good results if the charge is above the anode strip. The influence of the gap is appreciable if the charge is near to it. The extremes of the current shown in the uppermost drawings in Figs.(6.6) and (6.7) can be evaluated analytically (eqs.(6.15), (6.16)) for the model consisting of an continous conducting plate. The positive of these extremes is almost the same in the models with a real gap. So the domain of validity, which lies outside the extremes, can

be given explicitly.

Appendix A

Analytic Expressions for the Integrals $\mathcal{J}_n(a,b,c)$

Analytic expressions for the integrals, eq.(4.102)

$$\mathcal{J}_n(a,b,c) := \frac{1}{2\pi}\int_0^\infty d\zeta \frac{\sin(\zeta a)\cosh(\zeta b)\sinh^n(\zeta c)}{\sinh^{n+1}\zeta}\ , \quad 0 \le b < 1;\ 0 \le c < 1\ , \qquad \text{(A.1)}$$

have been obtained for $n = 0$ to $n = 6$ with the help of *Mathematica*. They can be expressed by trigonometric and hyperbolic functions multiplied by polynomials in a, b, c. For $n = 0$ and $n = 1$ this is a straigthforward procedure using the commands **Integrate**[], **FullSimplify**[] and **ComplexExpand**[**Re**[]]. For the other integrals $n = 2 - 6$ one gets lengthy expressions involving simple fractions of complex numbers containing a, b, c, trigonometric, hyperbolic and PolyGamma functions (whose arguments are complex linear polynomials in a, b, c) multiplied by polynomials in a, b, c. The contributions of the simple fractions add up to the value zero. The PolyGamma function as they occur here are just the logarithmic derivative of the Gamma function $\psi(z) = d(ln\Gamma(z))/dz$. They contain arguments $n/2 + g_i(a,b,c)$ with n being identical to the subscript n of $\mathcal{J}_n$ and $g_i(a,b,c)$ being a linear polynomial in (a,b,c). Recurrences using $\psi(z+1) = \psi(z)+1/z$ permit one to reduce the $\psi(n/2+g_i(a,b,c))$ to $\psi(1/2+g_i(a,b,c))$ and pure fractions. The contributions of the latter again sum up to the value zero. To every term containing $\psi(1/2 + g_i(a,b,c))$ there turns up a corresponding term containing $\psi(1/2 - g_i(a,b,c))$ such that the formula $\psi(1/2 + z) + \psi(1/2 - z) = \pi\ ctg(\pi z)$ may be applied. Then **FullSimplify**[] and **ComplexExpand**[**Re**[]] give the wanted expressions. As all these expressions have quite a regular structure all the operations are easily implemented in *Mathematica*. The final results are listed below:

$$\mathcal{J}_0(a,b,c) \ = \ +\frac{\sinh(a\,\pi)}{N_0(a,b,0)}; \qquad \text{(A.2)}$$

$$\mathcal{J}_1(a,b,c) = +\frac{z_1(a,b,c)}{2\ N_1(a,b,c)} - \frac{z_1(a,b,-c)}{2\ N_1(a,b,-c)}; \tag{A.3}$$

$$\mathcal{J}_2(a,b,c) = -\frac{z_2(a,b,0)}{N_2(a,b,0)} + \frac{z_2(a,b,2c)}{2\ N_2(a,b,2c)} + \frac{z_2(a,b,-2c)}{2\ N_2(a,b,-2c)}; \tag{A.4}$$

$$\mathcal{J}_3(a,b,c) = -\frac{z_3(a,b,c)}{2\ N_3(a,b,c)} + \frac{z_3(a,b,-c)}{2\ N_3(a,b,-c)} + \frac{z_3(a,b,3c)}{6\ N_3(a,b,3c)} - \frac{z_3(a,b,-3c)}{6\ N_3(a,b,-3c)}; \tag{A.5}$$

$$\begin{aligned}\mathcal{J}_4(a,b,c) = & -\frac{z_4(a,b,0)}{4\ N_4(a,b,0)} + \\ & + \frac{z_4(a,b,2c)}{6\ N_4(a,b,2c)} + \frac{z_4(a,b,-2c)}{6\ N_4(a,b,-2c)} - \frac{z_4(a,b,4c)}{24\ N_4(a,b,4c)} - \frac{z_4(a,b,-4c)}{24\ N_4(a,b,-4c)};\end{aligned} \tag{A.6}$$

$$\begin{aligned}\mathcal{J}_5(a,b,c) = & +\frac{z_5(a,b,c)}{12\ N_5(a,b,c)} - \frac{z_5(a,b,-c)}{12\ N_5(a,b,-c)} - \frac{z_5(a,b,3c)}{24\ N_5(a,b,3c)} + \frac{z_5(a,b,-3c)}{24\ N_5(a,b,-3c)} + \\ & + \frac{z_5(a,b,5c)}{120\ N_5(a,b,5c)} - \frac{z_5(a,b,-5c)}{120\ N_5(a,b,-5c)};\end{aligned} \tag{A.7}$$

$$\begin{aligned}\mathcal{J}_6(a,b,c) = & -\frac{z_6(a,b,0)}{36\ N_6(a,b,0)} + \frac{z_6(a,b,2c)}{48\ N_6(a,b,2c)} + \frac{z_6(a,b,-2c)}{48\ N_6(a,b,-2c)} - \\ & - \frac{z_6(a,b,4c)}{120\ N_6(a,b,4c)} - \frac{z_6(a,b,-4c)}{120\ N_6(a,b,-4c)} + \frac{z_6(a,b,6c)}{720\ N_6(a,b,6c)} + \frac{z_6(a,b,-6c)}{720\ N_6(a,b,-6c)};\end{aligned} \tag{A.8}$$

$$\begin{aligned}\mathcal{J}_7(a,b,c) = & +\frac{z_7(a,b,c)}{144\ N_7(a,b,c)} - \frac{z_7(a,b,-c)}{144\ N_7(a,b,-c)} - \frac{z_7(a,b,3c)}{240\ N_7(a,b,3c)} + \frac{z_7(a,b,-3c)}{240\ N_7(a,b,-3c)} + \\ & + \frac{z_7(a,b,5c)}{720\ N_7(a,b,5c)} - \frac{z_7(a,b,-5c)}{720\ N_7(a,b,-5c)} - \frac{z_7(a,b,7c)}{5040\ N_7(a,b,7c)} + \frac{z_7(a,b,-7c)}{240\ N_7(a,b,-7c)}.\end{aligned} \tag{A.9}$$

The denominators may be given by a single formula, namely

$$N_n(a,b,c) = 4\ 2^n\ [\cos[(b+c)\ \pi] + (-1)^n \cosh(a\pi)]\ . \tag{A.10}$$

Each numerator consists of two terms, whose parts are listed below:

$$z_n(a,b,c) = z_{n1}(a,b,c)\sin[(b+c)\pi] + z_{n2}(a,b,c)\sinh(a\pi); \tag{A.11}$$

$$z_{11}(a,b,c) = a; \tag{A.12}$$

$$z_{12}(a,b,c) = -(b+c); \tag{A.13}$$

$$z_{21}(a,b,c) = 2a(b+c); \tag{A.14}$$

$$z_{22}(a,b,c) = -1-a^2+b^2+2bc+c^2; \tag{A.15}$$

$$z_{31}(a,b,c) = a\left(-4-a^2+3b^2+6bc+3c^2\right); \tag{A.16}$$

$$z_{32}(a,b,c) = (b+c)\left(4+3a^2-b^2-2bc-c^2\right); \tag{A.17}$$

$$z_{41}(a,b,c) = 4a(b+c)[5+a^2-b^2-2bc-c^2]; \tag{A.18}$$

$$\begin{aligned} z_{42}(a,b,c) = {} & -9-a^4+10b^2-b^4+20bc-4b^3c+10c^2-6b^2c^2-4bc^3-c^4+ \\ & +2a^2(-5+3b^2+6bc+3c^2); \end{aligned} \tag{A.19}$$

$$\begin{aligned} z_{51}(a,b,c) = {} & a[64+a^4-60b^2+5b^4-120bc+20b^3c-60c^2+30b^2c^2+20bc^3+5c^4- \\ & -10a^2\left(-2+b^2+2bc+c^2\right)]; \end{aligned} \tag{A.20}$$

$$\begin{aligned} z_{52}(a,b,c) = {} & -(b+c)[64+5a^4-20b^2+b^4-40bc+4b^3c-20c^2+6b^2c^2+4bc^3+c^4- \\ & -10a^2(-6+b^2+2bc+c^2)]; \end{aligned} \tag{A.21}$$

$$\begin{aligned} z_{61}(a,b,c) = {} & 2a(b+c)[259+3a^4-70b^2+3b^4-140bc+12b^3c-70c^2+18b^2c^2+12bc^3+ \\ & +3c^4-10a^2(-7+b^2+2bc+c^2)]; \end{aligned} \tag{A.22}$$

$$\begin{aligned} z_{62}(a,b,c) = {} & -225-a^6+259b^2-35b^4+b^6+518bc-140b^3c+6b^5c+259c^2-210b^2c^2+15b^4c^2- \\ & -140bc^3+20b^3c^3-35c^4+15b^2c^4+6bc^5+c^6+5a^4(-7+3b^2+6bc+3c^2)- \\ & -a^2(259-210b^2+15b^4-420bc+60b^3c-210c^2+90b^2c^2+60bc^3+15c^4); \end{aligned} \tag{A.23}$$

$$\begin{aligned} z_{71}(a,b,c) = {} & a\Big[2304+a^6-7b^6-42b^5c-2352c^2+280c^4-7c^6+140b^3c\left(8-c^2\right)+ \\ & +35b^4\left(8-3c^2\right)+7a^4\left(8-3b^2-6bc-3c^2\right)- \\ & -14bc\left(336-80c^2+3c^4\right)-21b^2\left(112-80c^2+5c^4\right)+ \\ & +7a^2[112+5b^4+20b^3c-80c^2+5c^4-20bc\left(8-c^2\right)-10b^2\left(8-3c^2\right)]\Big]; \end{aligned} \tag{A.24}$$

$$\begin{aligned} z_{72}(a,b,c) = {} & (b+c)\Big[-2304-7a^6+b^6+6b^5c+784c^2-56c^4+c^6- \\ & -35a^4\left(8-b^2-2bc-c^2\right)-4b^3c\left(56-5c^2\right)-b^4\left(56-15c^2\right)+ \\ & +b^2\left(784-336c^2+15c^4\right)+b\left(1568c-224c^3+6c^5\right)- \\ & -7a^2[336+3b^4+12b^3c-80c^2+3c^4-4bc\left(40-3c^2\right)-2b^2\left(40-9c^2\right)]\Big]; \end{aligned} \tag{A.25}$$

Bibliography

[1] I. Crotty, E. Cerron Zeballos, J. Lamas Valverde, D. Hatzifotiadou, M. C. S. Williams and A. Zichichi, The Wide Gap Resistive Plate Chamber. Nucl. Instr. and Meth., A 360, 512 - 520, 1995.

[2] E. Cerron Zeballos, I. Crotty. D. Hatzifotiadou, J. Lamas Valverde, S. Neupane, S. Singh, M. C. S. Williams and A. Zichichi, High Rate Resistive Plate Chambers. Nucl. Instr. and Meth. A 367, 388 - 393, 1995.

[3] J. A. Lamas Valverde, Développement de la chambre à plaques résistives (RPC) et de la RPC multi-plaques (MRPC): Détecteurs gazeux déstinés au trigger de myons auprès des experiénces au LHC. Doctoral Dissertation, CERN European Laboratory for Particle Physics, Genf, CERN/LAA 97-03.

[4] H. Schöpf, Zeitabhaengige Theorie der Zählrohre. Doctoral Dissertation, Faculty of Science, Technische Universität Graz, 1991.

[5] H. Schöpf and B. Schnizer, Theory Describing Cathode Signals from Charges Moving in Counters with a Poorly Conducting Cathode. Nucl. Instr. and Meth. A 323, 338 - 344, 1992.

[6] H. Schöpf and B. Schnizer, Signals generated by uniformly moving charge in a counter. Kleinheubacher Berichte 35, 645 - 655, 1992.

[7] Th. Heubrandtner, B. Schnizer and H. Schöpf, Signals in a resistive plate chamber. Kleinheubacher Berichte 41, 484 - 489, 1998.

[8] Th. Heubrandtner, B. Schnizer and H. Schöpf, A simple theory for signals induced by a point charge moving in a resistive plate chamber. Nucl. Instr. and Meth. A 419, 721 - 725, 1998.

[9] L. Dedek, T. Bachorec. Evaluation of transient electric field in lossy media by means of ANSYS dynamical module. Proc. 8th Int. IGTE Symp. on Num. Field Calc. in Elect. Eng., September 21-24, 1998, Graz. 322-326.

[10] R. Weder. Spectral and scattering theory for wave propagation in perturbed stratified media. Springer (1991).

[11] Stratton, J. A., Electromagnetic Theory. McGraw-Hill, New York, 1941.

[12] Classical Electrodynamic, J. D. Jackson, 2. ed., John Wiley, New York, 1975.

[13] H. Buchholz, Elektrische und magnetische Potentialfelder, Springer, 1957, pp. 34-35.

[14] Ch. Carli and B. Schnizer, Green's function for a counter with a cathode of square cross section. Nucl.Inst.Meth. Phys. Res. A334 (1993) 409-419

[15] M. Abramowitz and I. Stegun, Handbook of Mathematical Functions. Dover Publ., New York, 1965.

[16] G. N. Watson, A treatise on the theory of Bessel functions. Cambridge University Press, Cambridge, 1966. p. 417

[17] Wolfram, The Mathematica book, Cambridge Univ.Press, Cambridge, 1996.

[18] Wolfram Research, Mathematica 3.0 Standard Add-On Packages, Cambridge University Press, 1996, pp.338-339.

[19] I. S. Gradshteyn and I. M. Ryzhik, Table of integrals, series, and products. 5. ed., 4. print. San Diego, Calif.: Acad. Press 1997.

[20] E. J. Weniger, Computer Physics Reports; Nonlinear Sequence Transformation for Acceleration of Convergence and Summation of Divergent series. North-Holland - Amsterdam 1989.

[21] V. Krebs, Sphärische Multipolentwicklung von Beugungsfeldern des elliptischen Kegels und ihre numerische Auswertung mit Hilfe von Reihentransformationen. Doctoral Dissertation, Faculty of Science, Ruhr-Universität Bochum, 1997.

[22] S. Singh, W. F. Richards, J. R. Zinecker, D. R. Wilton, Accelerating the Convergence of Series Representing the Free Space Periodic Green's Function. IEEE Transactions on Antennas and Propagation. Vol. 38. No. 12. December 1990.

Diese Arbeit wurde am Institut für Theoretische Physik der Technischen Universität Graz durchgeführt. Herzlich bedanken möchte ich mich bei Herrn Prof. Bernhard Schnizer für seine ausgezeichnete Betreuung und für die unzähligen klärenden Gespräche.

Auch bei allen anderen Mitgliedern des Institutes möchte ich mich für das angenehme Arbeitsklima und die schöne Zeit bedanken.